Exhaustive search for higher-order Kronrod-Patterson Extensions

R. Bourquin

Research Report No. 2015-11
April 2015

Seminar für Angewandte Mathematik
Eidgenössische Technische Hochschule
CH-8092 Zürich
Switzerland

Funding SNF: 140688

Exhaustive search for higher-order Kronrod-Patterson Extensions

R. Bourquin

April 30, 2015

Abstract

Gauss points are not nested and for this reason one searches for quadrature rules with nested points and similar efficiency. A well studied source of candidates are the Kronrod-Patterson extensions. Under suitable conditions it is possible to build towers of nested rules. We investigate this topic further and give a detailed description of the algorithms used for constructing such iterative extensions. Our new implementation combines several important ideas spread out in theoretical research papers. We apply the resulting algorithms to the classical orthogonal polynomials and build sparse high-dimensional quadrature rules for each class.

1 Introduction

The Gauss quadrature rules are among the most important techniques for numerical integration. Computation of their nodes and weights is an important task and makes these rules available for actual computation. This problem is by now solved at least for the classical orthogonal polynomials and quadrature rules Q_n are available for any number n of nodes even in the range up to several thousand.
The Gauss rules have a major drawback, namely that for two rules Q_n and Q_m with $m > n$, their sets of nodes Γ_n and Γ_m are in general different, except for very special points like the origin. We say that these rules are not *nested* because $\Gamma_n \not\subset \Gamma_m$ despite Γ_n being of smaller cardinality. This implies that almost all function evaluations can not be reused. This is an issue for example when one tries to recompute an integral with a higher order rule to obtain an error estimation.
Therefore Kronrod proposed [16] to extend a given Gauss quadrature rule Q_n with $n+1$ new points yielding a new rule. This is done in such a way that now the two rules are nested. A few years later Patterson showed [26] an optimal and numerically stable way to compute these new nodes. The close relation to the standard way of computing Gauss quadrature rules is shown in [17]. It is possible to iterate these constructions and build whole towers of nested quadrature rules [18]. We review this construction and give a detailed description of the algorithms for such iterated nested extensions to the Gauss quadrature rules related to the five classical orthogonal polynomials. The algorithms are implemented in an efficient code that is publicly available under the GPL license.

There are only few theoretical results on the existence of Kronrod-Patterson extensions and they are usually restricted to one single extension level [4, 5, 20, 21, 28]. Most of these results are for Legendre Polynomials and the branch stemming from specializations of Jacobi polynomials. For the case of Hermite polynomials, which is most interesting for the application we originally had in mind [9, 2], there is only a single result of limited use [14].
We take an algorithmic ansatz and explicitly find and enumerate extensions by an exhaustive recursive search. This gives huge families of nested quadrature rules for some cases. The evaluation of the best is not easy and partially left open. In other cases the choice is more limited and if we require a certain number of nested levels, there are only few possible rules left to try.
Quadrature rules that are not nested are a particularly bad starting point for the classical Smolyak ansatz that is often used for quadrature in higher dimensions. The set of quadrature point is then much larger than necessary and can be even larger than a full tensor product.
However, a tower of Kronrod extensions and the Smolyak composition formula yield efficient rules even for high dimensions and for more complex cases such as the unbounded case of Gauss-Hermite integration. It was proven [25] that this construction exactly yields the Genz-Keister quadrature rules [7]. Therefore we have an efficient way to actually build all these rules avoiding the explicit Smolyak formula. In the end we provide algorithms for the construction of sparse quadrature rules for any of the classical orthogonal polynomials. The rules are evaluated for accuracy as well as effectiveness. These algorithms are also implemented in the above mentioned code. The actual implementation follows closely the description given here in pseudo code.

2 Kronrod-Patterson Extensions

2.1 Mathematical principles

The n nodes $\{\gamma_i\}_{i=1}^n$ of any Gauss quadrature rule for a given density distribution $\omega(t)$ can be found as the roots of a polynomial P_n of degree n. The existence of corresponding weights $\{\omega_i\}_{i=1}^n$ is the ensured by the following theorem from [18] originally stated by Kronrod in [16]:

Theorem 1. *For every probability density function $\omega(t)$ and every set $\{\gamma_i\}_{i=1}^n \subset \mathbb{R}$ of n nodes there exists a set of unique weights $\{\omega_i\}_{i=1}^n$ such that the quadrature Formula for integration with respect to $\omega(t)$ has a polynomial degree of exactness of at least $n-1$. These weights are the unique solution of the linear system of equations:*

$$\sum_{i=1}^{n} \omega_i \gamma_i^k = \int_\Omega t^k \omega(t) \mathrm{d}t \tag{1}$$

for $k = 0, \ldots, n-1$.

Next we need another theorem giving the conditions under which we can extend a given set of nodes by a bunch of new nodes.

Theorem 2. *Let $\omega(t)$ be the probability density function of a distribution supported on $\Omega \subseteq \mathbb{R}$ with finite moments. Let $P_n(t)$ be a univariate polynomial of* *degree n with n distinct real roots, and suppose that there exists a polynomial E_p of degree p satisfying:*

$$\int_\Omega P_n(t)E_p(t)t^i\omega(t)\mathrm{d}t = 0 \tag{2}$$

for all $i = 0, \ldots, p-1$. Assume further that the roots of E_p are all real and of multiplicity one, and distinct from those of P_n. Then there exists a quadrature formula supported on the roots of P_nE_p, whose degree of polynomial exactness is at least $n + 2p - 1$.

A simple proof of this theorem is given in the original article [18]. Some more theoretical background on Kronrod extensions of Gauss quadrature rules can be found in [6, 22] and in the survey article [23].

2.2 Algorithmic procedure

The main algorithm consists of three steps building upon each other.

- Given the polynomial $P_n(t)$ of degree n defining the rule with nodes $\{\gamma_i\}_{i=1}^n$ and weights $\{\omega_i\}_{i=1}^n$.
- Choose $p \geq 1$. Find a new polynomial $E_p(t)$ with $\deg E_p = p$ such that:

$$\int_\Omega P_n(t)\, E_p(t)\, t^i\, \omega(t)\, \mathrm{d}t = 0 \tag{3}$$

  for all $i = 0, \ldots, p-1$, see theorem 2. We require that E_p is monic and obtain a square linear system. If this system is solvable, then the extension E_p exists. Otherwise we can *not* extend the given n point rule by adding exactly p new nodes to a $n + p$ point rule.

- Compute the roots $\{\gamma'_i\}_{i=1}^p$ of E_p. If not all roots lie within the region Ω then this extension does not construct a valid quadrature rule.
- Compute the weights $\{\omega'_i\}_{i=1}^{n+p}$ for the new quadrature rule. It is important to note that the weights of the old unextended rule usually will change too. Hence it is not possible to compute only new weights $\{\omega'_i\}_{i=n+1}^p$ but we must recompute all $n + p$ weights at once. For the unified final set of nodes:

$$\{\gamma_i\}_{i=1}^{n+p} := \{\gamma_i\}_{i=1}^n \cup \{\gamma'_i\}_{i=1}^p \tag{4}$$

  we compute the weights by formula (1):

$$\sum_{i=1}^{n+p} \omega'_i t_i^k = \int_\Omega t^k \omega(t)\mathrm{d}t \tag{5}$$

  for all $k = 0, \ldots, n + p - 1$. This is again a linear system of equations. On the right hand side we have the moments of the distribution $\omega(t)$. It can happen that some of the weights are negative. This might affect the overall stability on the quadrature rule but is tolerated for now.

The steps for computing a single extension E_p of P_n are shown in pseudo-code in Algorithm 1. Another version computing iteratively multiple nested extensions is shown in 2.

2.3 Find extensions

The general degree p monic polynomial E_p with symbolic coefficients is written as:

$$E_p(t) := t^p + \sum_{k=0}^{p-1} a_k t^k \tag{6}$$

and we need to determine the set of coefficients $\{a_i\}_{i=0}^{p-1}$. The theorem 2 from above and the integral formulation (2) gives:

$$\begin{aligned} 0 &= \int_\Omega P_n(t) E_p(t) t^i \omega(t) \,\mathrm{d}t = \int_\Omega P_n(t) \left(\sum_{k=0}^{p-1} a_k t^k + t^p \right) t^i \omega(t) \,\mathrm{d}t \\ &= \sum_{k=0}^{p-1} a_k \int_\Omega P_n(t) t^k t^i \omega(t) \,\mathrm{d}t + \int_\Omega P_n(t) t^p t^i \omega(t) \,\mathrm{d}t \,. \end{aligned} \tag{7}$$

We find from the last line the following linear system $\mathbf{A}\underline{a} = \underline{r}$ for the unknown coefficients $\underline{a} := \{a_i\}_{i=0}^{p-1}$:

$$\begin{bmatrix} & \vdots & \\ \cdots & \int_\Omega P_n(t) t^k t^i \omega(t) \,\mathrm{d}t & \cdots \\ & \vdots & \end{bmatrix} \begin{bmatrix} a_0 \\ \vdots \\ a_k \\ \vdots \\ a_{p-1} \end{bmatrix} = \begin{bmatrix} \vdots \\ -\int_\Omega P_n(t) t^p t^i \omega(t) \,\mathrm{d}t \\ \vdots \end{bmatrix} , \tag{8}$$

where the first index $i = 0, \ldots, p-1$ runs along a column and the second index $k = 0, \ldots, p-1$ runs along any row of the $p \times p$ matrix. On the right hand side we have essentially a bunch of moments of the probability density distribution $\omega(t)$. Provided a closed form for the moment generating function exists, this vector can be computed very easily.

2.4 Rational moments

A limitation of our current implementation (see section 2.8) is that we can work only with distributions $\omega(t)$ that have rational moments. However, in case of the most important distributions used as weight functions (see Table 1) for defining the Legendre, Chebyshev, Laguerre and Hermite orthogonal polynomials this is a well known truth.

By explicit computation one can easily show that the following closed form expressions for the moments hold:

[1]The Wigner semicircle distribution up to normalization.

Distribution	$\omega(t)$	$t \in \Omega$	Polynomial $P_n(t)$
Uniform	1	$[-1,1]$	Legendre P_n
Chebyshev T	$\frac{1}{\sqrt{1-x^2}}$	$[-1,1]$	Chebyshev T_n
Chebyshev U[1]	$\sqrt{1-x^2}$	$[-1,1]$	Chebyshev U_n
Exponential	$\exp(-t)$	$[0,\infty]$	Laguerre L_n
Normal	$\exp(-t^2)$	$[-\infty,\infty]$	Hermite H_n
Normal	$\exp\left(-\frac{t^2}{2}\right)$	$[-\infty,\infty]$	Hermite H_n

Table 1: Domain and weight function of classical orthogonal polynomials.

$$\int_{-1}^{1} t^n \mathrm{d}t = \frac{1+(-1)^n}{n+1} = \begin{cases} \frac{2}{n+1} & n \quad \text{even} \\ 0 & n \quad \text{odd} \end{cases} \tag{9}$$

$$\int_{-1}^{1} t^n \frac{1}{\sqrt{1-t^2}} \mathrm{d}t = \begin{cases} \frac{2\sqrt{\pi}}{n} \frac{\Gamma\left(\frac{n+1}{2}\right)}{\Gamma\left(\frac{n}{2}\right)} & n \quad \text{even}^{2} \\ 0 & n \quad \text{odd} \end{cases} \tag{10}$$

$$\int_{-1}^{1} t^n \sqrt{1-t^2} \mathrm{d}t = \begin{cases} \frac{\sqrt{\pi}}{2} \frac{\Gamma\left(\frac{n+1}{2}\right)}{\Gamma\left(2+\frac{n}{2}\right)} & n \quad \text{even} \\ 0 & n \quad \text{odd} \end{cases} \tag{11}$$

$$\int_{0}^{\infty} t^n \exp(-t) \mathrm{d}t = \Gamma\left(n+1\right) \tag{12}$$

$$\int_{-\infty}^{\infty} t^n \exp\left(-\frac{t^2}{2}\right) \mathrm{d}t = \begin{cases} 2^{\frac{n}{2}} \sqrt{2}\, \Gamma\left(\frac{n+1}{2}\right) & n \quad \text{even} \\ 0 & n \quad \text{odd} \end{cases} \tag{13}$$

$$\int_{-\infty}^{\infty} t^n \exp(-t^2) \mathrm{d}t = \begin{cases} \Gamma\left(\frac{n+1}{2}\right) & n \quad \text{even} \\ 0 & n \quad \text{odd} \end{cases} \tag{14}$$

In the case of the Hermite polynomial we find that for even n:

$$\Gamma\left(\frac{n+1}{2}\right) = \frac{\sqrt{\pi}}{2^{\frac{n}{2}}} \prod_{i=1}^{\frac{n}{2}} (2i-1) \tag{15}$$

The constant transcendental factor $\sqrt{\pi}$ will luckily drop out in our final equations because it is contained in every entry of the matrix $\mathbf{A}$ as well as the right hand side $\underline{r}$. This is a trick that allows us to omit any constant irrational or transcendental factor.

2.5 Computing nodes

Computing the nodes amounts to find all roots of a possibly high degree polynomial. In classical numerics there are various stability issues related to this task and a general solution is often not possible. Using arbitrary precision ball arithmetic as defined by van der Hoeven in [30, 29] we can avoid almost all of these issues by just increasing the precision whenever necessary. By making use

[2] For $n = 0$ one takes the limes or replaces $n\Gamma\left(\frac{n}{2}\right)$ by $2\Gamma\left(\frac{n}{2}+1\right)$

Algorithm 1 Compute an extension E_p of degree p over P_n

```
procedure ComputeExtension($P_n(x)$, $p$)
    $\mathbf{A} :=$ BuildMatrix($P_n, p$)          ▷ Construct the linear system as in (8)
    $\underline{r} :=$ BuildRHS($P_n, p$)
    $\{a_i\}_{i=0}^{p-1} :=$ SolveLinear($\mathbf{A}, \underline{r}$)
    if $\exists i : a_i \neq 0$ then                ▷ Check if system is solvable
        $E_p = t^p + \sum_{i=0}^{p-1} a_i t^i$
    else
        $E_p \equiv 0$
    end if
return $E_p$
end procedure
```

Algorithm 2 Compute a tower of k extensions $P_n \subset E_{p_1} \subset E_{p_2} \subset \ldots \subset E_{p_k}$

```
procedure ComputeExtensionTower($P_n(x)$, $[p_1, \ldots, p_k]$)
    $P_0 := P_n$
    for $i = 1, \ldots, k$ do
        $E_i :=$ ComputeExtension($P_{i-1}, p_i$)
        $P_i := P_{i-1} \cdot E_i$
    end for
return $E := \prod_{i=1}^{k} E_i$
end procedure
```

of the rigorous error bounds inherent in any ball we can easily decide when we have to increase precision to obtain fully accurate results in the end.
The following routine is shown here just for the sake of completeness. Internally we pass on by calling a suitable function from the `arb` library introduced below. The function called uses the Durand-Kerner method according to the library documentation. An assumption required for the specific implementation of this root-finding method to work is that the polynomial is square-free which is necessary for all valid extensions anyway.

Algorithm 3 Compute the nodes up to a given precision b_γ

```
procedure ComputeNodes($P_n(x)$, $b_\gamma$)
    $\{\gamma_i\}_{i=1}^{n} :=$ FindAllRoots($P_n(x), b_\gamma$)
return $\{\gamma_i\}_{i=1}^{n}$
end procedure
```

2.6 Computing weights

Given a set of n nodes $\{\gamma_i\}_{i=1}^{n}$, $\gamma_i \in \mathbb{R}$ we want to find the corresponding weights $\underline{\omega} := \{\omega_i\}_{i=1}^{n}$, $\omega_i \in \mathbb{R}$. We start with the equation (1) shown above:

$$\sum_{i=1}^{n} \omega_i \gamma_i^k = \int_\Omega t^k \omega(t) \mathrm{d}t \quad k = 0, \ldots, n-1 \tag{16}$$

This yields the following inhomogeneous linear system $\mathbf{A}\underline{\omega} = \underline{r}$:

$$\begin{bmatrix} \gamma_1^0 & \dots & \gamma_i^0 & \dots & \gamma_n^0 \\ \vdots & & \vdots & & \vdots \\ \gamma_1^k & \dots & \gamma_i^k & \dots & \gamma_n^k \\ \vdots & & \vdots & & \vdots \\ \gamma_1^{n-1} & \dots & \gamma_i^{n-1} & \dots & \gamma_n^{n-1} \end{bmatrix} \begin{bmatrix} \omega_1 \\ \vdots \\ \omega_i \\ \vdots \\ \omega_n \end{bmatrix} = \begin{bmatrix} \int_\Omega t^0 \omega(t) \, \mathrm{d}t \\ \vdots \\ \int_\Omega t^k \omega(t) \, \mathrm{d}t \\ \vdots \\ \int_\Omega t^{n-1} \omega(t) \, \mathrm{d}t \end{bmatrix} \tag{17}$$

where $k = 0, \dots, n-1$ is the row index and $i = 1, \dots, n$ is the column index of the matrix $\mathbf{A}$. This system is square and of shape $n \times n$. Theorem 1 ensures that there is a unique solution. Given that the nodes are in general algebraic numbers, we compute approximations by complex balls. Even in case we knew the nodes in closed form, there is obviously no way to solve this system within the rationals and we would have to resort to the algebraic number field. Therefore we approximate the weights by complex balls in the same way. Computing the solution vector $\underline{\omega}$ to a target precision of b_ω bits is actually not straight forward, because we know the nodes with a precision of b_γ bits only which could be not precise enough to solve the system and retrieve b_ω bits for the weights.
The way out of this dilemma consists of an iterative ansatz. First we try to solve the system and then check the precision b'_ω of the weights. If $b'_\omega \geq b_\omega$, then the precision goal was met and we can stop. Otherwise, we double the required precision $b'_\gamma := 2b_\gamma$ and recompute the nodes first. After that we can retry to solve this system and see if the precision goal is met. If not yet, we let the algorithm iterate until the goal of b_ω bits is eventually fulfilled or an upper bound on the number of bits is hit. The procedure is shown in pseudo-code in listing 4.

Algorithm 4 Compute the weights up to a given precision b_ω

```
**procedure** ComputeWeights($P_n(x)$, $\omega(t)$, $b_\omega$)
    $b_\gamma := \frac{1}{2} b_\omega$
    **repeat**
        $b_\gamma := 2b_\gamma$
        $\{\gamma_i\}_{i=1}^n :=$ ComputeNodes($P_n(x), b_\gamma$)
        $\mathbf{A} :=$ BuildMatrix($\{\gamma_i\}_{i=1}^n$)
        $\underline{r} :=$ BuildRHS($\omega(t)$)
        $\{\omega_i\}_{i=1}^n :=$ SolveLinear($\mathbf{A}, \underline{r}$)
        $b'_\omega :=$ CheckAccuracy($\{\omega_i\}_{i=1}^n$)
    **until** $b'_\omega \geq b_\omega$
**return** $\{\omega_i\}_{i=1}^n$
**end procedure**
```

2.7 Validation of nodes and weights

Validation of the extensions computed is necessary and happens in two separate steps where the second one is optional. Even if we can solve equation (8) and Algorithm 1 does return a non-vanishing polynomial E_p, this does not guarantee we have found a suitable extension. As an example we look at possible extensions E_p of the Gauss-Laguerre rule given by the polynomial $L_2 = \frac{1}{2}t^2 - 2t + 1$, having two quadrature points $t = 2 \pm \sqrt{2}$. Searching for an extension E_3 of degree 3 we get the polynomial $E_3 = t^3 - 9t^2 + 9t - 33$. Computing the roots and therewith the quadrature nodes algebraically we get:

$$t = 3 - \frac{1}{2}\left(1 \pm \imath\sqrt{3}\right)\sqrt[3]{30 - 6\sqrt{19}} - \frac{1}{2}\left(1 \mp \imath\sqrt{3}\right)\sqrt[3]{30 + 6\sqrt{19}}$$
$$t = 3 + \sqrt[3]{30 - 6\sqrt{19}} + \sqrt[3]{30 + 6\sqrt{19}}\,.$$

Numerical computation with at least 20 digits of precision by ball arithmetic gives the following numbers (midpoint) and error bars (radius):

Midpoint	Radius
$8.39619697401 - 5.58635992795 \cdot 10^{-56}\imath$	$\pm(3.07 \cdot 10^{-55}, 3.07 \cdot 10^{-55}\imath)$
$0.301901512994 + 1.95938927647\imath$	$\pm(2.16 \cdot 10^{-58}, 2.16 \cdot 10^{-58}\imath)$
$0.301901512994 - 1.95938927647\imath$	$\pm(8.96 \cdot 10^{-63}, 8.96 \cdot 10^{-63}\imath)$

Obviously two of the nodes are complex-valued. The balls that contain the roots do not intersect with the real line, so this is not a valid extension. Looking for an extension of order 4 we find $E_4 = t^4 - \frac{272}{13}t^3 + \frac{1512}{13}t^2 - \frac{1824}{13}t + \frac{552}{13}$. Computing the roots of E_4 again up to at least 20 digits of precision gives:

Midpoint	Radius
$12.486507079 + 1.54779865518 \cdot 10^{-135}\imath$	$\pm(2.26 \cdot 10^{-61}, 2.26 \cdot 10^{-61}\imath)$
$6.92395654571 - 9.45876955945 \cdot 10^{-136}\imath$	$\pm(4.77 \cdot 10^{-61}, 4.77 \cdot 10^{-61}\imath)$
$1.04067484064 - 1.40662202686 \cdot 10^{-176}\imath$	$\pm(1.16 \cdot 10^{-61}, 1.16 \cdot 10^{-61}\imath)$
$0.471938457685 + 4.23901787652 \cdot 10^{-155}\imath$	$\pm(1.04 \cdot 10^{-61}, 1.04 \cdot 10^{-61}\imath)$

The imaginary parts are tiny and we may safely assume that the roots are indeed all real and positive. The balls do all intersect the real line but also extend into the complex plane. We can recompute these numbers with higher precision and obtain smaller radii up to a point where we are satisfied with the result. The extension E_4 has one drawback, namely there are negative weights for the resulting quadrature rule. Numerical computation of the weights (ordered by nodes) yields:

Midpoint	Radius
$2.72885335563 \cdot 10^{-5} + 1.81693615677 \cdot 10^{-140}\imath$	$\pm(4.59 \cdot 10^{-31}, 3.19 \cdot 10^{-61}\imath)$
$0.00425721115051 + 2.50073034862 \cdot 10^{-138}\imath$	$\pm(6.87 \cdot 10^{-30}, 4.77 \cdot 10^{-60}\imath)$
$0.0923319982492 - 9.18105623974 \cdot 10^{-138}\imath$	$\pm(6.32 \cdot 10^{-29}, 4.38 \cdot 10^{-59}\imath)$
$1.05270222681 + 8.51307944261 \cdot 10^{-137}\imath$	$\pm(4.4 \cdot 10^{-28}, 3.03 \cdot 10^{-58}\imath)$
$-3.25091510452 - 2.96660678416 \cdot 10^{-136}\imath$	$\pm(1.83 \cdot 10^{-27}, 1.24 \cdot 10^{-57}\imath)$
$3.10159637977 + 2.1819204052 \cdot 10^{-136}\imath$	$\pm(2.24 \cdot 10^{-27}, 1.53 \cdot 10^{-57}\imath)$

Turning our attention to the extension $E_5 = t^5 - \frac{1625}{47}t^4 + \frac{55000}{141}t^3 - \frac{76200}{47}t^2 + \frac{87000}{47}t - \frac{8840}{47}$ we will find that all its roots are on the positive real axis and all weights are strictly positive.
To validate an extension E_p of P_n we first check that the roots $\{\gamma_i\}_{i=1}^p$ of this polynomial E_p actually lie within the region Ω. The subset Ω of $\mathbb{R}$ is the region where the original polynomials P_n are orthogonal and where we want the quadrature to happen, see Table 1 for details. We require that:

$$\{\gamma_i\}_{i=1}^p \subset \Omega\,. \tag{18}$$

The second step in the validation of an extension concerns the weights. While we infer from (17) that the weights are all real, they can still be negative. Negative weights can affect the stability of a quadrature rule. For that reason one usually drops rules having negative weights. We filter out invalid extensions with the condition:

$$\omega_i > 0 \quad i = 1, \ldots, p + n \,. \tag{19}$$

These steps apply in the same way also to nested towers $P_n \subset E_{p_1} \subset E_{p_2} \subset \ldots \subset E_{p_k}$ of extensions. The nodes can be validated for each level k independently. In contrast, the weights need to be computed and examined in the end for all levels together.

2.8 Implementation aspects

The whole algorithm is implemented in `C` and relies heavily on the computational number theory library `flint` [11, 10]. This library provides among many other things highly efficient exact rational numbers with arbitrary large numerator and denominator integers. Therefore we have the complete arithmetics of the field $\mathbb{Q}$ available. It also implements the polynomial rings $\mathbb{Z}[x]$ and $\mathbb{Q}[x]$ and hence we can compute and express the polynomials defining the nodes of our nested extension tower. There are at least two reasons we require an efficient implementation of $\mathbb{Q}[x]$. First, we need to be able to do fast arithmetics with polynomials, specifically multiplication and checking whether a given polynomial is indeed square-free. Second, the coefficients grow exponentially large and we must use arbitrary precision rational numbers for expressing them. Other things we use from `flint` are matrices over $\mathbb{Z}$ and $\mathbb{Q}$. The matrices module provides us with means to solve linear systems by integral or rational arithmetic using a specially adapted fraction free version of Gauss elimination.
Given all that, we can check whether an extension E_p to any given rule P_n exists by using only exact rational arithmetic. The price we pay is that we can handle only distributions $\omega(t)$ that have rational moments.
Johansson implemented arbitrary-precision floating point ball arithmetic in a library called `arb` [13]. This library enables us to compute and refine the nodes to any number of bits precision while always obtaining rigorous error radii for each floating point ball computed. In detail, the library implements, among some more things, real and complex floating point balls, polynomials having ball-valued coefficients and matrices with balls as entries. Furthermore this library plays very well together with `flint` making it the ideal choice for our purpose. However it should not be neglected that all this comes at a higher cost in computation time compared to normal hardware-accelerated floating point arithmetic. The comparison has to be made against *software* based arbitrary precision floating point arithmetic as for example implemented in the GNU `MPFR` library [3]. In that case the ball arithmetic of `arb` is claimed to be usually much less than a factor of 2 slower than the plain `MPFR` floating point numbers. This is actually very good and a perfectly fair price to pay for the additional confidence put into the computed numbers. Even though `arb` is highly optimized, computing many roots to a high working precision can still take some time.

3 Direct Search for single Extensions

We consider now only single Kronrod extensions. Given a polynomial P_n of either Legendre, Chebyshev, Laguerre or Hermite type and of degree n, we compute the extension E_p of order p for some suitable choice of p. We make use of Algorithm 1 to obtain the polynomial E_p defining the extension in the first place. Next, we compute nodes and weights. If requested, validity checks are performed to ensure that the nodes are within the region of integration and that all the weights are positive.
Since the aim of this work is an exhaustive search for valid rules, we use this algorithm for a series of increasing n and test all p up to some upper bound. We obtain all extensions of some given Gauss type rule P_n up to extension order $p_{\max}$. To cover as much as possible the range of rules used in practice, we set $n_{\max} = 100$ and also $p_{\max} = 100$. In the extreme case there is now a polynomial of degree 200 defining a rule with the same number of node-weight pairs.

Algorithm 5 Exhaustive search up to $n_{\max}$ and $p_{\max}$

```
procedure ExhaustiveSearch($n_{\max}$, $p_{\max}$)
    $\mathbf{M} \in \{0,1\}^{n \times p}$                ▷ Bitmap for storing the found rules
    for $n = 1, \dots, n_{\max}$ do
        Get $P_n(t)$                ▷ Suitable orthogonal polynomial of order $n$
        for $p = n+1, \dots, p_{\max}$ do
            $E_p :=$ ComputeExtension($P_n, p$)
            if $E_p \not\equiv 0$ then
                $\mathbf{M}_{n,p} := 1$
            else
                $\mathbf{M}_{n,p} := 0$
            end if
        end for
    end for
end procedure
```

The output of this algorithm applied to the three polynomial classes mentioned above is shown in the Figures 1a, 1d and 1e.

3.1 Existence and non-existence results

From the rather sparse theory on this subject we know only of very few rigorous existence results for Kronrod-Patterson extensions.
In the Legendre case there is a proof that for each n there is always an extension with $p = n+1$ [28]. This is recovered by our computation and shows up in Figure 1a as the first upper diagonal line. Additionally to their existence, these rules also have positive weights in all cases as shown in [20]. The existence theorems can be generalized to hold also for Chebyshev, Gegenbauer and ultimatively Jacobi polynomials [4, 5, 24, 21].
For Laguerre polynomials there are no classical Kronrod extensions with $p = n+1$ at all. Higher order extensions are very sparse too, we could not find extensions for any $12 < n \leq 100$ while keeping $p \leq 150$. There is no strong reason to believe this would change if allowing for even higher p. Apart from that, such rules would probably be of no practical use anyway.

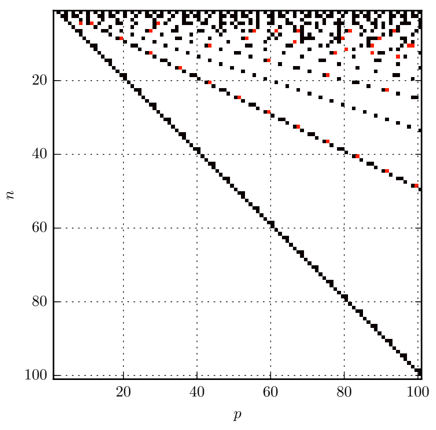

(a) Gauss-Legendre rules P_n.

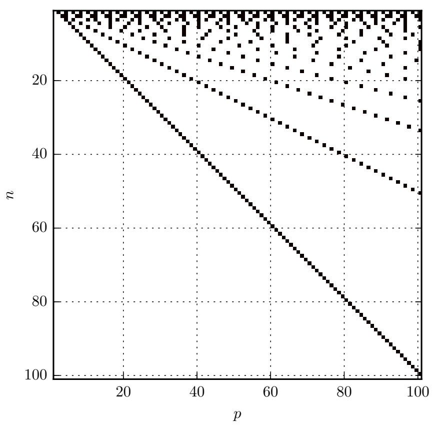

(b) Gauss-Chebyshev rules T_n.

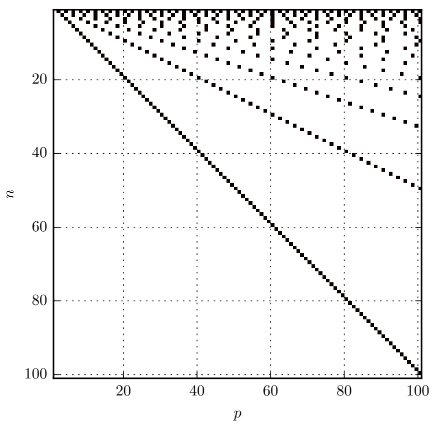

(c) Gauss-Chebyshev rules U_n.

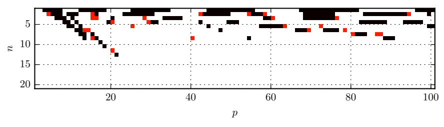

(d) Gauss-Laguerre rules L_n.

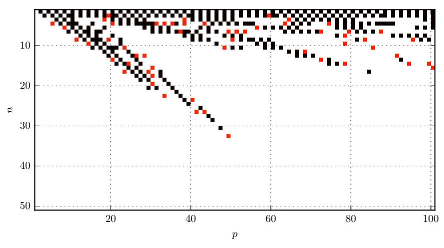

(e) Gauss-Hermite rules H_n.

Figure 1: Map of the extensions E_p of Gauss quadrature rules for $n \leq 100$ and p up to 100. The parts with $n \leq 100$ not shown do not contain any single valid extension. Red points represent rules with non-positive weights. Compare the Laguerre case also to Table 1 in [15].

In the case of Hermite polynomials our computation indeed reveals the three possible classical Kronrod rules for $n = 1, p = 2$ and $n = 2, p = 3$ and $n = 4, p = 5$. This can be seen in the very top left corner of Figure 1e and is in perfect agreement with the literature [19, 14, 31]. In fact if we examine the three rules more closely, we will find that the case $n = 4, p = 5$ does not have positive weights and is in turn ruled out by the authors of the aforementioned papers.

4 Recursive Enumeration of nested Extensions

In the last section we computed a single extensions E_p over a given rule P_n. This is enough in case of adaptive quadrature where all one wants is to make an error

estimate of the Gaussian quadrature by evaluation of another quadrature rule having higher order. In that case the property of nested nodes $\{\gamma_i\}_{i=1}^{n} \subset \{\gamma_i\}_{i=1}^{n+p}$ can reduce computation cost.
The construction of quadrature rules for higher dimensional integrals needs more than that. For the number of dimensions in the range from 4 up to some ten such quadrature rules can be done efficiently by the well known Smolyak construction.
Given an initial polynomial P_n of degree n, we want to find the set of all extension towers[3] $P_n \equiv E_{p_0} \subset E_{p_1} \subset \ldots \subset E_{p_k} \subset \ldots \subset E_{p_{k_{\max}}}$ over P_n having finite height $k_{\max}$. Additionally, we truncate this potentially infinite set by requiring that the degrees p_k of all polynomials E_{p_k} never exceed a fixed upper bound $p_{\max}$. This will in turn give a finite tree of nested extensions. In the end, we denote a single extension from this set by $\mathcal{K} = (n, p_1, \ldots, p_{k_{\max}}) \in \mathbb{N}^{k_{\max}+1}$.
Given the polynomial $P_{k-1}(x) := \prod_{i=0}^{k-1} E_{p_i}(x)$ that defines the lower part $E_{p_0} \subset \ldots \subset E_{p_{k-1}}$ of this tower, we can call Algorithm 6 with P_{k-1} to compute recursively the remaining upper layers $k, \ldots, k_{\max}$ as far as they exist. This algorithm will perform a flat exhaustive search on layer k and then call itself for the next layer $k+1$. To get this process started, we make an initial call for $k = 1$ with $P_0 := P_n \equiv E_{p_0}$ as shown in 7.
We denote by $\mathcal{Q}[p_0, \ldots, p_k]$ the quadrature rule and explicitly the nodes and weights that can be computed from the nested Kronrod extension $\mathcal{K} = (p_0, \ldots, p_k)$. Of course $\mathcal{Q}[n]$ is simple the original quadrature rule we started with. In all cases considered here this will be a Gauss rule of order n having n points.
If we run this algorithm for recursive enumeration, it finds a multitude of higher order nested Kronrod extensions. Depending on the kind of orthogonal polynomial we start with, there are large differences in the number and nesting degree of the extensions. For polynomials which are specializations of the Jacobi polynomials, we find the most regular structure which displays a vast number of extensions. For other polynomials like the Laguerre polynomials there are almost no extensions and the average nesting level is very low. From this large zoo of possible $\mathcal{K}$ tuples, some of the more interesting ones are summarized in the Tables 2, 3, 4, 5 and 6 in the appendix A.

[3]By abuse of notation, let E_{p_k} denote the polynomial of degree p_k as well as the abstract extension over $E_{p_{k-1}}$ defined by it.

Algorithm 6 Recursive search for extensions over P_{k-1} on layer k

```
procedure RecursiveSearch($P_{k-1}$, $p_{\max}$, $k$, $k_{\max}$)
                    ▷ Search for possible extensions of $P_{k-1}$ of order $p \le p_{\max}$
    for $p = 1, \ldots, p_{\max}$ do
        $E_p :=$ ComputeExtension($P_{k-1}, p$)
        if $E_p \not\equiv 0$ then
            valid := ValidateRoots($E_p$)
        else
            valid := false
        end if
        if valid = true then
                    ▷ Valid extension $E_p$ of order $p$ found for $P_{k-1}$ on layer $k$
            $p_k := p$
            $\mathcal{K} := (p_0, \ldots, p_{k-1}, p_k) \in \mathbb{N}^{k+1}$
            $\mathcal{R} := \mathcal{R} \cup \mathcal{K}$
            if $k < k_{\max}$ then
                    ▷ Follow the recursion down, descending to new layer $k+1$
                $P_k := P_{k-1}E_p$
                RecursiveSearch($P_k, p_{\max}, k+1, k_{\max}$)
            else
                    ▷ Maximum recursion depth reached, not descending
            end if
        else
                    ▷ No valid extension of order $p$ found for $P_{k-1}$ on layer $k$
        end if
    end for
                    ▷ Maximal extension order $p_{\max}$ reached, ascending
end procedure
```

Algorithm 7 Exhaustive recursive search up to $p_{\max}$ and $k_{\max}$

```
procedure ExhaustiveRecursiveSearch($P$, $p_{\max}$, $k_{\max}$)
    $\mathcal{R} := \{\}$                    ▷ Storage for all the rules $\mathcal{K}$ found
    $p_0 := \deg P$
    RecursiveSearch($P, p_{\max}, 1, k_{\max}$)
end procedure
```

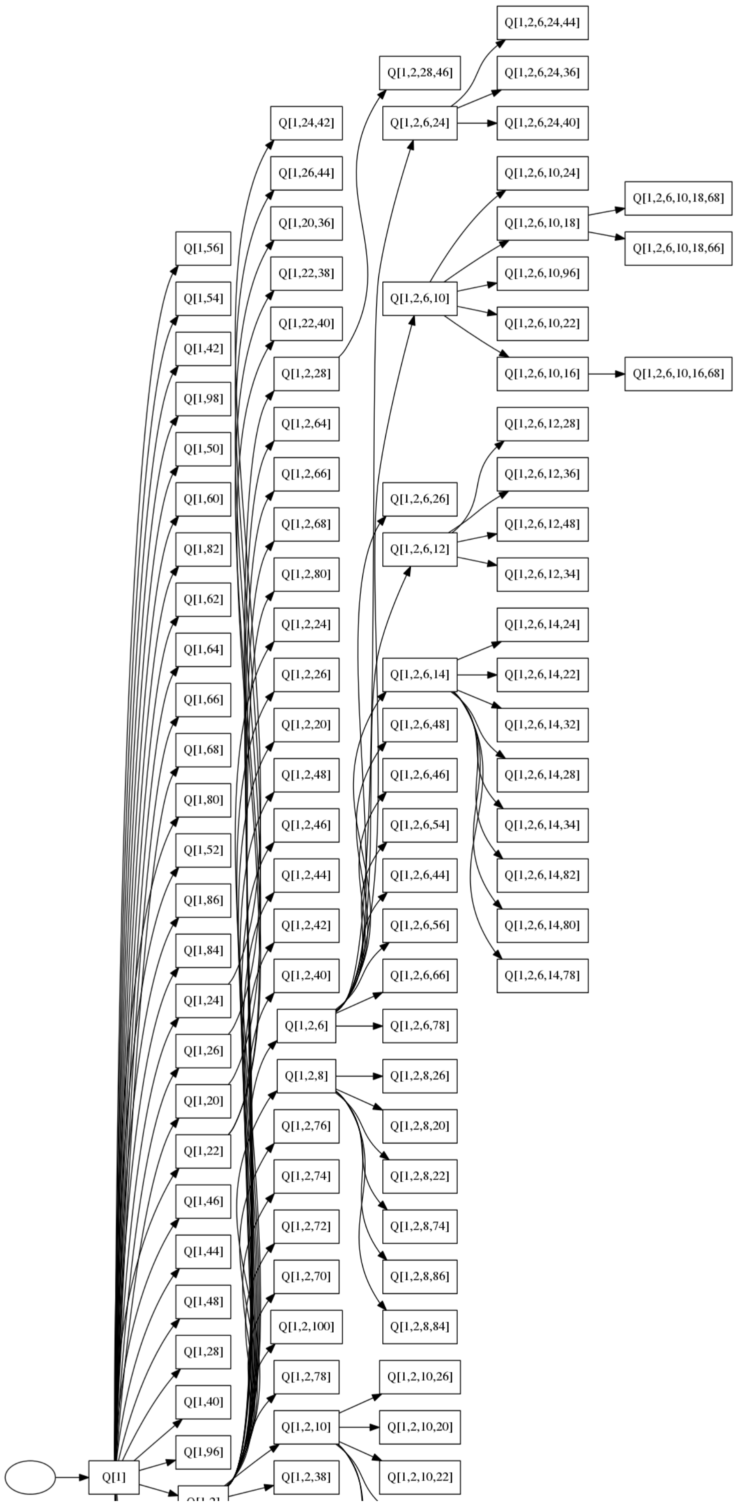

Figure 2: Part of the tree of nested higher order Kronrod Extensions of the single point Gauss-Hermite rule $\mathcal{Q}[1]$. The new and for us most important rules are in the top right corner.

5 Genz-Keister Multidimensional Construction

Genz and Keister found an explicit construction by which efficient special quadrature rules for an arbitrary number of dimensions can be built. The resulting rules are called *fully-symmetric* for reasons that will become clear later. In this section we review this construction of Genz and Keister as given in [7, 8]. We follow mostly their development but focus mainly on the computational aspects and less the theoretical derivation. Additionally we extend the construction to Gauss-Chebyshev quadrature (both kinds) and analyze the resulting rules.

5.1 The construction

The quadrature rule $Q^{D,K}$ of *level* $K \geq 0$ and for use in D dimensions is defined as:

$$\int_\Omega f(\underline{x}) \mathrm{d}x =: I[f] \approx Q^{D,K}[f] := \sum_{\mathbf{p}\in\mathcal{P}} f\left(\Gamma_{\mathbf{p}}\right) \omega_{\mathbf{p}} \tag{20}$$

where $\mathcal{P}$ is the set of all integer partitions as defined below. The node sets Γ and weights ω are indexed by partitions $\mathbf{p} \in \mathcal{P}$. Define the set $\mathcal{P}$ of all admissible integer partitions $\mathbf{p} := (\mathbf{p}_1, \ldots, \mathbf{p}_D) \in \mathbb{N}_0^D$ having D parts (some of which can be zero) and $|\mathbf{p}| \leq K$ with $K \geq 0$ as:

$$\mathcal{P} := \{\mathbf{p}\,| K \geq \mathbf{p}_1 \geq \cdots \geq \mathbf{p}_D \geq 0 \wedge |\mathbf{p}| \leq K\} \,. \tag{21}$$

A method for computing that set $\mathcal{P}$ is shown in Algorithm 14. Before we look deeper into the details of this construction, we need to introduce the set Λ of so called *generators*:

$$\Lambda := \{\lambda_0, \lambda_1, \ldots, \lambda_J\} \tag{22}$$

where we require that $\lambda_0 \equiv 0$ and all λ_i be pair-wise distinct. There are obviously $J+1$ real non-negative generators. A single quadrature point $\gamma \in \mathbb{R}^D$ is then an ordered multiset of size D of elements from Λ. Note that γ is not just a subset because elements are allowed to appear multiple times. The specific items are then selected by an integer vector $\mathbf{k} \in \mathbb{N}_0^D$, explicitly:

$$\gamma_{\mathbf{k}} := \Lambda_{\mathbf{k}} = (\lambda_{k_1}, \ldots, \lambda_{k_D}) \,. \tag{23}$$

We define δ as the number of components of $\gamma_{\mathbf{k}}$ that are 0. As we require that only λ_0 is zero, δ is equivalent to the number of zeros in $\mathbf{k}$. Next we define the set $\overline{\gamma_{\mathbf{k}}}$ containing all possible sign flips:

$$\overline{\gamma_{\mathbf{k}}} := \sigma\gamma_{\mathbf{k}} = \{(\sigma_1\gamma_1, \ldots, \sigma_D\lambda_D)\}_{\sigma\in\{-1,0,1\}^D} \tag{24}$$

where $\sigma_d \in \{-1, 1\}$ or $\sigma_d = 0$ if and only if $\gamma_d = 0$. The point $\gamma_{\mathbf{k}}$ gets mirrored into all 2^D orthants by σ. Clearly, this set $\overline{\gamma_{\mathbf{k}}}$ is of size $2^{D-\delta}$ for the reason that some points coincide with their own mirror images.
At this point we can go back and understand the notation of equation (20) where $\Gamma_{\mathbf{p}}$ stands for a whole set of nodes given by:

$$\Gamma_{\mathbf{p}} := \bigcup_{\mathbf{q}\in\mathcal{S}_{\mathbf{p}}} \overline{\gamma_{\mathbf{q}}} \tag{25}$$

and $\mathcal{S}_{\mathbf{p}}$ is the set of all permutations of the D elements of $\mathbf{p} \in \mathcal{P}$. An algorithm for the enumeration of all permutations is given in 15. Finally we find:

$$f\left(\Gamma_{\mathbf{p}}\right) := \sum_{\mathbf{q} \in \mathcal{S}_p} \sum_{\gamma \in \overline{\gamma_{\mathbf{q}}}} f\left(\gamma_1, \ldots, \gamma_D\right) . \tag{26}$$

What remains is the explanation of $\omega_{\mathbf{p}}$. The formula (2.4) given in [7] looks quite simple but the efficient implementation needs some care. For every admissible partition $\mathbf{p} \in \mathcal{P}$ the corresponding weight can be computed by:

$$\omega_{\mathbf{p}} := 2^{-(D-\delta)} \sum_{|\mathbf{k}| \leq K - |\mathbf{p}|} \prod_{d=1}^{D} \frac{a_{\mathbf{k}_d + \mathbf{p}_d}}{P(\mathbf{k}_d, \mathbf{p}_d)} \tag{27}$$

where we define the denominator:

$$P(\mathbf{k}_d, \mathbf{p}_d) := \prod_{\substack{i=0 \\ i \neq \mathbf{p}_d}}^{\mathbf{k}_d + \mathbf{p}_d} \left(\lambda_{\mathbf{p}_d}^2 - \lambda_i^2\right) \tag{28}$$

and use the multi-index $\mathbf{k} \in \mathbb{N}_0^D$. Note that the prefactor is exactly $1/|\overline{\gamma_{\mathbf{k}}}|$. Algorithm 16 implements a procedure for enumeration of all relevant multi-indices. This formula above presents us with several parts we need to compute. Some of these parts can even be tabulated once for a maximal and fixed J value and independent of the dimension D. Let us start with the numerator. There we need the value a_i which is defined by:

$$a_i := \int_{\Omega} p_i(x) w(x) \mathrm{d}x, \quad i = 0, \ldots, J+1 , \tag{29}$$

whereas the domain Ω and the weight function $w(x)$ are chosen appropriately (see below). The polynomials $p_i(x)$ are defined as:

$$\begin{aligned} p_0(x) &:= 1 \\ p_i(x) &:= \prod_{j=0}^{i-1} \left(x^2 - \lambda_j^2\right) \end{aligned} \tag{30}$$

where the empty product equals 1. It holds that $\deg p_i = 2i$. Since all the real numbers λ_j are known, we can indeed expand the product and write p_i as $\sum_{j=0}^{2i} c_j x^j$ for some coefficients c_j. This enables us to compute the integral in equation (29) term-wise by using linearity:

$$a_i = \sum_{j=0}^{2i} c_j \int_{\Omega} x^j w(x) \mathrm{d}x = \sum_{j=0}^{2i} c_j M_j \tag{31}$$

where M_j is the j-th moment and chosen according to Table (1) and the explicit formulae shown thereafter. For the Legendre, Chebyshev and Hermite case, the explicit formulae are (9), (10), (10) and (14). Optionally, we can replace very small values by zero. As we will see later, it is important to be able to decide whether $a_i = 0$. Because we compute with real numbers (either floating point

Algorithm 8 Compute table $\underline{A}$ of a_i factors

```
procedure ComputeAValues($\Lambda$, $\underline{M}$)
    $\underline{A} := \underline{0} \in \mathbb{R}^{J+1}$
    $p := 1$
    for $i = 0, \ldots, J+1$ do
        $a := 0$
        for $c_j$ in $\sum_{j=0}^{2i} c_j x^j = p$ do
            $a := a + c_j \underline{M}_j$
        end for
        $\underline{A}_i := a$
        $p := p\left(x^2 - \lambda_i^2\right)$
    end for
end procedure
```

numbers or real ball arithmetic) we can however never solve this problem exactly like in rational arithmetic.
Computing the denominator as defined in (28) is straight forward. Since we required the λ_i to be pairwise distinct this value never becomes zero and division poses no issue.
We notice that the product in formula (27) only depends on $\mathbf{p}_d =: \xi$ and the sum $\mathbf{p}_d + \mathbf{k}_d =: \eta$. Therefore we can precompute a table of size $J+1 \times J+1$ indexed by (ξ, η) whose entries are given by:

$$\mathbf{T}_{\xi,\eta} := \frac{a_{\mathbf{k}_d+\mathbf{p}_d}}{P(\mathbf{k}_d, \mathbf{p}_d)} \,. \tag{32}$$

In the example below, the top left corner of $\mathbf{T}$ is shown and we only ever need the upper right triangular part:

	$\eta = 0$	$\eta = 1$	$\eta = 2$	$\eta = 3$
$\xi = 0$	$\frac{a_0}{1}$	$\frac{a_1}{(\lambda_0^2-\lambda_1^2)}$	$\frac{a_2}{(\lambda_0^2-\lambda_1^2)(\lambda_0^2-\lambda_2^2)}$	$\frac{a_3}{(\lambda_0^2-\lambda_1^2)(\lambda_0^2-\lambda_2^2)(\lambda_0^2-\lambda_3^2)}$
$\xi = 1$	0	$\frac{a_1}{(\lambda_1^2-\lambda_0^2)}$	$\frac{a_2}{(\lambda_1^2-\lambda_0^2)(\lambda_1^2-\lambda_2^2)}$	$\frac{a_3}{(\lambda_1^2-\lambda_0^2)(\lambda_1^2-\lambda_2^2)(\lambda_1^2-\lambda_3^2)}$
$\xi = 2$	0	0	$\frac{a_2}{(\lambda_2^2-\lambda_0^2)(\lambda_2^2-\lambda_1^2)}$	$\frac{a_3}{(\lambda_2^2-\lambda_0^2)(\lambda_2^2-\lambda_1^2)(\lambda_2^2-\lambda_3^2)}$
$\xi = 3$	0	0	0	$\frac{a_3}{(\lambda_3^2-\lambda_0^2)(\lambda_3^2-\lambda_1^2)(\lambda_3^2-\lambda_2^2)}$

Given the list Λ of generators and all the values a_i collected into the list $\underline{A}$, we can compute the table $\mathbf{T}$ efficiently by Algorithm 9. By the use of this table, the implementation of formula (27) transforms into a series of trivial table look-up steps. However, precomputation of $\mathbf{T}$ is expensive for larger J, on the other hand it needs to be done only once for each Λ and $w(x)$. The numerator and denominator of the entries in $\mathbf{T}$ can become really large numbers (remember that most moments include gamma functions), while their quotient stays within reasonable range for floating point representation. For this reason one can compute $\mathbf{T}$ to high precision with specialized software packages like `flint` [11, 10] and afterwards use these tabulated values during usual floating point computations.
At the end of the day we arrive at the following two Algorithms 10 and 11 for computing the node set $\Gamma_{\mathbf{p}}$ and weights $\omega_{\mathbf{p}}$ for an arbitrary given partition $\mathbf{p} \in \mathcal{P}$.

Algorithm 9 Compute table $\mathbf{T}_{\xi,\eta}$ of weight factors

```
procedure WeightFactors($\Lambda$, $\underline{A}$)
    $n := |\Lambda|$
    $\mathbf{T} \in \mathbb{R}^{n \times n}$                                    ▷ Compute $T$ row by row
    for $\xi = 0, \dots, n-1$ do
        $t := 1$
        for $\eta = 0, \dots, n-1$ do
            if $\xi \neq \eta$ then
                $t := t\left(\lambda_\xi^2 - \lambda_\eta^2\right)$
            end if
            if $\eta \geq \xi$ then
                $\mathbf{T}_{\xi,\eta} := \frac{a_\eta}{t}$
            end if
        end for
    end for
end procedure
```

Algorithm 10 Compute nodes $\Gamma_\mathbf{p}$ for given $\mathbf{p} \in \mathcal{P} \subset \mathbb{N}_0^D$

```
procedure Nodes($\mathbf{p}$, $\Lambda$)
    $\Gamma_\mathbf{p} := \{\}$
    $\delta :=$ NumberOfZeros($\mathbf{p}$)
    $\mathcal{S} :=$ Permutations($D, \mathbf{p}$)
    for $\mathbf{q} \in \mathcal{S}$ do
        for $v = 0, \dots, 2^{(D-\delta)} - 1$ do
            $u := 0$
            for $d = 0, \dots, D-1$ do
                $\gamma_d := \Lambda_{\mathbf{q}_d}$
                if $\mathbf{q}_d \neq 0$ then                             ▷ Compute sign flip
                    if $\lfloor \frac{v}{2^u} \rfloor \mod 2 = 1$ then
                        $\gamma_d := -\gamma_d$
                    end if
                    $u := u + 1$
                end if
            end for
            $\Gamma_\mathbf{p} := \Gamma_\mathbf{p} \cup \gamma$
        end for
    end for
end procedure
```

The last ingredient we need is the integer sequence $\underline{z} = (z_0, \dots, z_J)$ defined as:

$$\begin{aligned} z_0 &= 0 \\ z_i &= l \quad \Leftrightarrow \quad a_{i+k} = 0 \quad \forall\, k = 0, \dots, l-1\,. \end{aligned} \tag{33}$$

The reasoning behind this sequence and the specific definition summarizes to the fact that we like to get many summands with $\omega_\mathbf{p} = 0$ in equation (20). Looking at the definition of the weights in equation (27) we have a sum-product structure. A single product becomes zero if the numerator $a_{\mathbf{k}_d + \mathbf{p}_d} = 0$. This then must

Algorithm 11 Compute weight $\omega_{\mathbf{p}}$ for given $\mathbf{p} \in \mathcal{P} \subset \mathbb{N}_0^D$

```
procedure WEIGHTS($\mathbf{p}$, $K$, $\mathbf{T}$)
    $\delta :=$ NUMBEROFZEROS($\mathbf{p}$)
    $\omega_{\mathbf{p}} := 0$
    $\mathcal{L} :=$ ENUMERATELATTICEPOINTS($D, K - |\mathbf{p}|$)
    for $\mathbf{k} \in \mathcal{L}$ do
        $w := 1$
        for $d = 0, \ldots, D-1$ do
            $w := w\, \mathbf{T}_{\mathbf{p}_d, \mathbf{k}_d + \mathbf{p}_d}$
        end for
        $\omega_{\mathbf{p}} := \omega_{\mathbf{p}} + w$
    end for
    $\omega_{\mathbf{p}} := 2^{-(D-\delta)} \omega_{\mathbf{p}}$
end procedure
```

happen for all summands in the sum. A simple algorithm to find $\underline{z}$ is given in 12 below. It is limited in rigor because of the zero test on floating point numbers.

Algorithm 12 Compute the $\underline{z}$ sequence

```
procedure COMPUEZSEQUENCE($\underline{A}$)
    $\underline{z} := \underline{0} \in \mathbb{R}^{J+1}$
    $v := 0$
    for $i = 0, \ldots, J$ do
        if $v = 0$ then
            while $\underline{A}_{i+v} = 0$ do
                $v := v + 1$
            end while
        else
            $v := v - 1$
        end if
        $\underline{z}_i := v$
    end for
end procedure
```

Finally, we cite theorem 3.1 from [7] but omit the proof:

Theorem. *A fully symmetric rule using a generator set* Λ *has weights* $\omega_{\mathbf{p}} = 0$ *if* $|\mathbf{p}| + |\underline{z}(\mathbf{p})| > K$.

This theorem tells us which partitions $\mathbf{p}$ we can omit when assembling the quadrature rule. The full algorithm for the construction of fully symmetric quadrature rules in D dimensions and of level K is shown in 13. The whole procedure is general in the sense that we can apply it to both the Legendre and Hermite cases as it was already done in [7] and [8] respectively. Further we can repeat the very same computations for both kinds of Gauss-Chebyshev quadrature which is new. As we have seen in the last section, there exists a plethora of nested higher order Kronrod extensions for some orthogonal polynomials. Each of these can serve as the basis $\mathcal{K}$ for the generator set Λ. Genz and Keister used in the Hermite case the Kronrod extensions $\mathcal{K} = (1, 2, 6, 10, 16)$ and $\mathcal{K} = (1, 2, 8, 20)$.

One should note that not all rules are equally well suited. A criterion on the expected *sparsity* of the final rule is the number of zero elements in the $\underline{z}$ sequence. The more non-zero elements the better, but unfortunately such sequences are rare. Additionally there appears the question of stability which was discussed in [7]. Novak and Ritter show in [25], section 6, that the Genz-Keister construction produces quadrature rules which are of classical Smolyak form. This is convenient for two reasons. First, we can construct D dimensional rules either by direct full Genz-Keister construction or by Smolyak construction applied to the set of one-dimensional Genz-Keister rules. Second, the convergence and error analysis from Smolyak theory is also valid for this construction.

Algorithm 13 Genz-Keister construction

```
procedure GenzKeisterConstruction($D, K$)
    $\Gamma := \{\}$                                   ▷ Nodes and weights as ordered sets
    $\Omega := \{\}$
                                                       ▷ Precompute fundamental tables
    $\Lambda :=$ ComputeGenerators($\mathcal{K}$)
    $\underline{M} :=$ ComputeMoments()
    $\underline{A} :=$ ComputeAValues($\Lambda, \underline{M}$)
    $\mathbf{T} :=$ WeightFactors($\Lambda, \underline{A}$)
                                                       ▷ Construct multi-dimensional rule
    $\mathcal{P} :=$ EnumeratePartitions($D, K$)
    for $\mathbf{p} \in \mathcal{P}$ do
        if $|\mathbf{p}| + |\underline{z}(\mathbf{p})| \leq K$ then
            $\Gamma_{\mathbf{p}} :=$ Nodes($\mathbf{p}, \Lambda$)
            $\omega_{\mathbf{p}} :=$ Weights($\mathbf{p}, K, \mathbf{T}$)
            $\Gamma := \Gamma \cup \Gamma_{\mathbf{p}}$
            $\Omega := \Omega \cup \omega_{\mathbf{p}}$                 ▷ Add $|\Gamma_{\mathbf{p}}|$ times the weight $\omega_{\mathbf{p}}$
        end if
    end for
end procedure
```

5.1.1 Combinatorial Algorithms

In this section we summarize the combinatorial algorithms that can be used during the Genz-Keister construction. In the programming language `python` they can be implemented very efficiently by the use of `yield` statements inside so called *generator expressions.*
The Algorithm 14 can be used for enumeration of the set $\mathcal{P}$ defined in (21). This works for any given value of $D \geq 1$ and maximal element size $K \geq 0$. The elements $\mathbf{p} \in \mathcal{P}$ will be generated by increasing value of $|\mathbf{p}|$ until the boundary K is hit.
An algorithm to enumerate the set $\mathcal{S}$ of all entry-wise permutations of a given vector $\mathbf{p} \in \mathbb{N}_0^D$ is shown next in 15. This algorithm will generate the permutations in reverse lexicographic order, starting with $\mathbf{p}$.
In the definition of the weights in formula (27) we need to iterate over the set $\mathcal{L} := \{\mathbf{k_i}\}$ of all lattice points $\mathbf{k} \in \mathbb{N}_0^D$ up to some maximal value of the l_1 norm. The Algorithm 16 shows an efficient method for the enumeration of all such

Algorithm 14 Enumerate the set $\mathcal{P}$ of all integer partitions

```
procedure EnumeratePartitions($D$, $K$)
    $\mathcal{P} := \{\}$
    $\mathbf{p} := \underline{0} \in \mathbb{N}_0^D$
    while $|\mathbf{p}| \leq K$ do
        $\tau :=$ false
        $p := \mathbf{p}_0$
        for i = 1, ... D-1 do
            $p := p + \mathbf{p}_i$
            if $\mathbf{p}_0 \leq \mathbf{p}_i + 1$ then
                $\mathbf{p}_i := 0$
            else
                $\mathbf{p}_0 := p - i(\mathbf{p}_i + 1)$
                for j = 1, ..., i do
                    $\mathbf{p}_j := \mathbf{p}_i + 1$
                end for
                $\mathcal{P} := \mathcal{P} \cup \mathbf{p}$
                $\tau :=$ true
                break
            end if
        end for
        if $\tau =$ false then
            $\mathbf{p}_0 := p + 1$
            if $|\mathbf{p}| \leq K$ then
                $\mathcal{P} := \mathcal{P} \cup \mathbf{p}$
            end if
        end if
    end while
end procedure
```

points. It is well known that the cardinality of $\mathcal{L}$ is:

$$|\mathcal{L}| = \left(\frac{K+1}{D}\right) \binom{D+K}{K+1}. \tag{34}$$

For more details see for example [27].

Algorithm 15 Enumerate the set $\mathcal{S}$ of all permutations of the entries of $\mathbf{p} \in \mathbb{N}_0^D$

```
procedure PERMUTATIONS($D$, $\mathbf{p}$)
    $\mathcal{S} := \{\mathbf{p}\}$
    $\tau :=$ true
    while $\tau =$ true do
        $\tau :=$ false
        for $i = 1, \ldots, D-1$ do
            $p := \mathbf{p}_i$
            if $\mathbf{p}_{i-1} > p$ then
                $I := i$
                if $i > 1$ then
                    $J := I$
                    for $j = 0, \ldots, \lfloor \frac{I}{2} \rfloor - 1$ do
                        $q := \mathbf{p}_j$
                        if $q \leq p$ then
                            $I := I - 1$
                        end if
                        $\mathbf{p}_j := \mathbf{p}_{i-j-1}$
                        $\mathbf{p}_{i-j-1} := q$
                        if $\mathbf{p}_j > p$ then
                            $J := j + 1$
                        end if
                    end for
                    if $\mathbf{p}_{I-1} \leq p$ then
                        $I := J$
                    end if
                end if
                $\mathbf{p}_i := \mathbf{p}_{I-1}$
                $\mathbf{p}_{I-1} := p$
                $\mathcal{S} := \mathcal{S} \cup \mathbf{p}$
                $\tau :=$ true
                break
            end if
        end for
    end while
end procedure
```

Algorithm 16 Enumerate lattice points in $\{\mathbf{k_i}\} =: \mathcal{L} \subset \mathbb{N}_0^D$ with $\|\mathbf{k_i}\|_1 \leq N$

```
procedure EnumerateLatticePoints($D$, $N$)
    $\mathcal{L} := \{\}$
    for $n = 0, \ldots, N$ do
        $\mathbf{k} := \underline{0} \in \mathbb{N}_0^D$
        $\mathbf{k}_0 := n$
        $\mathcal{L} := \mathcal{L} \cup \mathbf{k}$
        $c := 1$
        while $\mathbf{k}_{D-1} < n$ do
            if $c = D$ then
                for $i = c - 1, \ldots, 1$ do
                    $c := i$
                    if $\mathbf{k}_{i-1} \neq 0$ then
                        break
                    end if
                end for
                $\mathbf{k}_{c-1} := \mathbf{k}_{c-1} - 1$
                $c := c + 1$
                $\mathbf{k}_{c-1} := n$
                for $i = 0, \ldots, c - 2$ do
                    $\mathbf{k}_{c-1} := \mathbf{k}_{c-1} - \mathbf{k}_i$
                end for
                if $c < D$ then
                    for $i = c, \ldots, D - 1$ do
                        $\mathbf{k}_i := 0$
                    end for
                end if
                $\mathcal{L} := \mathcal{L} \cup \mathbf{k}$
            end if
        end while
    end for
end procedure
```

6 Nested Rules for Orthogonal Polynomials

In this section we present various results for the classical orthogonal polynomials and related Gauss quadrature schemes. For each scheme we could find at least one replacement having nested nodes based on the Genz-Keister construction. The generator set Λ is in each case obtained by recursive higher order Kronrod extensions $\mathcal{K} := (k_1, \ldots, k_p)$. For each extension level k_i we then get a subset of nodes $\{\lambda_{i_1}, \ldots, \lambda_{i_q}\}$ from the corresponding polynomial E_{k_i}. The final rule now depends on the ordering of these generators and different orderings can lead to a non-negligible difference in overall stability. Permutation of the nodes λ_{i_j} within each subset does not change the number of function evaluations required. The original authors came up with the following heuristic for sorting the generators: begin each subset with its largest generator and then alternate the remaining generators always using extremal values. They claim that this procedure yields rules with a good (but not necessarily optimal) stability factor. In our notation this factor reads:

$$C := \sum_{\mathbf{p} \in \mathcal{P}} N_{\mathbf{p}} |\omega_{\mathbf{p}}|$$

where for any partition $\mathbf{p}$ with n distinct parts $\mathbf{p}_j$ each having multiplicity m_j the value $N_{\mathbf{p}}$ is given by:

$$N_{\mathbf{p}} = \frac{2^{|m|} D!}{(D - |m|)! \, m_1! \cdots m_n!} \, .$$

In principle one could test all permutations of the generators and search for one minimizing this stability constant. We will choose this alternating ordering as default. The order of a quadrature rule Q^K is given by theorem 2.1 in [7] and shown to be:

$$2K + 1 \, . \tag{35}$$

The K in this formula is, for each fixed quadrature rule, the maximal value of K for which the Genz-Keister construction results in the given rule. For example in the Hermite case $K = 9, \ldots, 14$ all yield the same node-weight pairs. The order os this rule is then $2 \cdot 14 + 1 = 29$.
Lemma 4.1 in [12] gives conditions on the one-dimensional rules such that the Smolyak construction of level K from these rules has order at least $2K - 1$. It can be seen from Figures 11, 13, 15 and 17 that the rules discussed here fulfill the required conditions as their orders are always large enough.

6.1 Legendre Quadrature

For the Legendre polynomials P_n we can find various Kronrod extensions. The most suitable one seems to be $\mathcal{K} = (1, 2, 4, 8, 16, 32)$. The Genz-Keister construction built upon this set of generators has the following $\underline{z}$ sequence:

$$\underline{z} = (0, 0, 1, 0, 2, 1, 0, 0, 4, 3, 2, 1, 0, 0, 0, 0, 11, 10, 9, 8, 7, 6, 5, 4, 3, 2, 1, 0, 5, 4, 3, 2, 1)$$

where a large number of non-zero elements occur. Also we can in principle arbitrarily extend $\mathcal{K}$ by doubling the degree. If we use this extension we get the one-dimensional quadrature nodes with a constellation as in Figure 3 and weights shown in Figure 7. For most values of the level K the weights behave

well but for some they start oscillating and even become negative. These special values of K correlate with extra zeros in the $\underline{z}$ sequence. The number of nodes relative to Gauss-Legendre Quadrature is shown in Figure 11 for one dimension and compared across dimensions in Figure 12. Figure 19 shows the sparse node distribution in the plane for two-dimensional quadrature rules.
Notice that for $D < 3$, using the Genz-Keister construction results in more quadrature points than the full tensor product Ansatz. This fact is examined in Figures 23a and 23b. The other Figure 23c displays the same comparison, this time with respect to the Smolyak construction.
For testing the quadrature rules in D dimensions, the following integral over multi-variate monomials with $\underline{n} \in \mathbb{N}_0^D$ is used:

$$\int_{\underline{x} \in [-1,1]^D} \cdots \int \prod_{d=1}^{D} x_d^{n_d} \mathrm{d}\underline{x} = \prod_{d=1}^{D} \frac{1 + (-1)^{n_d}}{1 + n_d} \tag{36}$$

where we know the exact solution in closed form. The results are shown in Figure 27 for $D = 1$ and for $2 \leq D \leq 6$ in Figures 28 and 29. Finally, the Figure 40 shows the minimal level K necessary to correctly integrate the term $x^m y^n$.

6.2 Chebyshev Quadrature of the first kind

As in the case of Legendre polynomials, both Chebyshev polynomials T_n and U_n possess many different Kronrod extensions. For the first kind T_n we choose $\mathcal{K} = (1, 2, 4, 6, 12, 24)$ with the $\underline{z}$ sequence:

$$\underline{z} = (0, 0, 1, 0, 2, 1, 0, 5, 4, 3, 2, 1, 0, 11, 10, 9, 8, 7, 6, 5, 4, 3, 2, 1, 0, 1) \,.$$

Again we can in principle extend $\mathcal{K}$ by doubling the degree. Using this extension we get the one-dimensional quadrature nodes with a constellation as in Figure 4 and weights shown in Figure 8. The number of nodes relative to Gauss-Chebyshev Quadrature is shown in Figure 13 for one dimension and compared across dimensions in Figure 14.
Figure 20 shows the sparse node distribution in the plane for two-dimensional quadrature rules. Notice that for $D < 3$, using the Genz-Keister construction results in more quadrature points than the full tensor product Ansatz, however there are some exceptions. This fact is examined in Figures 24a and 24b. The other Figure 24c displays the same comparison, this time with respect to the Smolyak construction.
For testing the quadrature rules in D dimensions, the following integral over multi-variate monomials with $\underline{n} \in \mathbb{N}_0^D$ is used:

$$\int_{\underline{x} \in [-1,1]^D} \cdots \int \prod_{d=1}^{D} x_d^{n_d} \frac{1}{\sqrt{1 - x_d^2}} \mathrm{d}\underline{x} = \left(\frac{\sqrt{\pi}}{2}\right)^D \prod_{d=1}^{D} \left(1 + (-1)^{n_d}\right) \frac{\Gamma\left(\frac{n_d}{2} + \frac{1}{2}\right)}{\Gamma\left(\frac{n_d}{2} + 1\right)} \tag{37}$$

where we know the exact solution in closed form. The results are shown in Figure 30 for $D = 1$ and for $2 \leq D \leq 6$ in Figures 31 and 32. The last Figure 41 shows the minimal level K necessary to correctly integrate the term $x^m y^n$.

6.3 Chebyshev Quadrature of the second kind

For the second kind U_n of Chebyshev polynomials we use $\mathcal{K} = (1, 2, 4, 8, 16, 32)$ with the $\underline{z}$ sequence:

$$\underline{z} = (0, 0, 1, 0, 3, 2, 1, 0, 7, 6, 5, 4, 3, 2, 1, 0, 15, 14, 13, 12, 11, 10, 9, 8, 7, 6, 5, 4, 3, 2, 1, 0, 1)\,.$$

Once more we could extend $\mathcal{K}$ by doubling the degree. Using this extension we get the one-dimensional quadrature nodes with a constellation as in Figure 5 and weights shown in Figure 9. The number of nodes relative to Gauss-Chebyshev Quadrature is shown in Figure 15 for one dimension and compared across dimensions in Figure 16. Figure 21 shows the sparse node distribution in the plane for two-dimensional quadrature rules.
For $D = 2$ there are levels where Genz-Keister is better than Gauss-Chebyshev tensor products but there are also levels where it behaves the other way round. The details are shown in Figures 25a and 25b. The third Figure 25c shows the same comparison with respect to the Smolyak construction. Notice that although some of the Gauss rules are already nested, this has (as expected) almost no effect when applying the Smolyak construction. The only difference between this figure and its siblings is the point $D = 4$ and $K = 8$ which here is white instead of black. Also the boundary will reach $D = 5$ a few levels later. However there is obviously still room for improvement.
For testing the quadrature rules in D dimensions, the following integral over multi-variate monomials with $\underline{n} \in \mathbb{N}_0^D$ is used:

$$\int_{\underline{x}\in[-1,1]^D} \cdots \int \prod_{d=1}^{D} x_d^{n_d} \sqrt{1 - x_d^2}\,\mathrm{d}\underline{x} = \left(\frac{\sqrt{\pi}}{4}\right)^D \prod_{d=1}^{D} (1 + (-1)^{n_d}) \frac{\Gamma\left(\frac{n_d}{2} + \frac{1}{2}\right)}{\Gamma\left(\frac{n_d}{2} + 2\right)} \tag{38}$$

where we know the exact solution in closed form. The results are shown in Figure 33 for $D = 1$ and for $2 \leq D \leq 6$ in Figures 34 and 35. Figure 42 shows the minimal level K necessary to correctly integrate the term $x^m y^n$.

6.4 Hermite Quadrature

Figure 26c shows the comparison of a full tensor and a Smolyak construction based on the usual Gauss-Hermite points. Obviously the region where Smolyak is disadvantageous extends to higher dimensions and this at even relatively low levels. This is clearly an issue and should give some motivation for studying the Genz-Keister constructions. For Hermite polynomials H_n Kronrod extensions are rare, especially extensions having a high nesting degree. One of the best such extensions found so far is $\mathcal{K} = (1, 2, 6, 10, 16, 68)$ with the z sequence:

$$\underline{z} = (0, 0, 1, 0, 0, 3, 2, 1, 0, 0, 5, 4, 3, 2, 1, 0, 0, 0, 8, 7, 6, 5, 4, 3, 2, 1, 0, 0, 0, 0, 0, 0, \ldots)$$

Using this extension we get the one-dimensional quadrature nodes with a constellation as in Figure 6 and weights shown in Figure 10. The number of nodes relative to Gauss-Hermite Quadrature is shown in Figure 17 for one dimension and compared across dimensions in Figure 18. Figure 22 shows the sparse node distribution in the plane for two-dimensional quadrature rules.
By comparing to Figure 36 we can confirm that the rules with $K < 18$ are stable. The rule obtained with $K = 17$ has 35 nodes and is of order 51. In the range

$18 < K \leq 25$ we get no new rules but rather the same nodes and weights as with $K = 17$. Rules with even higher $K > 25$ were found to be highly unstable.
Notice that for $D < 3$, using the Genz-Keister construction results in more quadrature points than the full tensor product Ansatz. This can be read off from Figures 26a and 26b. The last Figure 26c displays the same comparison, this time with respect to the Smolyak construction.
For testing the quadrature rules in D dimensions, the following integral over multi-variate monomials with $\underline{n} \in \mathbb{N}_0^D$ is used:

$$\underset{\underline{x}\in\mathbb{R}^D}{\int \cdots \int} \prod_{d=1}^{D} x_d^{n_d} \exp\left(-x_d^2\right) \mathrm{d}\underline{x} = \frac{1}{2^D} \prod_{d=1}^{D} \left(1 + (-1)^{n_d}\right) \Gamma\left(\frac{n_d + 1}{2}\right) \tag{39}$$

where we know the exact solution in closed form. The results are shown for $2 \leq D \leq 6$ in Figures 38 and 39. The Figure 43 shows the minimal level K necessary to correctly integrate the term $x^m y^n$.

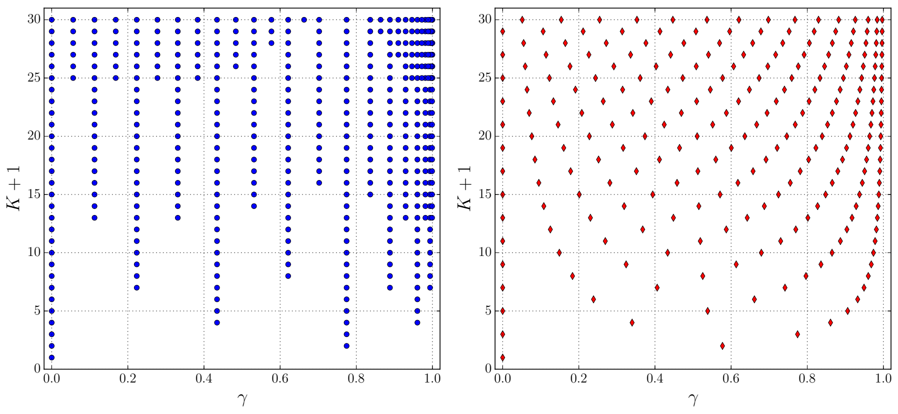

Figure 3: Comparison of Gauss-Legendre nodes (right) and nested Genz-Keister nodes (left) based on the $\mathcal{K} = (1, 2, 4, 8, 16, 32)$ Kronrod extension. The points are nicely nested and well suited for sparse grids.

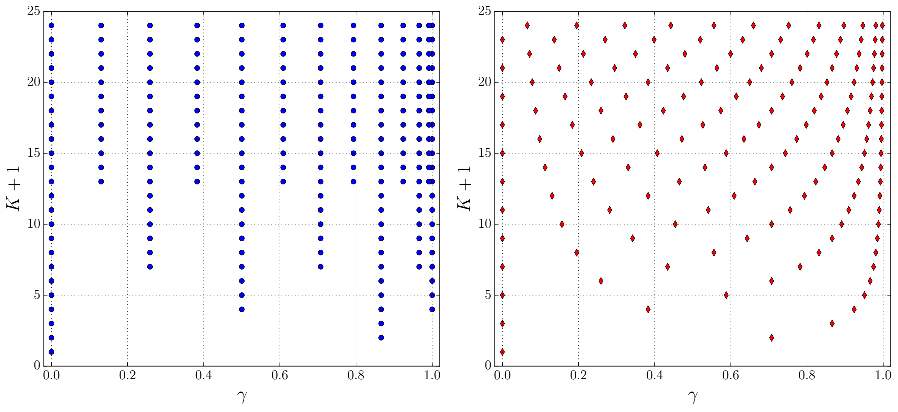

Figure 4: Comparison of Gauss-Chebyshev-T nodes (right) and nested Genz-Keister nodes (left) based on the $\mathcal{K} = (1, 2, 4, 6, 12, 24)$ Kronrod extension. The points are nicely nested and well suited for sparse grids.

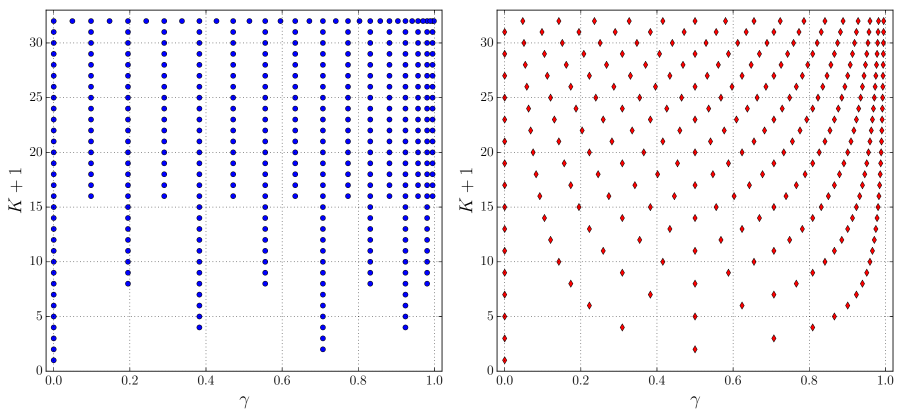

Figure 5: Comparison of Gauss-Chebyshev-U nodes (right) and nested Genz-Keister nodes (left) based on the $\mathcal{K} = (1, 2, 4, 8, 16, 32)$ Kronrod extension. The points are nicely nested and well suited for sparse grids.

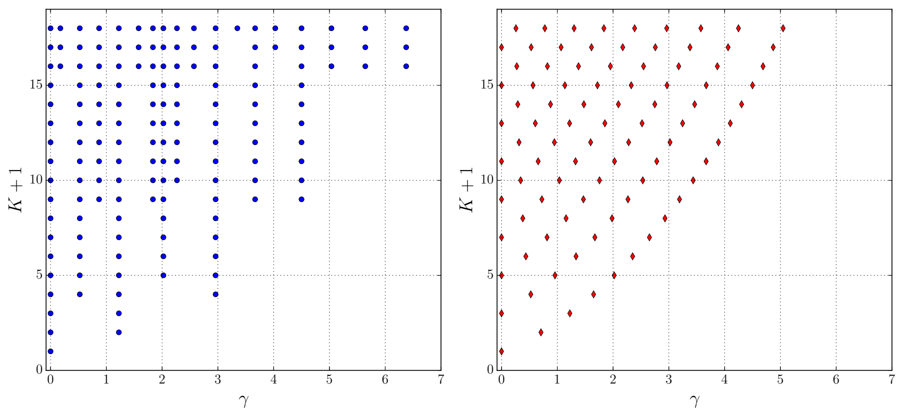

Figure 6: Comparison of Gauss-Hermite nodes (right) and nested Genz-Keister nodes (left) based on the $\mathcal{K} = (1, 2, 6, 10, 16, 68)$ Kronrod extension. The points are nicely nested and well suited for sparse grids.

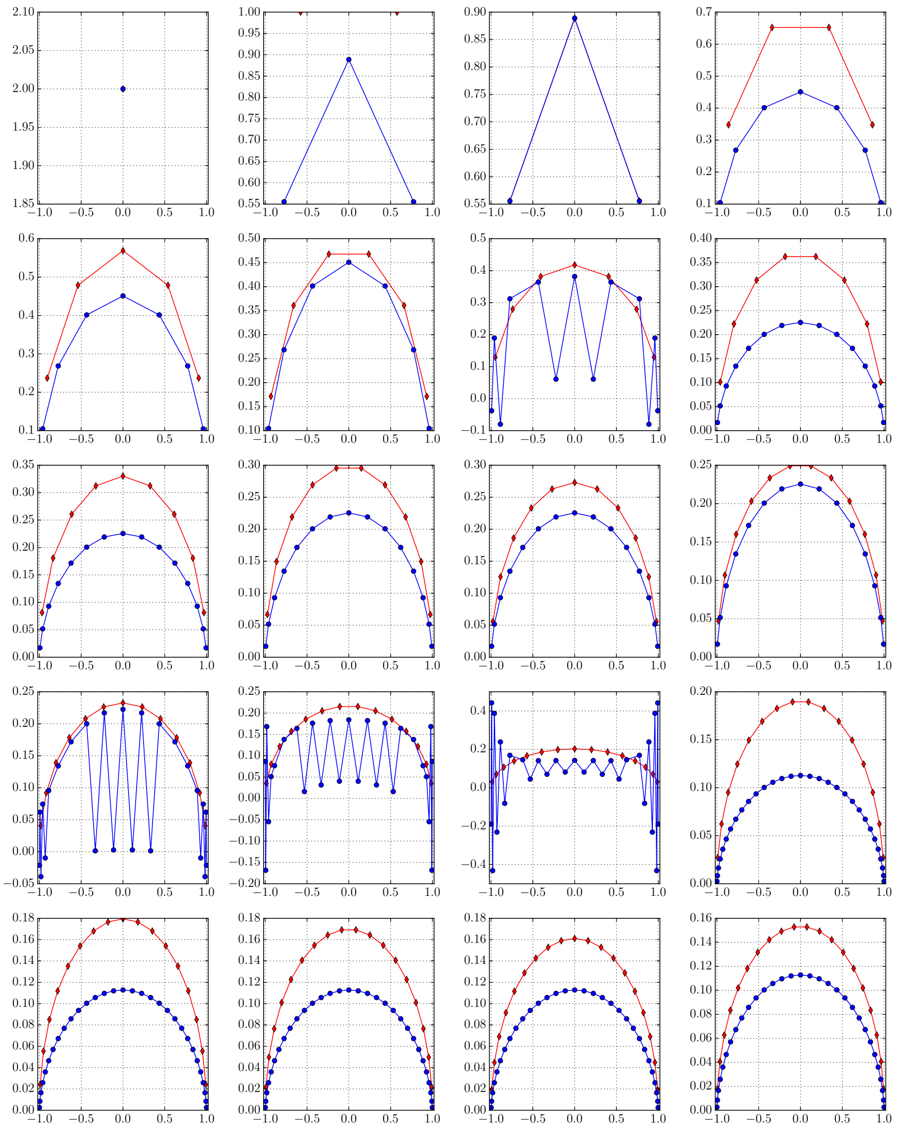
Figure 7: Gauss-Legendre (red) and Genz-Keister (blue) nodes versus corresponding weights. The 1- and 3-point rules are identical. Note that a few rules have oscillations in the weights, some of them are almost zero, others become increasingly negative. This affects the stability of the corresponding rules.

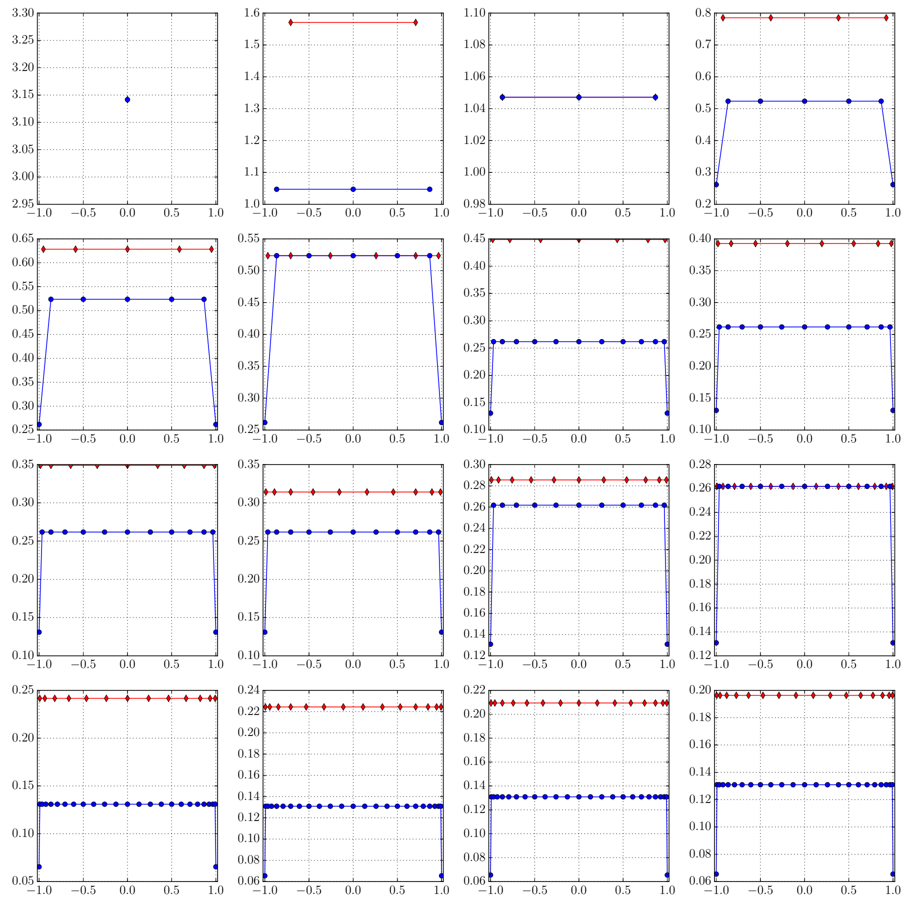
Figure 8: Gauss-Chebyshev-T (red) and Genz-Keister (blue) nodes versus corresponding weights. The 1- and 3-point rules are identical.

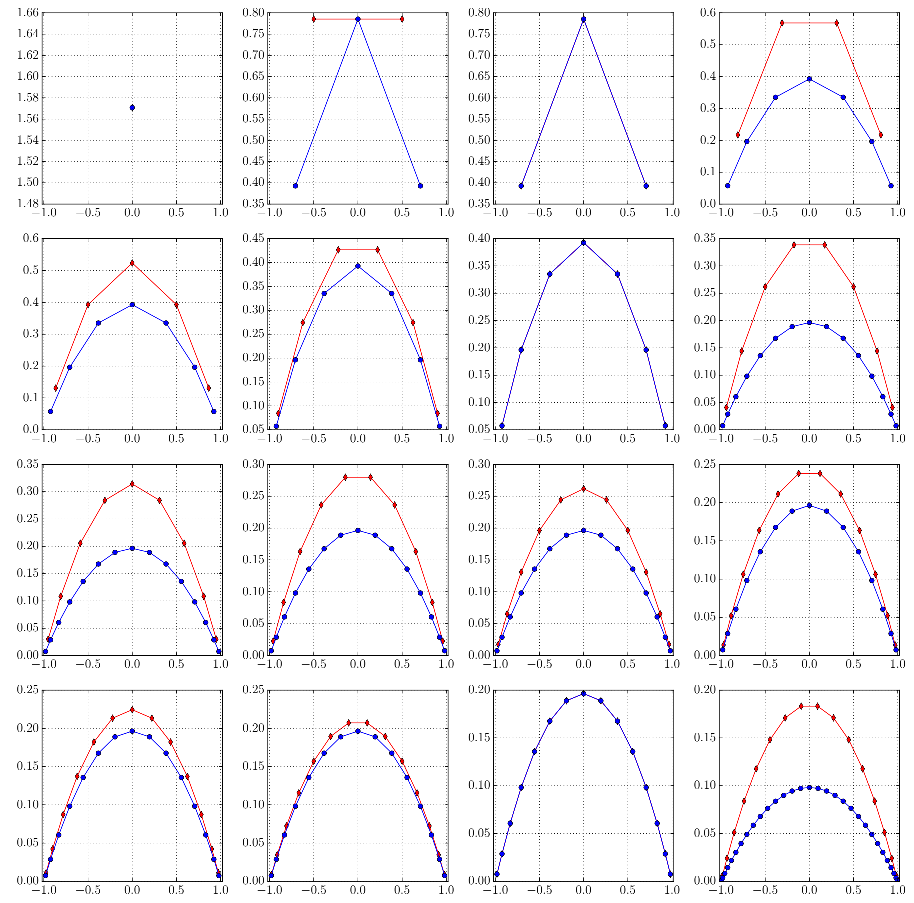
Figure 9: Gauss-Chebyshev-U (red) and Genz-Keister (blue) nodes versus corresponding weights. All $(2^i - 1)$-point rules are identical.

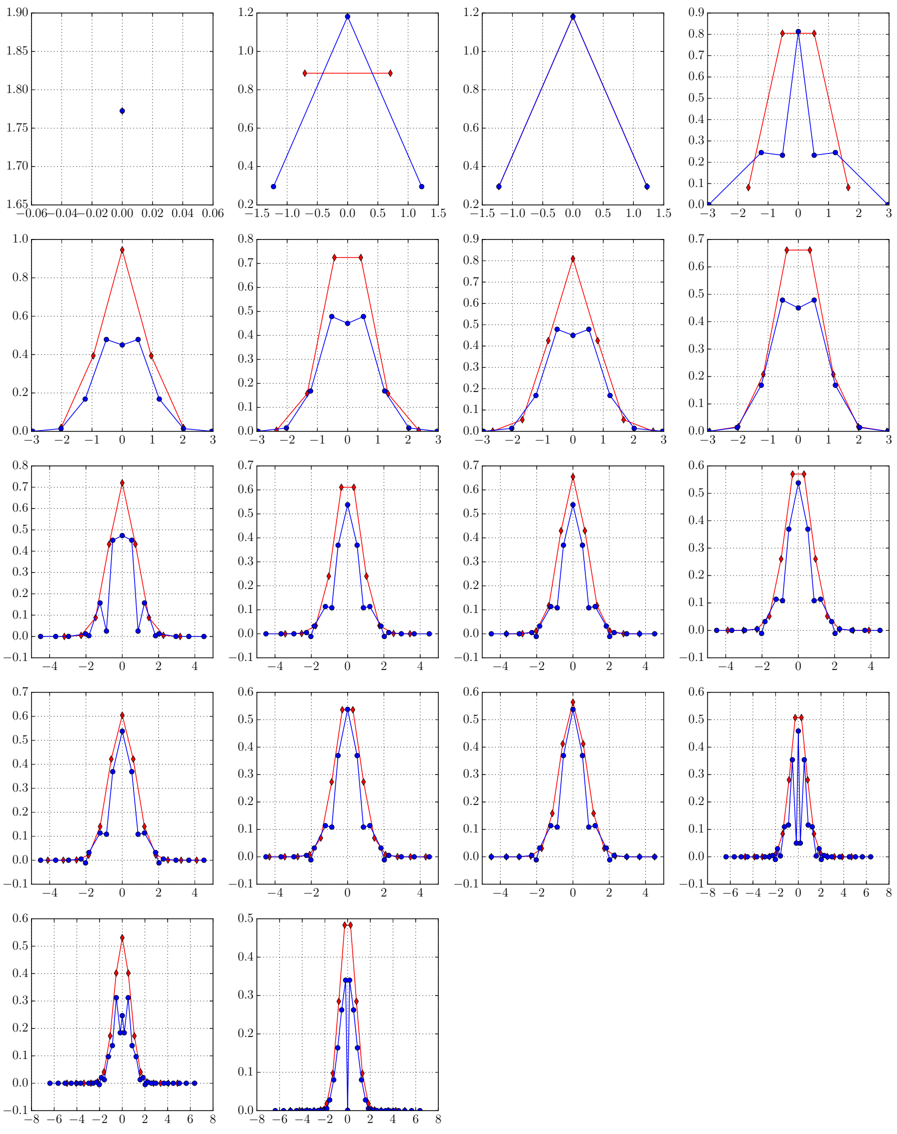
Figure 10: Gauss-Hermite (red) and Genz-Keister (blue) nodes versus corresponding weights. The 1- and 3-point rules are identical.

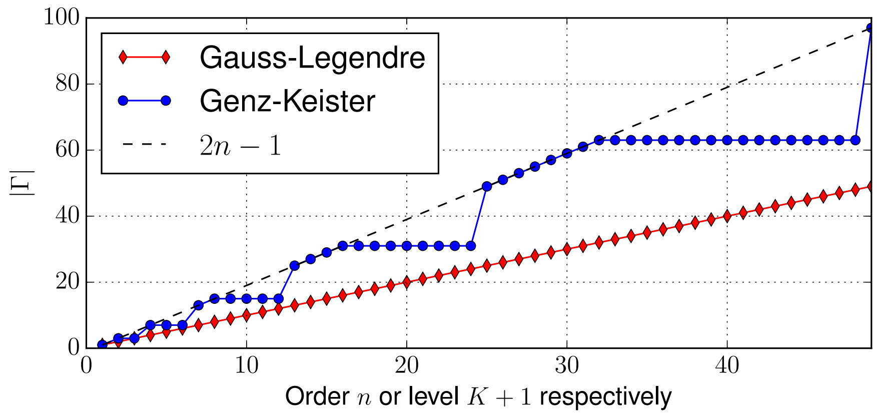

Figure 11: Number of nodes for the one-dimensional Gauss-Legendre and Genz-Keister quadrature rules of order n or level K respectively.

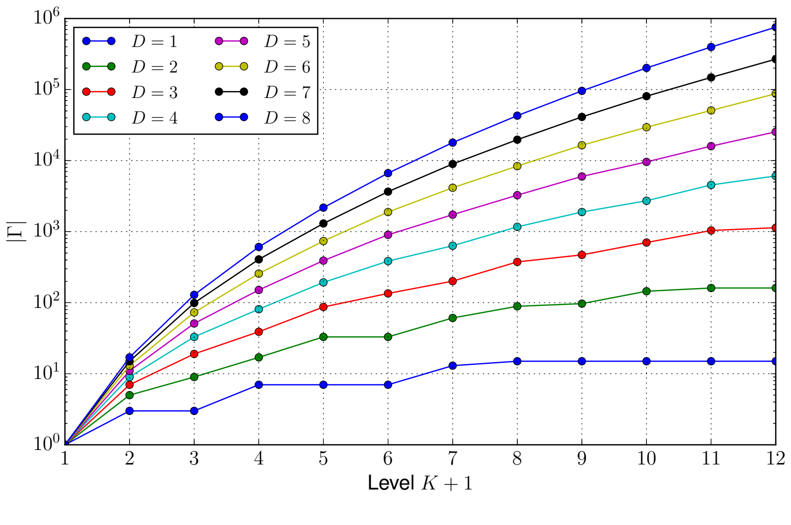

Figure 12: Number $|\Gamma|$ of Genz-Keister quadrature nodes for various levels K and dimensions D in the Legendre case.

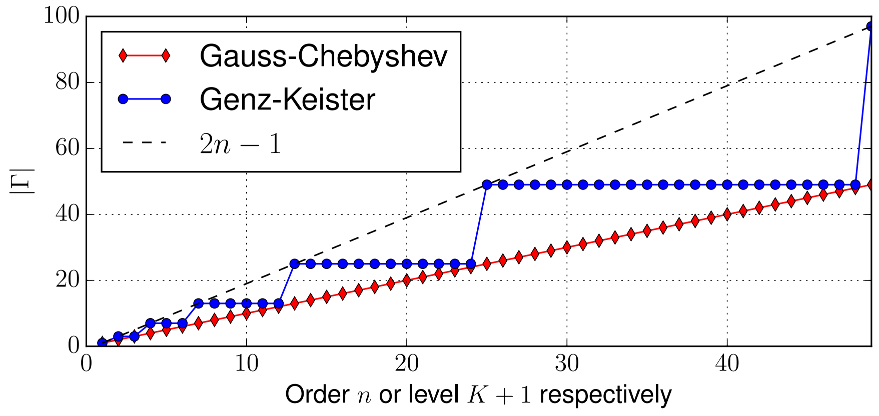

Figure 13: Number of nodes for the one-dimensional Gauss-Chebyshev-T and Genz-Keister quadrature rules of order n or level K respectively.

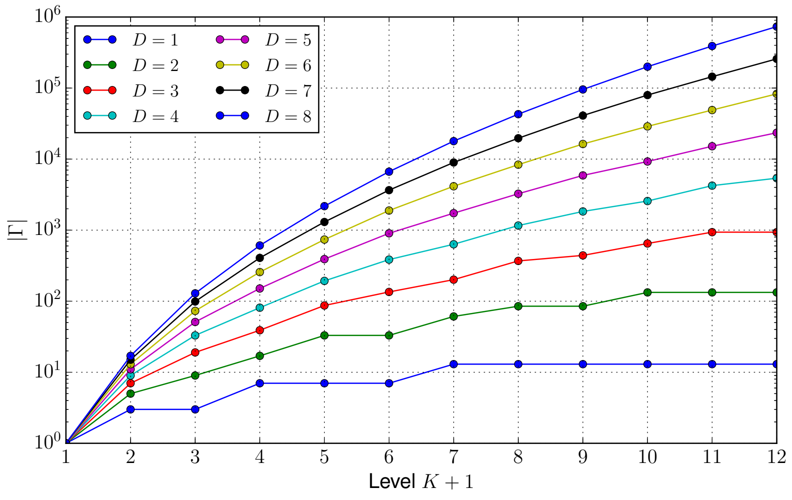

Figure 14: Number $|\Gamma|$ of Genz-Keister quadrature nodes for various levels K and dimensions D in the Chebyshev-T case.

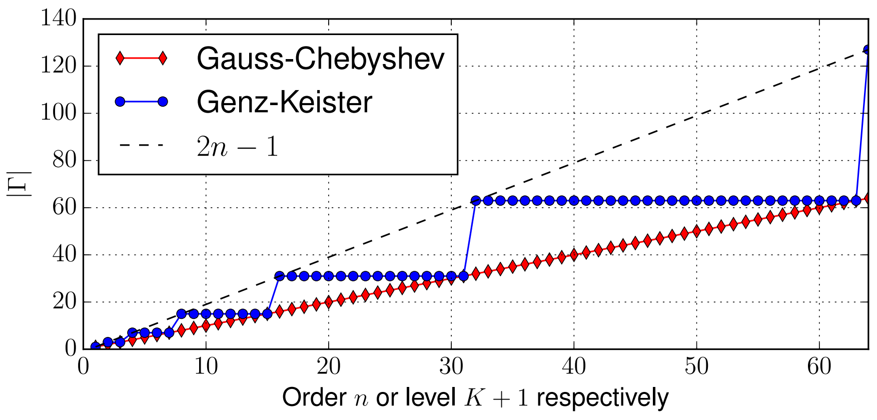

Figure 15: Number of nodes for the one-dimensional Gauss-Chebyshev-U and Genz-Keister quadrature rules of order n or level K respectively.

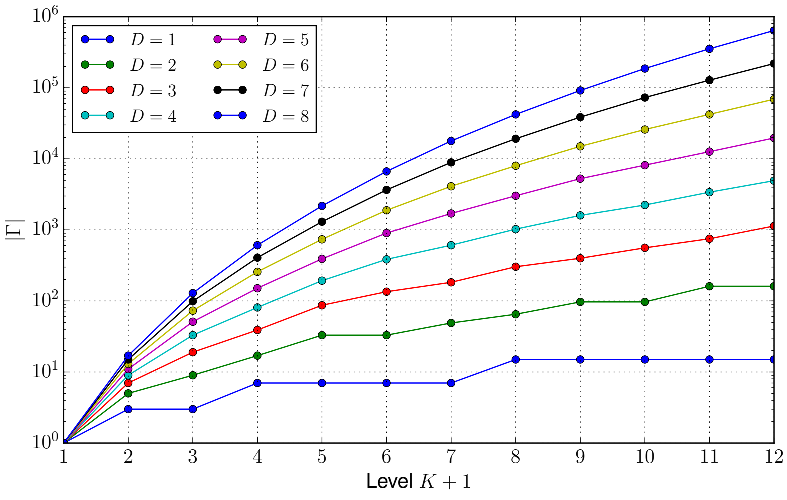

Figure 16: Number $|\Gamma|$ of Genz-Keister quadrature nodes for various levels K and dimensions D in the Chebyshev-U case.

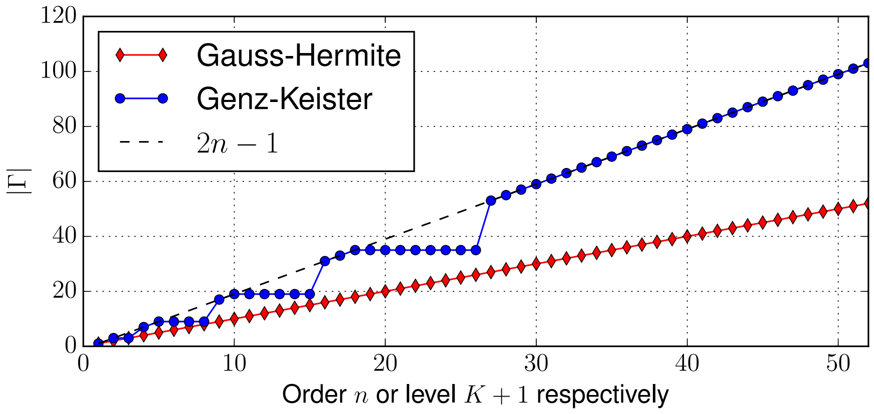

Figure 17: Number of nodes for the one-dimensional Gauss-Hermite and Genz-Keister quadrature rules of order n or level K respectively.

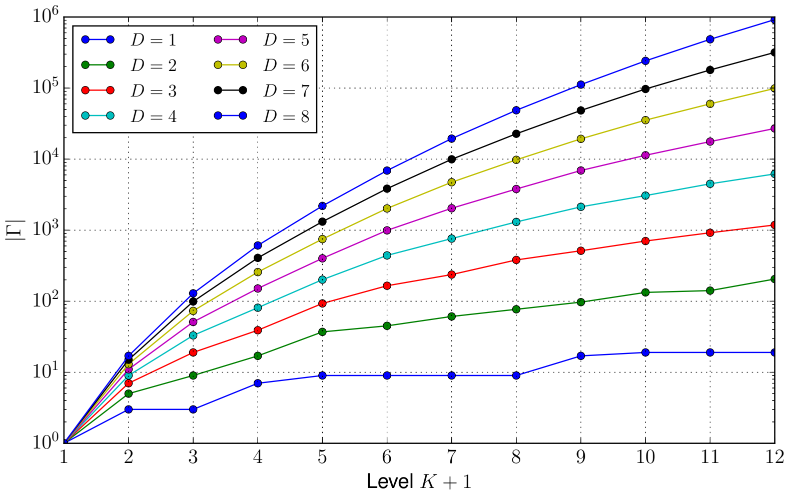

Figure 18: Number $|\Gamma|$ of Genz-Keister quadrature nodes for various levels K and dimensions D in the Hermite case.

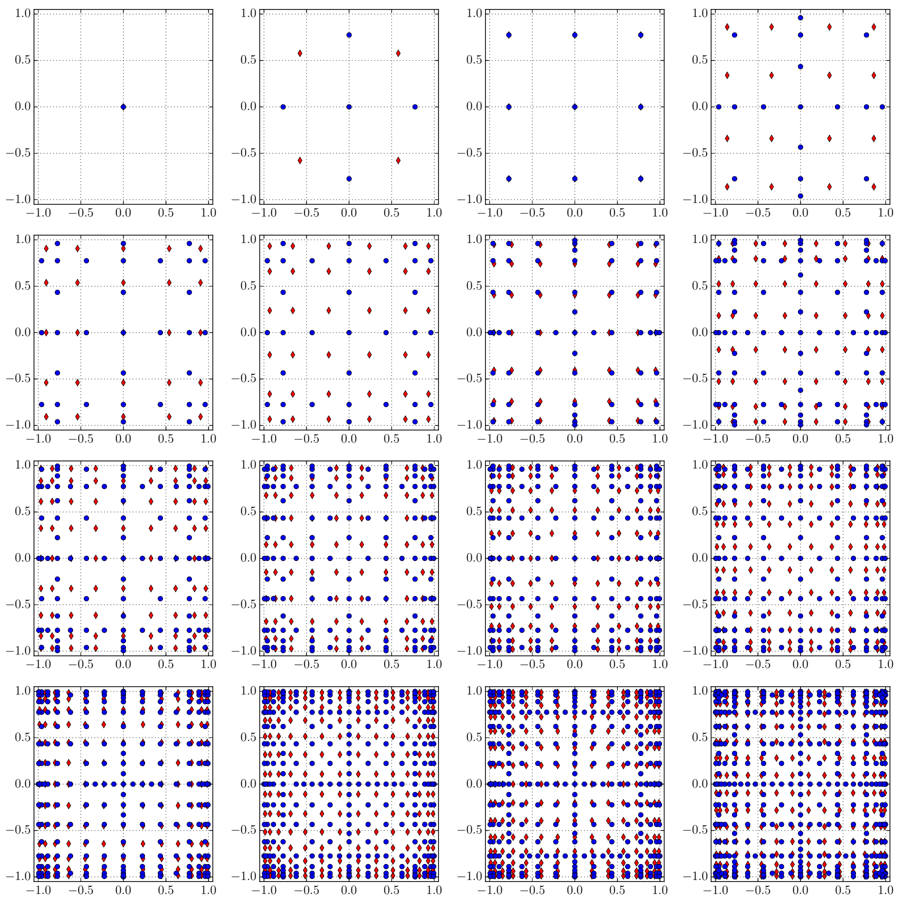

Figure 19: Gauss-Legendre (red) and Genz-Keister (blue) nodes for two-dimensional rules. The Gauss-Legendre points form a full tensor product.

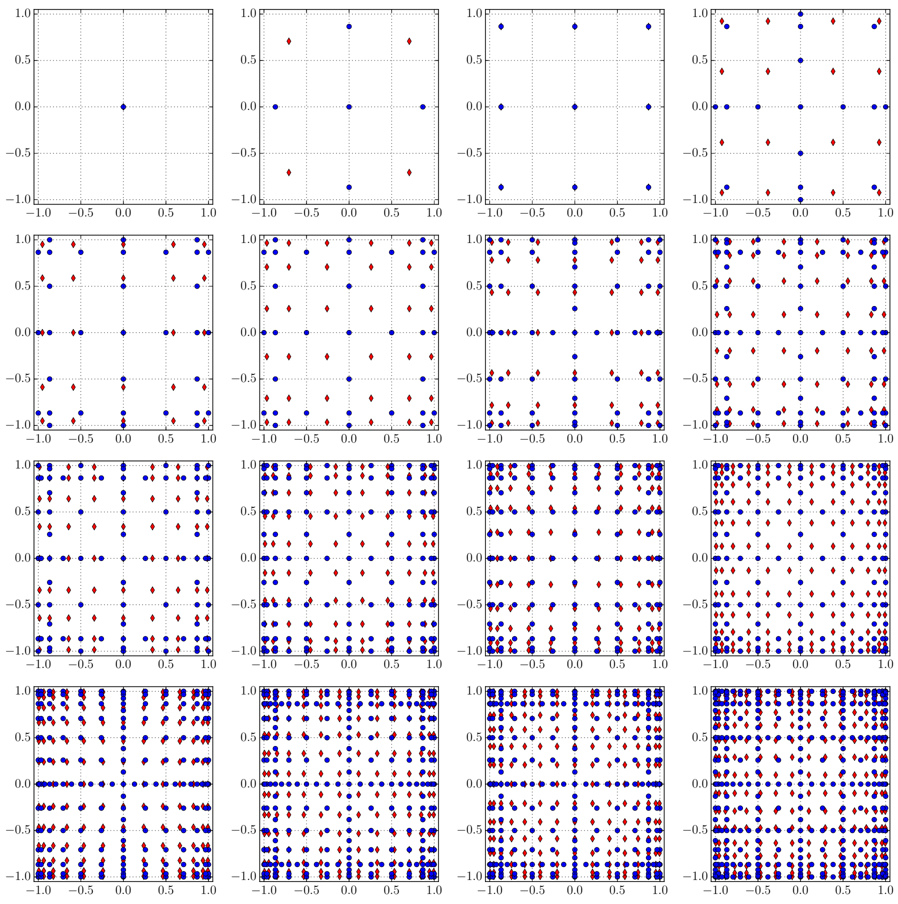
Figure 20: Gauss-Chebyshev-T (red) and Genz-Keister (blue) nodes for two-dimensional rules. The Gauss-Chebyshev points form a full tensor product.

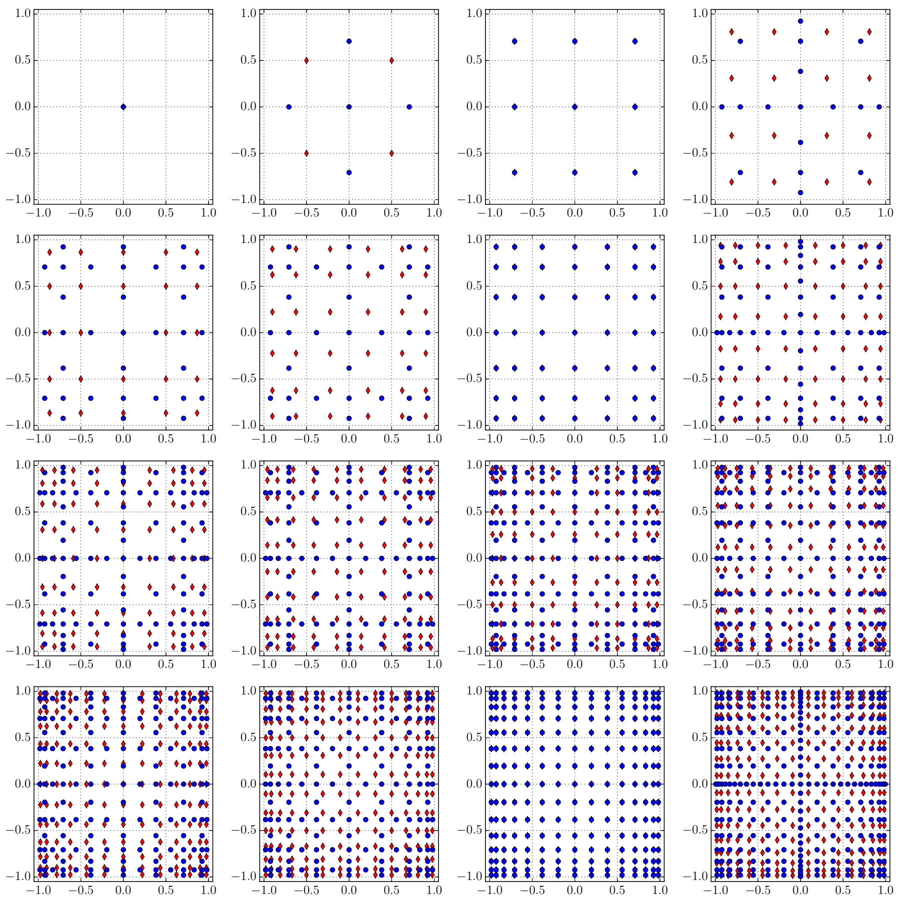

Figure 21: Gauss-Chebyshev-U (red) and Genz-Keister (blue) nodes for two-dimensional rules. The Gauss-Chebyshev points form a full tensor product.

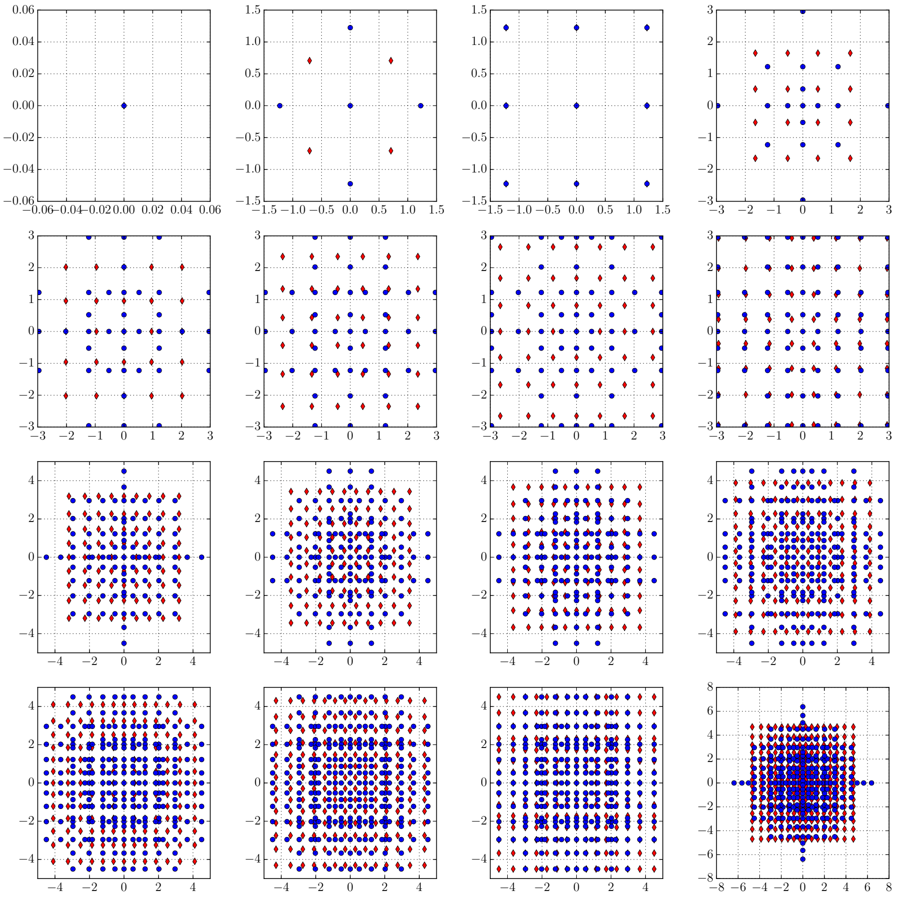

Figure 22: Gauss-Hermite (red) and Genz-Keister (blue) nodes for two-dimensional rules. The Gauss-Hermite points form a full tensor product.

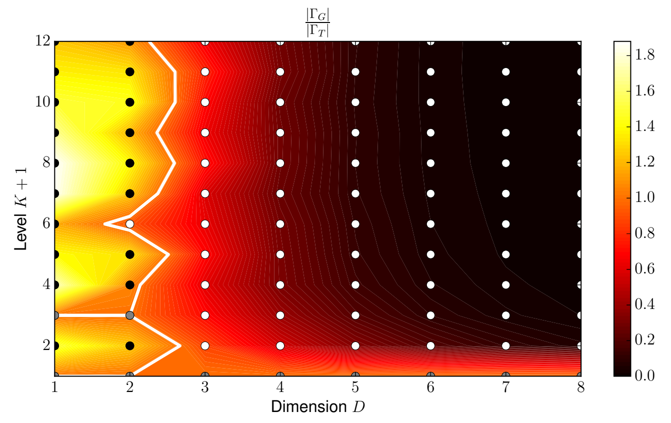

(a) Dimension $D \leq 8$ and Level $K \leq 12$.

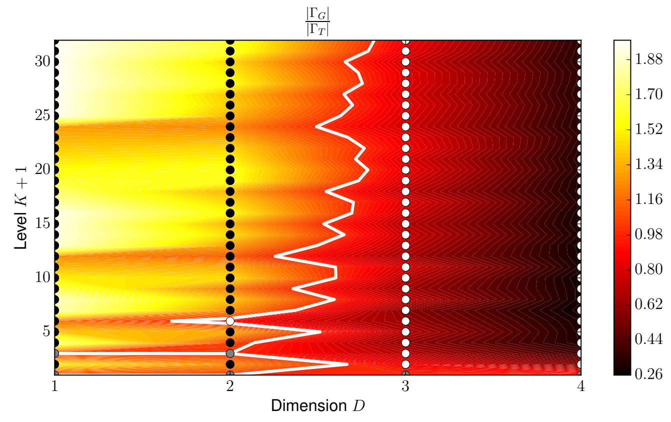

(b) Dimension $D \leq 4$ and Level $K \leq 32$. Notice the tendency of the white boundary to go to the right and eventually reach dimensions $D \geq 3$.

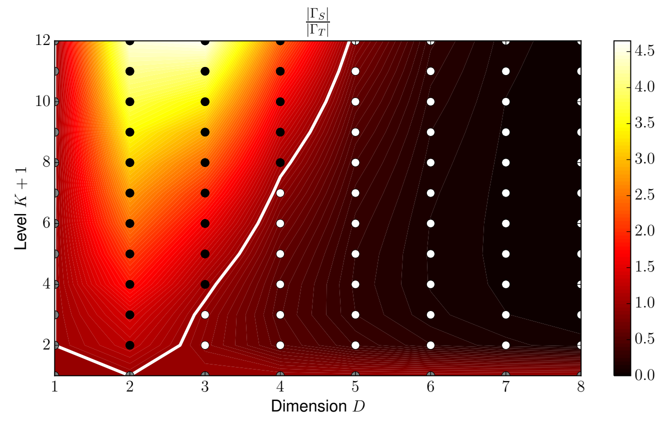

(c) Ratio comparing tensor product and classical Smolyak construction.

Figure 23: Ratio of the number of Genz-Keister and Gauss-Legendre tensor product points for some dimensions and Levels. White dots are D, K combinations where Genz-Keister is advantageous, while for black dots Genz-Keister is worse and for gray dots the ratio equals 1.

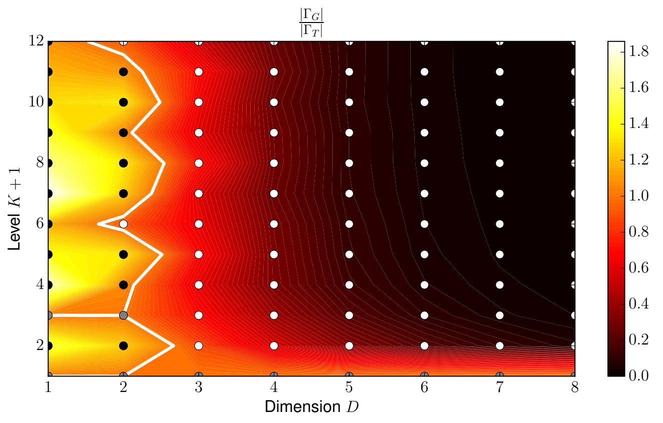

(a) Dimension $D \leq 8$ and Level $K \leq 12$.

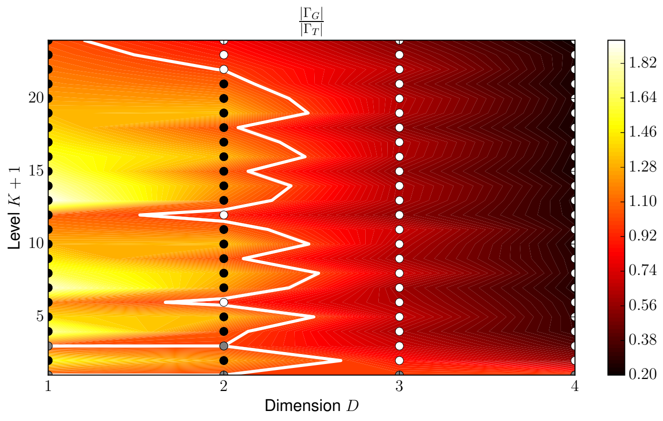

(b) Dimension $D \leq 4$ and Level $K \leq 32$.

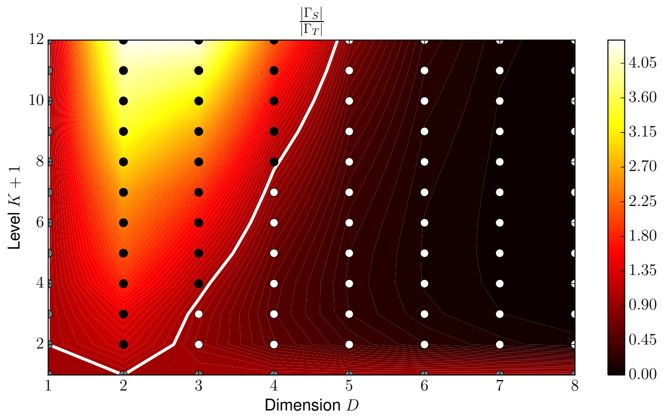

(c) Ratio comparing tensor product and classical Smolyak construction.

Figure 24: Ratio of the number of Genz-Keister and Gauss-Chebyshev-T tensor product points for some dimensions and Levels. White dots are D, K combinations where Genz-Keister is advantageous, while for black dots Genz-Keister is worse and for gray dots the ratio equals 1.

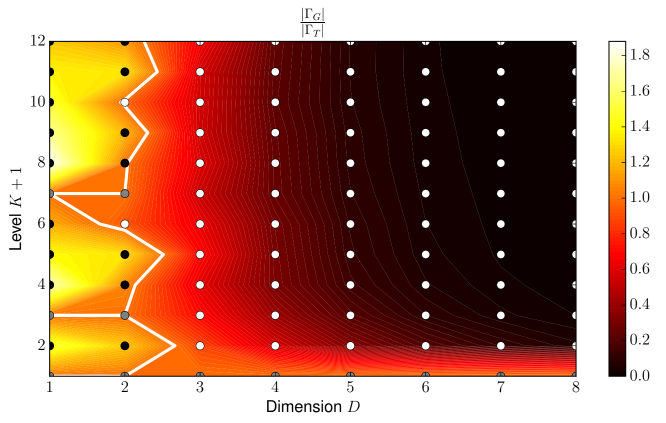

(a) Dimension $D \leq 8$ and Level $K \leq 12$.

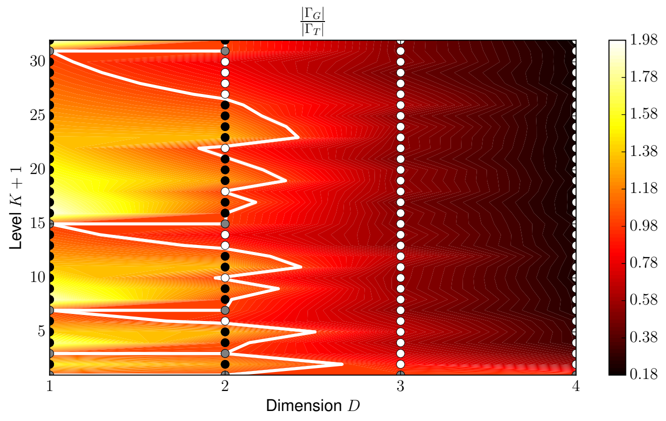

(b) Dimension $D \leq 4$ and Level $K \leq 32$.

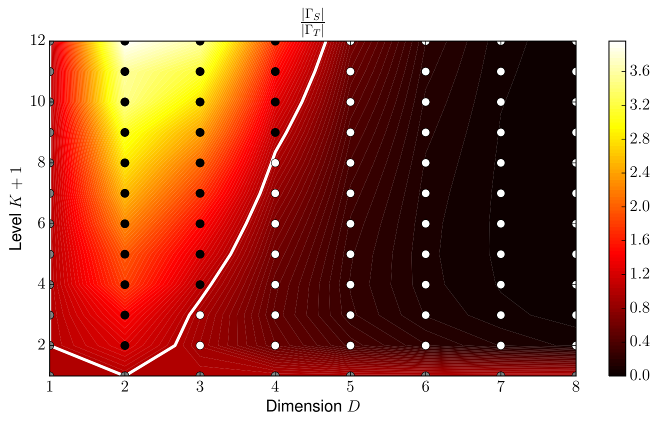

(c) Ratio comparing tensor product and classical Smolyak construction.

Figure 25: Ratio of the number of Genz-Keister and Gauss-Chebyshev-U tensor product points for some dimensions and Levels. White dots are D, K combinations where Genz-Keister is advantageous, while for black dots Genz-Keister is worse and for gray dots the ratio equals 1.

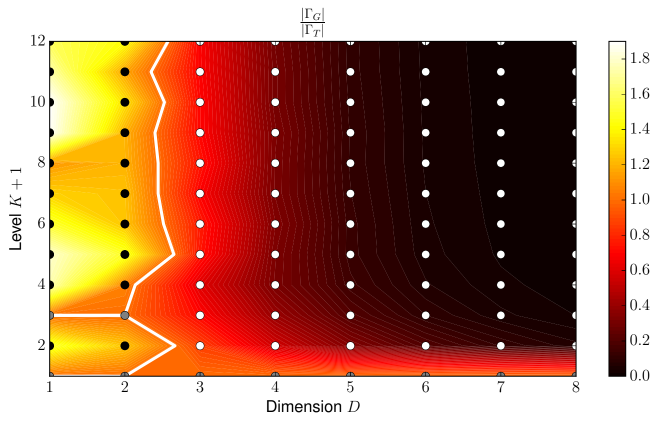

(a) Dimension $D \leq 8$ and Level $K \leq 12$.

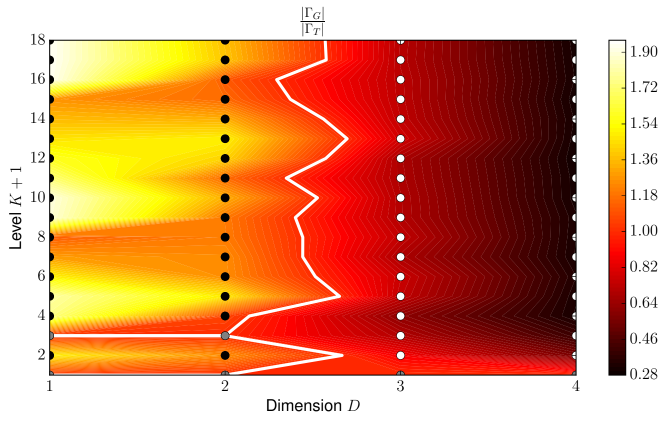

(b) Dimension $D \leq 4$ and Level $K \leq 32$. Even if not visible here, the white boundary will go more to the right and reach dimension $D = 3$ at level $K = 51$.

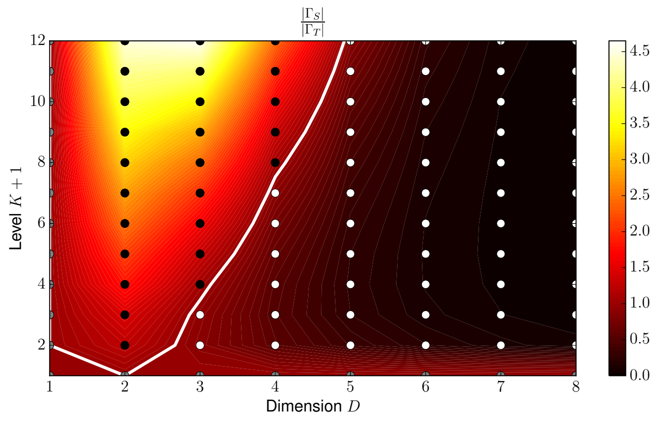

(c) Ratio comparing tensor product and classical Smolyak construction.

Figure 26: Ratio of the number of Genz-Keister and Gauss-Hermite tensor product points for some dimensions and Levels. White dots are D, K combinations where Genz-Keister is advantageous, while for black dots Genz-Keister is worse and for gray dots the ratio equals 1.

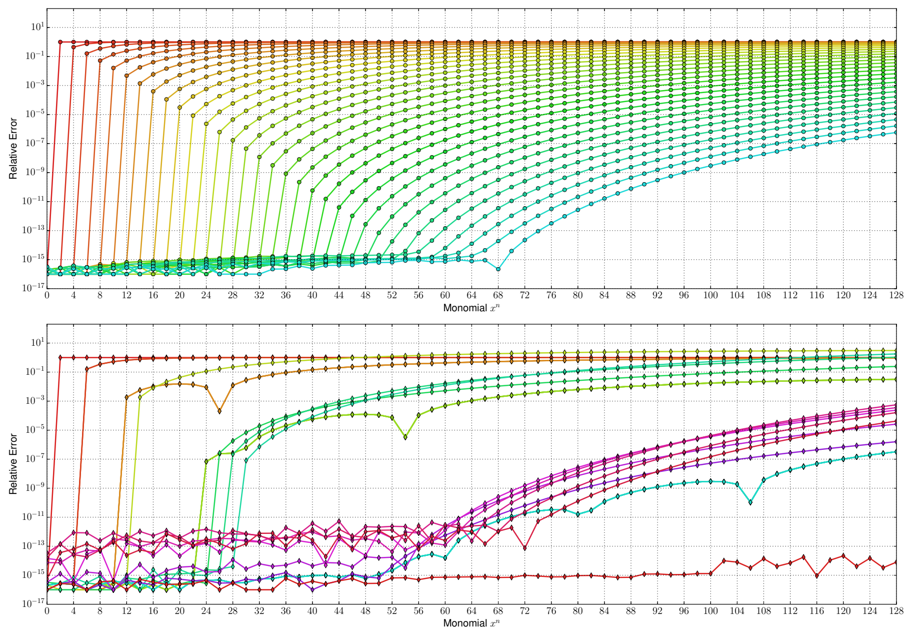

Figure 27: Relative quadrature error for integration of single univariate monomials x^n of increasing degree n. Each line represents a quadrature rule and the color indicates the number of nodes (colors wrap around once though). The upper plot shows Gauss-Legendre rules as reference while the lower one shows the Genz-Keister rules. The number of nodes for each of these rules is: 1, 3, 7, 13, 15, 25, 27, 29, 31, 49, 51, 53, 55, 57, 59, 61, 63 and the orders according to (35) are: 1, 5, 11, 13, 23, 25, 27, 29, 47, 49, 51, 53, 55, 57, 59, 61, 95 which perfectly agrees with the figure. Starting with the 31 point rule, the rules become somewhat unstable and do not reach the machine epsilon error level. This can be explained by growing oscillations in the weights for some of the rules. (Refer to Figure 7 though the rules affected are beyond the range of that plot.) The rule having 63 nodes is very stable again.

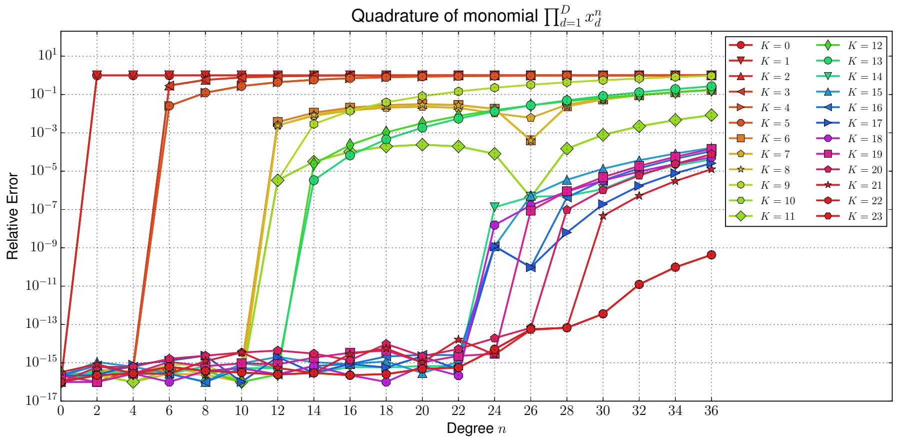

(a) Dimension $D = 2$

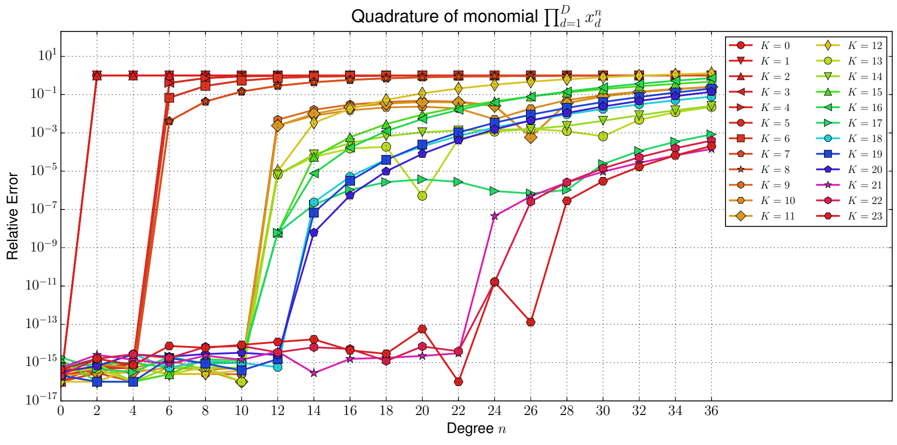

(b) Dimension $D = 3$

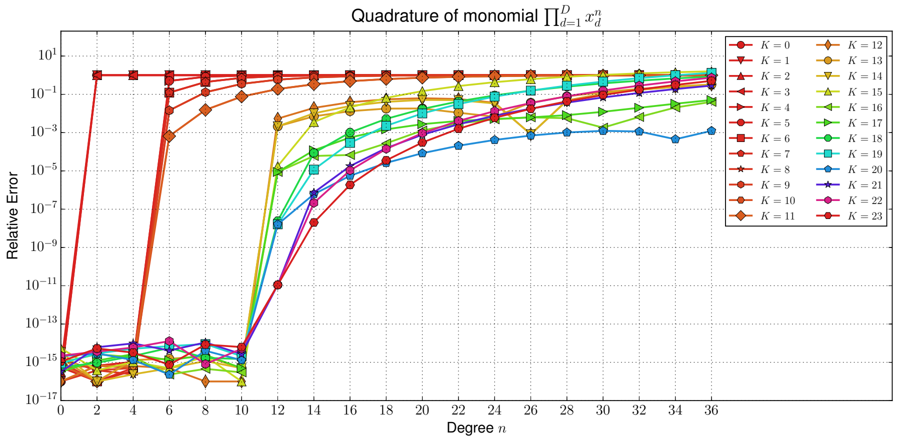

(c) Dimension $D = 4$

Figure 28: Relative errors in the Legendre case for the integral (36) in different dimensions. All variables x_d share the same exponent n.

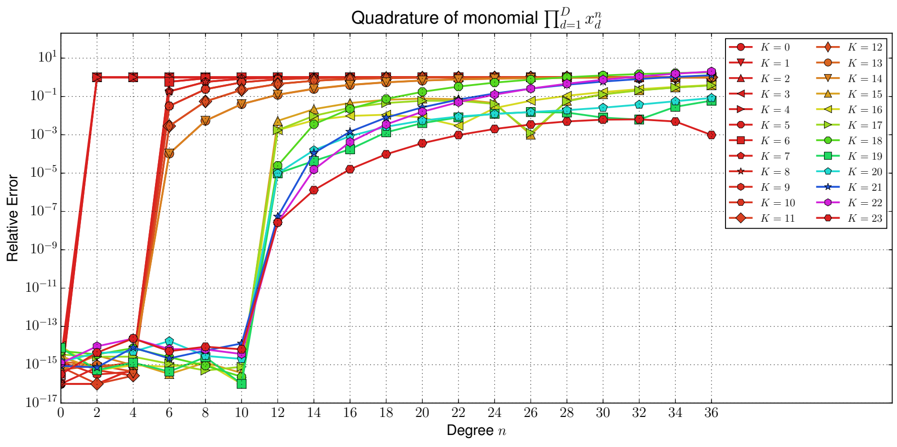

(a) Dimension $D = 5$

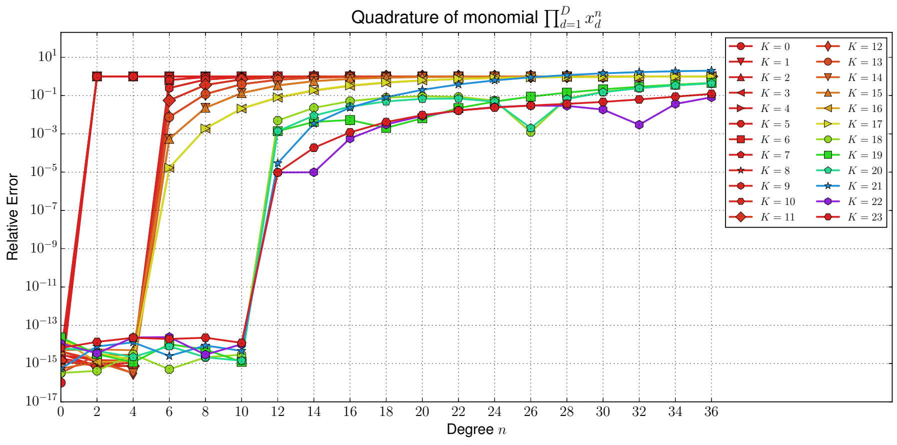

(b) Dimension $D = 6$

Figure 29: Relative errors in the Legendre case for the integral (36) in different dimensions. All variables x_d share the same exponent n.

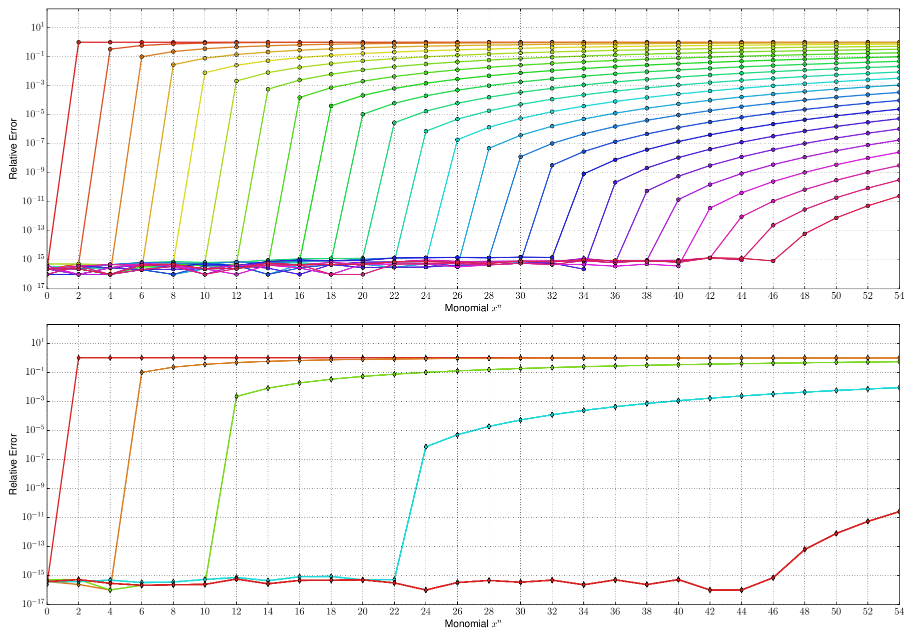

Figure 30: Relative quadrature error for integration of single univariate monomials x^n of increasing degree n. Each line represents a quadrature rule and the color indicates the number of nodes (colors wrap around once though). The upper plot shows Gauss-Chebyshev-T rules as reference while the lower one shows the Genz-Keister rules. The number of nodes for each of these rules is: 1, 3, 7, 13, 25 and the orders according to (35) are: 1, 5, 11, 23, 47 which perfectly agrees with the figure. All rules examined here are very stable up to machine precision.

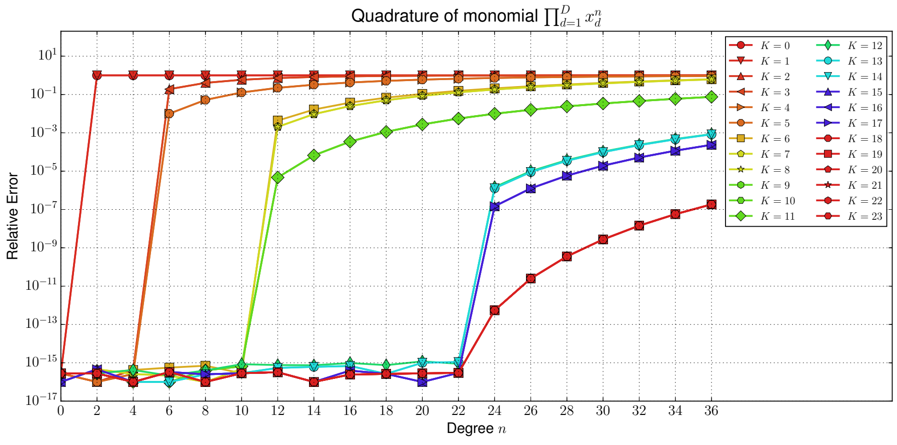

(a) Dimension $D = 2$

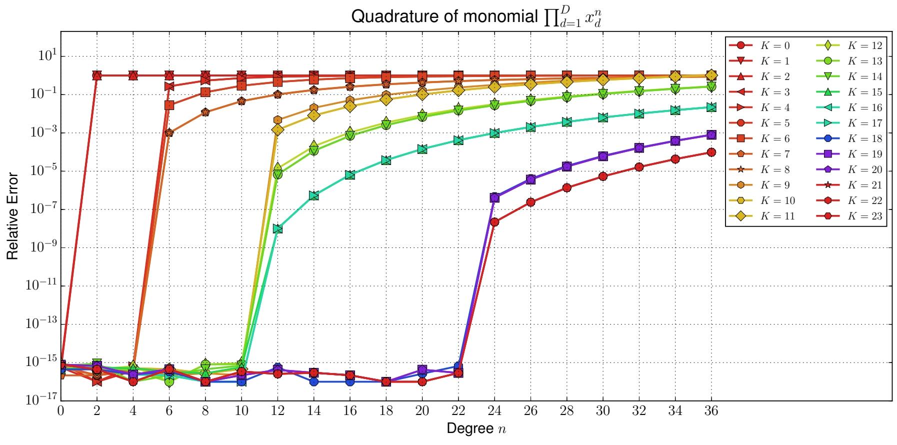

(b) Dimension $D = 3$

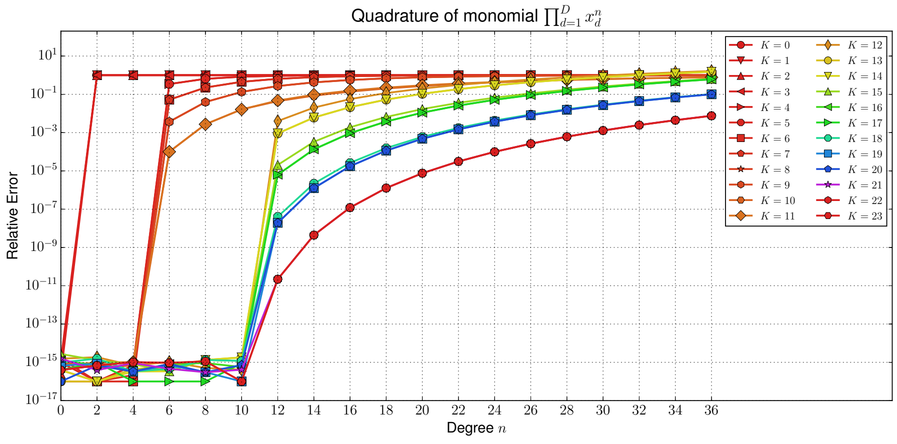

(c) Dimension $D = 4$

Figure 31: Relative errors in the Chebyshev-T case for the integral (37) in different dimensions. All variables x_d share the same exponent n.

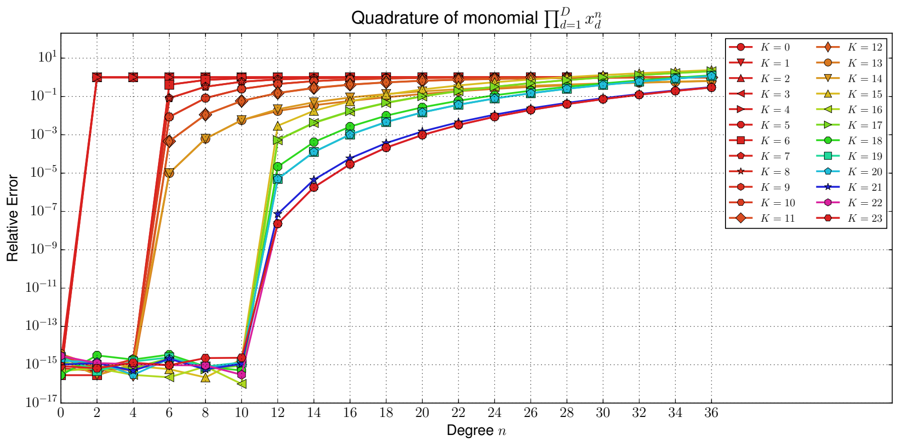

(a) Dimension $D = 5$

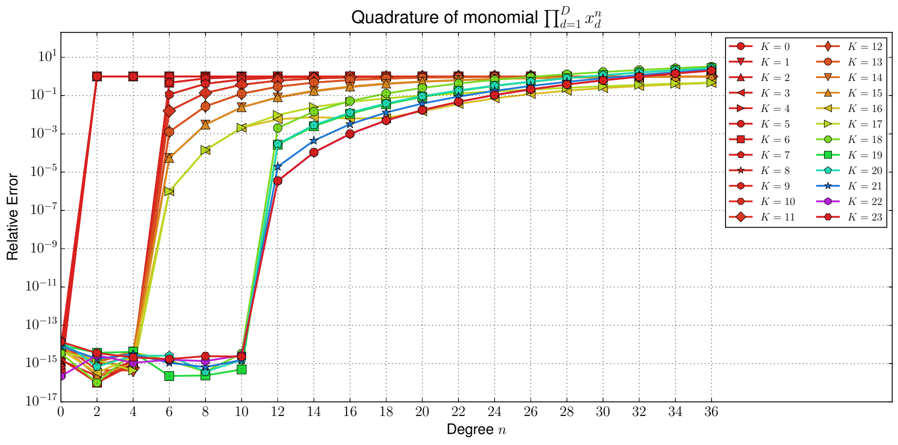

(b) Dimension $D = 6$

Figure 32: Relative errors in the Chebyshev-T case for the integral (37) in different dimensions. All variables x_d share the same exponent n.

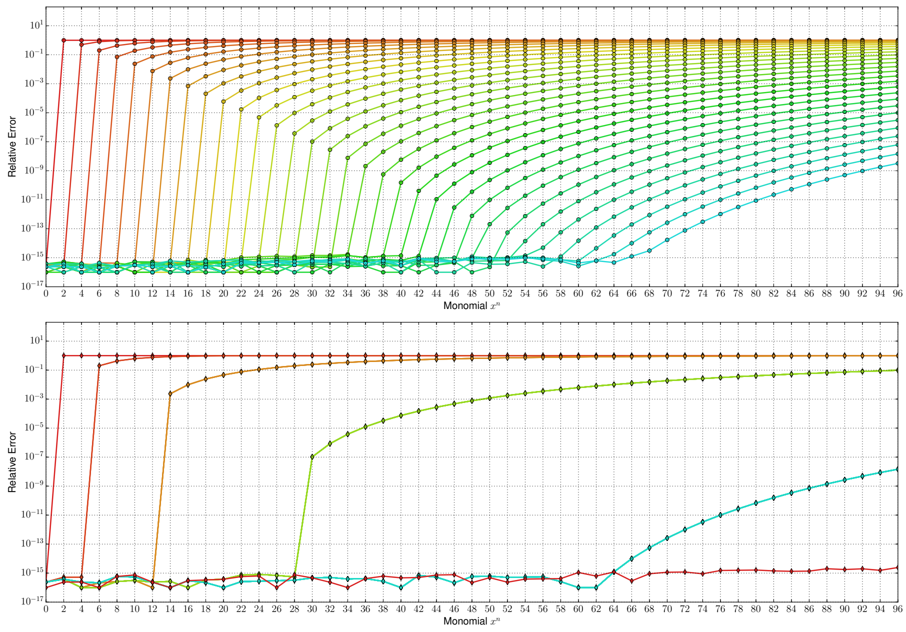

Figure 33: Relative quadrature error for integration of single univariate monomials x^n of increasing degree n. Each line represents a quadrature rule and the color indicates the number of nodes (colors wrap around once though). The upper plot shows Gauss-Chebyshev-U rules as reference while the lower one shows the Genz-Keister rules. The number of nodes for each of these rules is: 1, 3, 7, 15, 31, 63 and the orders according to (35) are: 1, 5, 13, 29, 61, 125 which perfectly agrees with the figure. The error is in good agreement with the Gauss-Chebyshev rules which is of course expected because the rules are identical.

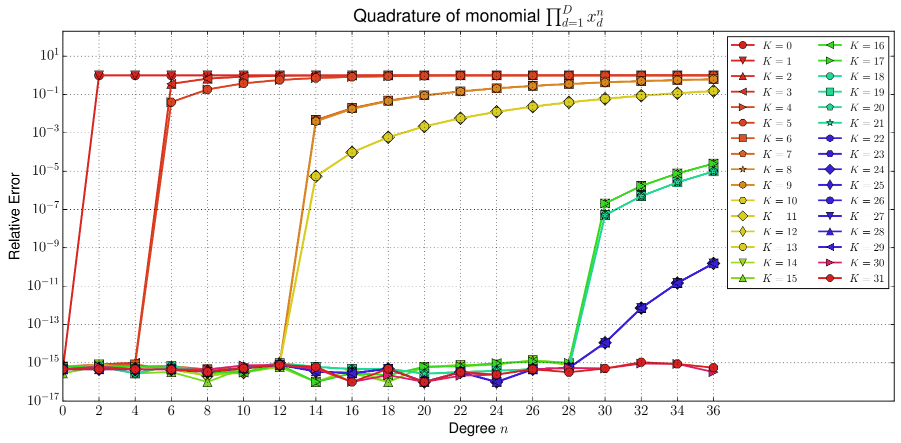

(a) Dimension $D = 2$

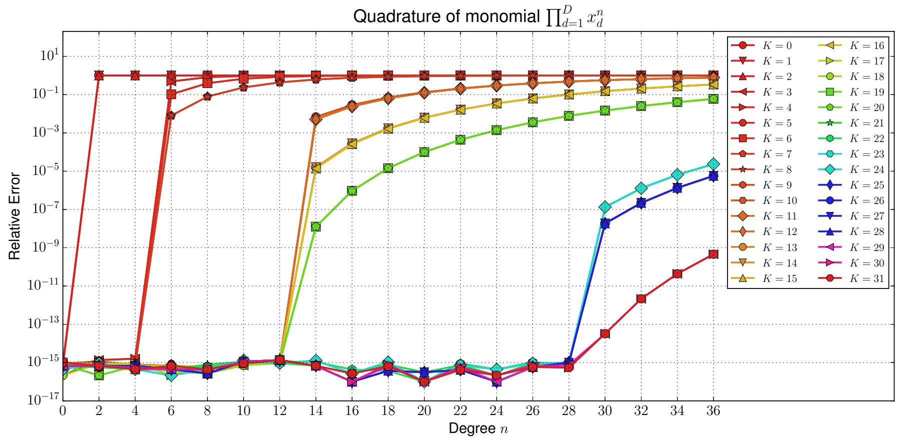

(b) Dimension $D = 3$

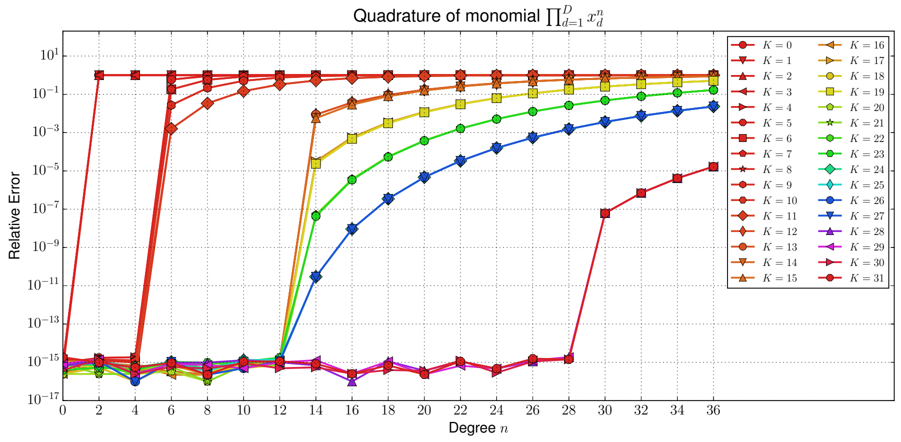

(c) Dimension $D = 4$

Figure 34: Relative errors in the Chebyshev-U case for the integral (38) in different dimensions. All variables x_d share the same exponent n.

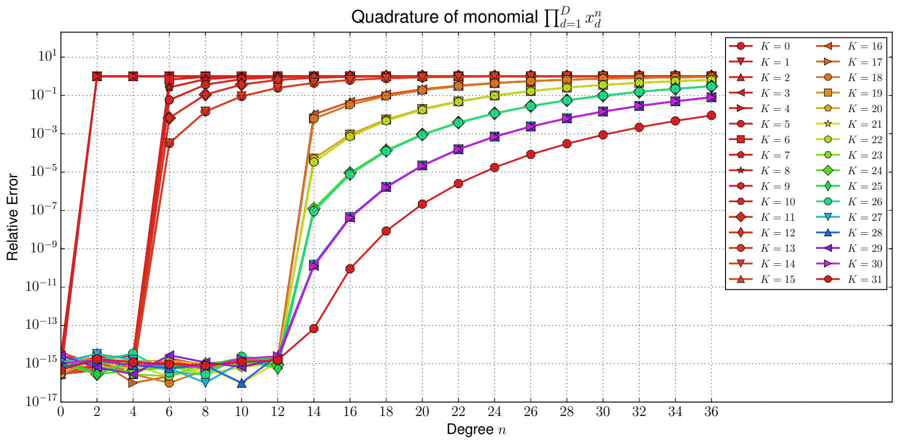

(a) Dimension $D = 5$

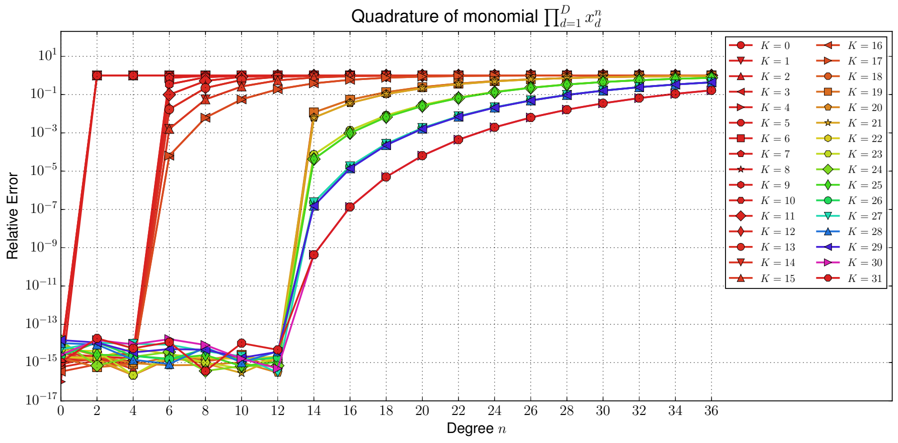

(b) Dimension $D = 6$

Figure 35: Relative errors in the Chebyshev-U case for the integral (38) in different dimensions. All variables x_d share the same exponent n.

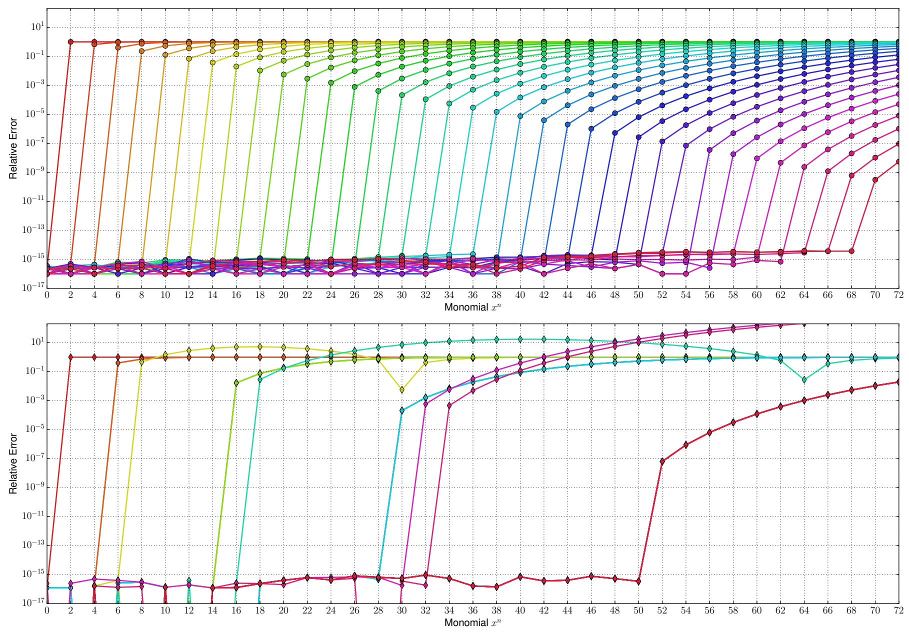

Figure 36: Relative quadrature error for integration of single univariate monomials x^n of increasing degree n. Each line represents a quadrature rule and the color indicates the number of nodes (colors wrap around once though). The upper plot shows Gauss-Hermite rules as reference while the lower one shows the Genz-Keister rules. The number of nodes for each of these rules is: 1, 3, 7, 9, 17, 19, 31, 33, 35 and the orders according to (35) are: 1, 5, 7, 15, 17, 29, 31, 33, 51 which perfectly agrees with the figure. Given that none of the higher order rules agree with any Gauss-Hermite rule, the stability and error behavior is excellent. On the other hand, the rule with 35 points integrates monomials correctly only up to x^{51} with $51 = 2 \cdot 25 + 1$ instead of up to $n = 2 \cdot 35 - 1 = 69$.

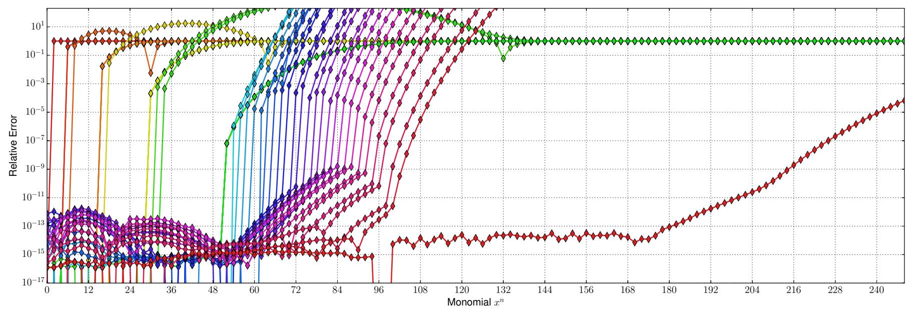

Figure 37: Relative quadrature error for integration of single univariate monomials x^n of increasing degree n. Each line represents a quadrature rule and the color indicates the number of nodes (colors wrap around once though). The number of nodes for each of these rules is: 53, 55, 57, 59, 61, 63, 65, 67, 69, 71, 73, 75, 77, 79, 81, 83, 85, 87, 89, 91, 93, 95, 97, 99, 101, 103. The rules for $K > 25$ become soon highly unstable. A notable exception is the last rule with $K = 51$ having 103 nodes which shows good behavior and is of order 103. This is obviously extremely inefficient for practical use.

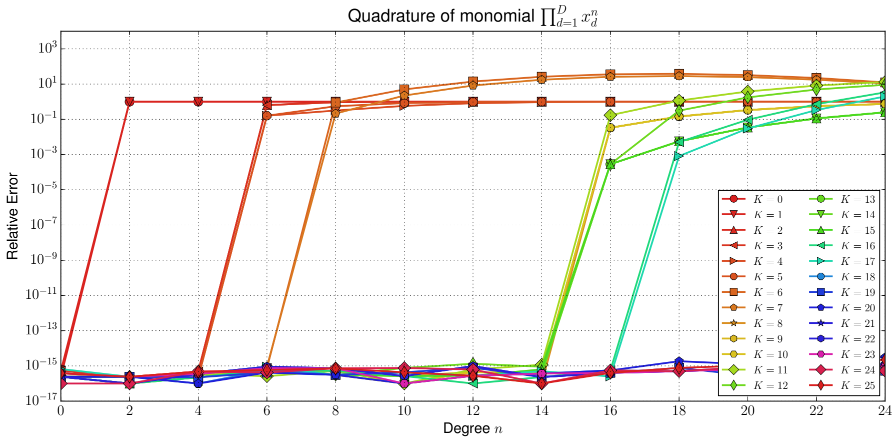

(a) Dimension $D = 2$

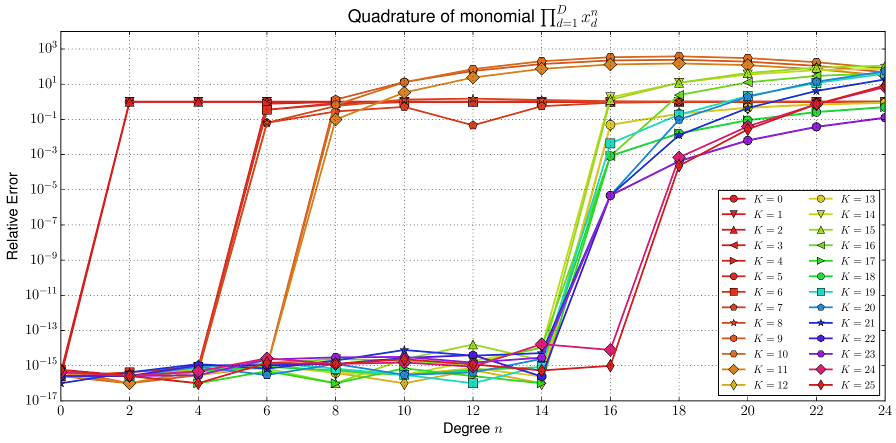

(b) Dimension $D = 3$

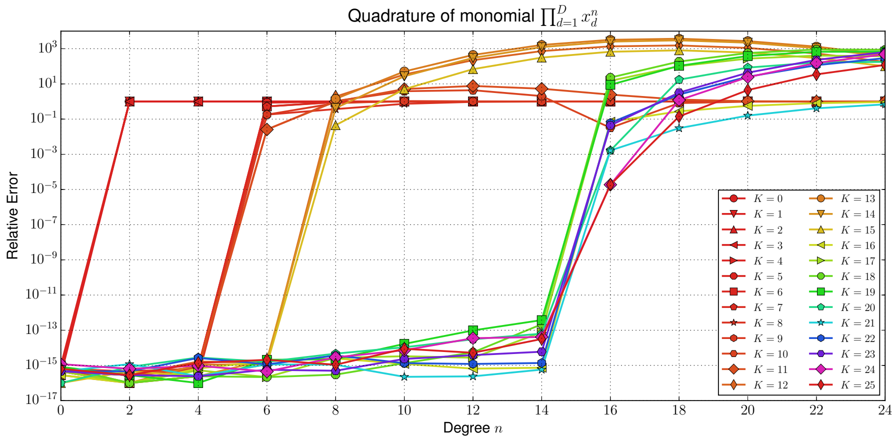

(c) Dimension $D = 4$

Figure 38: Relative errors in the Hermite case for the integral (39) in different dimensions. All variables x_d share the same exponent n.

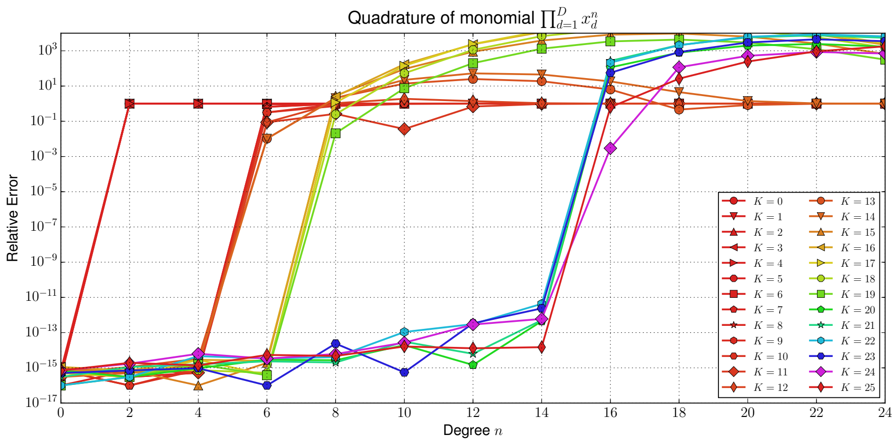

(a) Dimension $D = 5$

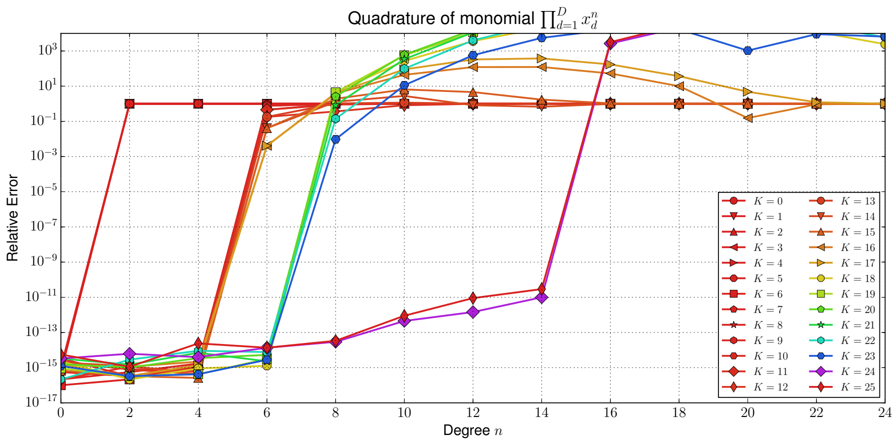

(b) Dimension $D = 6$

Figure 39: Relative errors in the Hermite case for the integral (39) in different dimensions. All variables x_d share the same exponent n.

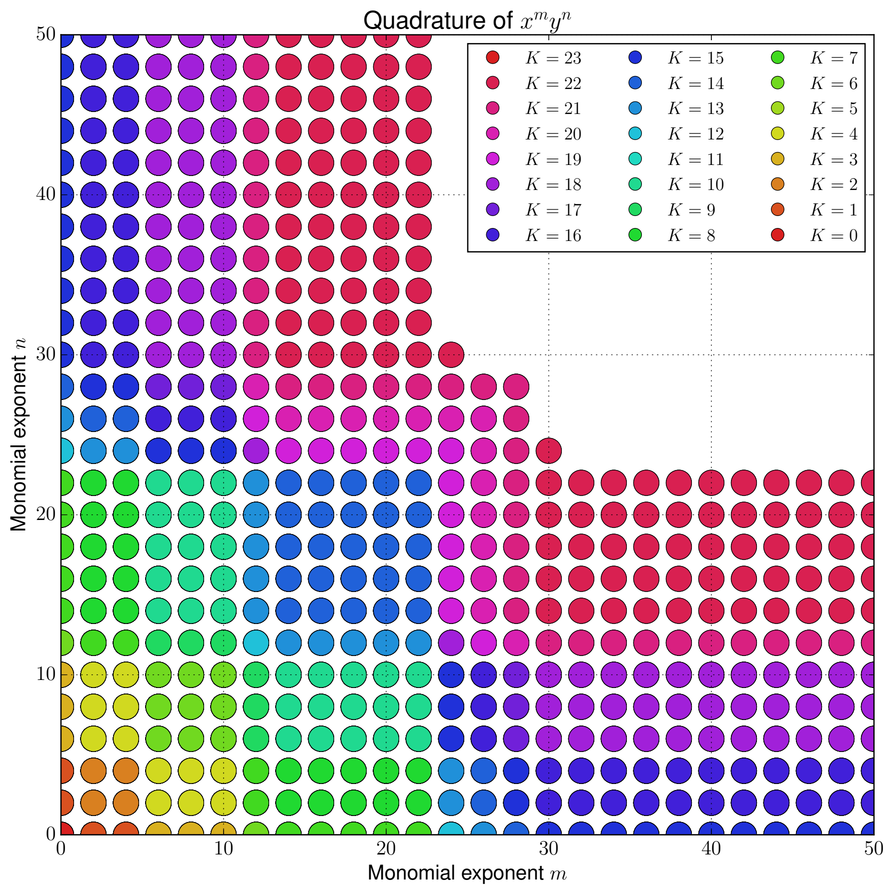

Figure 40: Quadrature of the bivariate monomials $x^m y^n$ for $0 \le n, m \le 50$ in the Legendre case. Each pair (m, n) is color-coded by the lowest level K rule that correctly integrates the monomial with a relative error not larger than 10^{-13}.

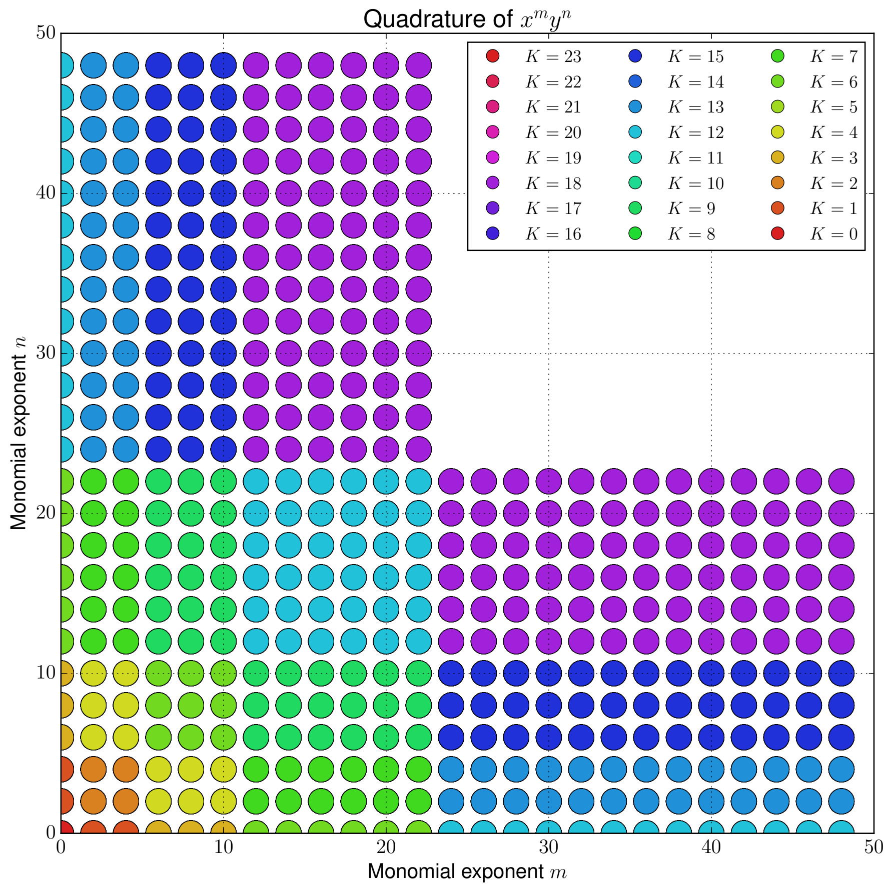

Figure 41: Quadrature of the bivariate monomials $x^m y^n$ for $0 \leq n, m \leq 50$ in the Chebyshev-T case. Each pair (m, n) is color-coded by the lowest level K rule that correctly integrates the monomial with a relative error not larger than 10^{-13}.

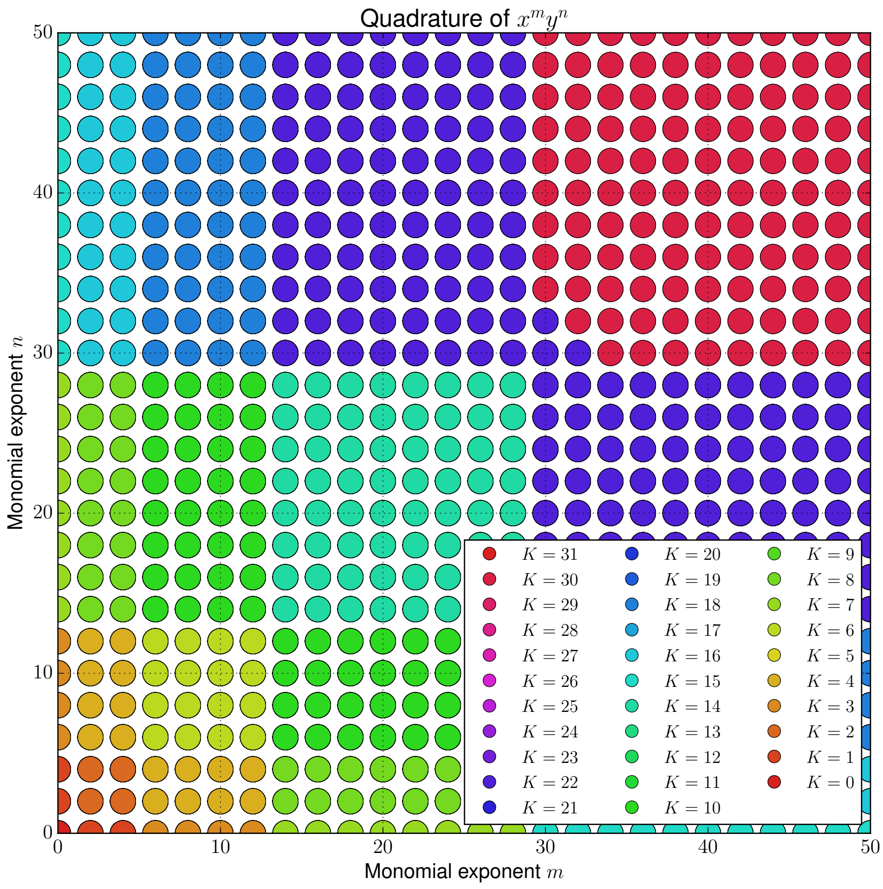

Figure 42: Quadrature of the bivariate monomials $x^m y^n$ for $0 \leq n, m \leq 50$ in the Chebyshev-U case. Each pair (m, n) is color-coded by the lowest level K rule that correctly integrates the monomial with a relative error not larger than 10^{-13}.

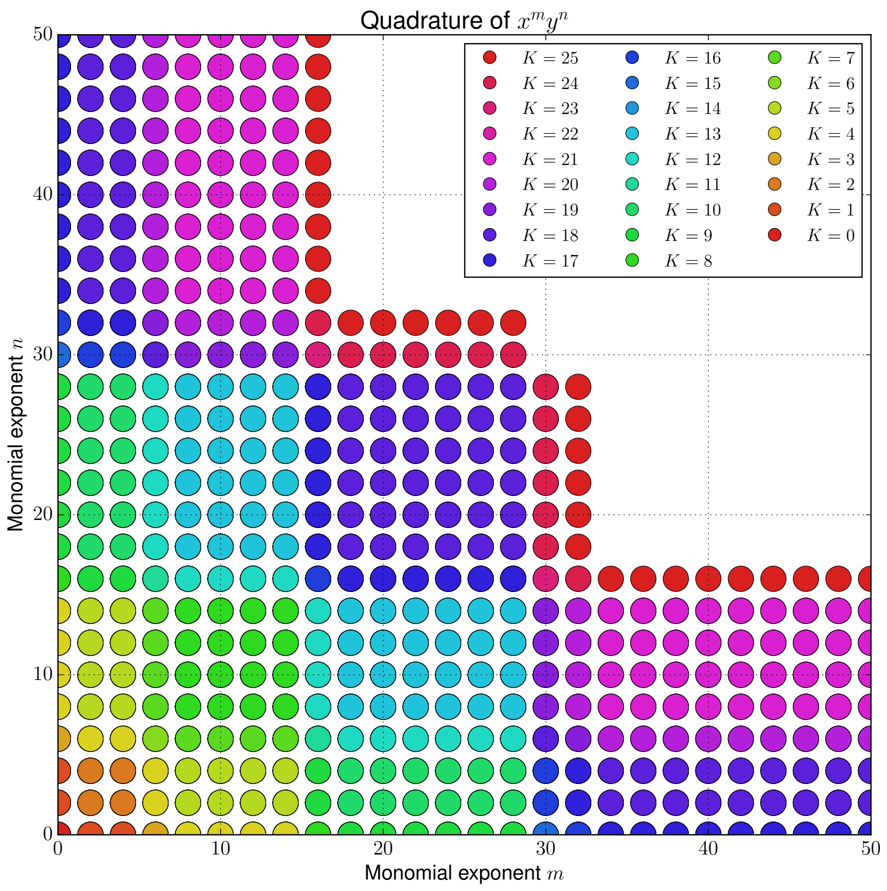

Figure 43: Quadrature of the bivariate monomials $x^m y^n$ for $0 \leq n, m \leq 50$ in the Hermite case. Each pair (m, n) is color-coded by the lowest level K rule that correctly integrates the monomial with a relative error not larger than 10^{-13}.

7 Software

The complete software used for this project can be downloaded at:

https://github.com/raoulbq/kes.git

and is released as free software under the GNU General Public License.

8 Future work

A question is whether it would be computationally more efficient to compute everything with arbitrary precision floating point ball arithmetic. By doing that it might be possible to better handle the exponential growth of coefficients. On the other hand, computing roots and solving for the weights seems to be the most expensive part already.
By having efficient root isolation and counting algorithms in `flint` we would not have to compute all roots of E_p numerically to high precision just for answering the question if some of them are complex hence marking the whole extension invalid [4].
Finally, this work is based on empirical studies on the outcome of algorithmic searches. It would be desirable to have a rigorous mathematical foundation for the claims made.
Some of the techniques presented here could theoretically be generalized to Gegenbauer polynomials $C_n^{(\alpha)}(x)$ and ultimately Jacobi polynomials $P_n^{(\alpha,\beta)}(x)$. The parametric nature of these polynomials makes the implementation more complex. Also, results will depend on the explicit values of these parameters α and β.
Similar techniques are actually applied in practical computations, for example in the simulation of the Schrödinger equation [1].

[4]This solution is also not fully satisfying since we can only decide that a complex root is really complex but not if a candidate is for sure real.

A Tables of higher order Kronrod extensions $\mathcal{K}$

P_n	$\mathcal{K} = (p_0, p_1, \ldots, p_k)$
P_1 $k \geq 6$	$(1,2,4,8,16,32,64)$, $(1,2,4,8,30,46,92)$, $(1,2,4,14,22,44,88)$, $(1,2,4,14,22,44,90)$, $(1,4,6,12,24,48,96)$
P_2 $k \geq 5$	$(2,3,6,12,44,68)$, $(2,3,6,22,34,68)$, $(2,3,10,16,32,64)$, $(2,3,10,16,32,66)$, $(2,3,16,22,44,88)$, $(2,3,16,22,44,90)$, $(2,4,6,22,35,70)$, $(2,4,6,22,36,70)$, $(2,4,6,22,36,71)$, $(2,4,6,22,36,72)$, $(2,4,6,29,42,84)$, $(2,4,14,20,40,82)$, $(2,4,15,22,44,88)$, $(2,4,15,22,44,90)$, $(2,4,16,22,44,90)$, $(2,4,16,22,45,92)$, $(2,6,9,32,50,100)$, $(2,6,16,25,50,100)$, $(2,7,10,20,40,80)$
P_3 $k \geq 5$	$(3,4,8,16,32,64)$, $(3,4,8,30,46,92)$, $(3,4,14,22,44,88)$, $(3,4,14,22,44,90)$
P_4 $k \geq 5$	$(4,5,10,20,40,80)$
P_5 $k \geq 4$	$(5,6,12,24,48,96)$, $(5,6,12,24,48)$, $(5,6,12,46,70)$, $(5,6,22,34,68)$, $(5,6,34,46,92)$
P_6 $k \geq 4$	$(6,7,14,28,56)$, $(6,7,14,30,58)$, $(6,7,14,54,82)$, $(6,7,26,40,80)$, $(6,8,14,29,58)$, $(6,8,14,30,58)$, $(6,8,14,30,59)$, $(6,8,14,55,84)$, $(6,8,14,56,84)$, $(6,8,14,56,85)$, $(6,8,15,54,84)$, $(6,8,26,40,80)$, $(6,8,26,40,81)$, $(6,8,26,40,82)$
P_7 $k \geq 4$	$(7,8,16,32,64)$, $(7,8,16,34,66)$, $(7,8,16,62,94)$, $(7,8,16,64,96)$, $(7,8,30,46,92)$
P_8 $k \geq 4$	$(8,9,18,36,72)$, $(8,9,18,38,74)$
P_9 $k \geq 4$	$(9,10,20,40,80)$, $(9,10,20,42,82)$
P_{10} $k \geq 4$	$(10,11,22,44,88)$, $(10,11,22,46,90)$, $(10,12,22,45,90)$, $(10,12,22,45,92)$, $(10,12,24,46,93)$, $(10,12,24,47,94)$, $(10,12,24,47,96)$, $(10,12,24,48,94)$, $(10,12,24,48,95)$, $(10,12,24,48,96)$

Table 2: Nested higher order Kronrod extensions $\mathcal{K}$ of the Legendre polynomials P_n. The table lists the most deeply nested extensions for $n \leq 10$ which were found. The maximal order $p_{\max}$ was set to 100 and the recursion limit $k_{\max}$ was never reached. Notice that extensions and especially highly nested extensions are very abundant in the case of Legendre polynomials.

T_n	$\mathcal{K} = (p_0, p_1, \ldots, p_k)$
T_1 $k \geq 6$	$(1,2,4,6,12,24,48,96)$, $(1,2,4,6,12,24,48)$, $(1,2,4,6,12,24,96)$, $(1,2,4,6,12,48,72)$, $(1,2,4,6,12,72,96)$, $(1,2,4,6,24,36,72)$, $(1,2,4,6,36,48,96)$, $(1,2,4,12,18,36,72)$, $(1,2,4,18,24,48,96)$, $(1,2,6,10,18,36,72)$, $(1,2,10,12,24,48,96)$, $(1,4,6,10,20,40,80)$
T_2 $k \geq 6$	$(2,3,4,8,16,32,64)$, $(2,3,4,8,16,64,96)$, $(2,3,4,8,32,48,96)$, $(2,3,4,16,24,48,96)$, $(2,3,8,12,24,48,96)$, $(2,4,7,12,24,48,96)$
T_3 $k \geq 5$	$(3,4,6,12,24,48,96)$, $(3,4,6,12,24,48)$, $(3,4,6,12,24,96)$, $(3,4,6,12,48,72)$, $(3,4,6,12,72,96)$, $(3,4,6,24,36,72)$, $(3,4,6,36,48,96)$, $(3,4,12,18,36,72)$, $(3,4,18,24,48,96)$, $(3,6,10,18,36,72)$, $(3,10,12,24,48,96)$
T_4 $k \geq 5$	$(4,5,8,16,32,64)$, $(4,5,8,16,64,96)$, $(4,5,8,32,48,96)$, $(4,5,16,24,48,96)$, $(4,8,13,24,48,96)$
T_5 $k \geq 4$	$(5,6,10,20,40,80)$, $(5,6,10,20,40)$, $(5,6,10,20,80)$, $(5,6,10,40,60)$, $(5,6,10,60,80)$, $(5,6,10,80,100)$, $(5,6,20,30,60)$, $(5,6,20,60,90)$, $(5,6,30,40,80)$, $(5,6,40,50,100)$, $(5,10,16,30,60)$, $(5,10,16,60,90)$, $(5,10,30,46,90)$, $(5,16,20,40,80)$, $(5,20,26,50,100)$
T_6 $k \geq 4$	$(6,7,12,24,48,96)$, $(6,7,12,24,48)$, $(6,7,12,24,96)$, $(6,7,12,48,72)$, $(6,7,12,72,96)$, $(6,7,24,36,72)$, $(6,7,36,48,96)$, $(6,12,19,36,72)$, $(6,19,24,48,96)$
T_7 $k \geq 4$	$(7,8,14,28,56)$, $(7,8,14,56,84)$, $(7,8,28,42,84)$, $(7,14,22,42,84)$
T_8 $k \geq 4$	$(8,9,16,32,64)$, $(8,9,16,64,96)$, $(8,9,32,48,96)$, $(8,16,25,48,96)$
T_9 $k \geq 4$	$(9,10,18,36,72)$
T_{10} $k \geq 4$	$(10,11,20,40,80)$

Table 3: Nested higher order Kronrod extensions $\mathcal{K}$ of the Chebyshev polynomials T_n. The table lists the most deeply nested extensions for $n \leq 10$ which were found. The maximal order $p_{\max}$ was set to 100 and the recursion limit $k_{\max}$ was never reached. The Chebyshev polynomials also possess a rich structure of deeply nested extensions.

U_n	$\mathcal{K} = (p_0, p_1, \ldots, p_k)$
U_1 $k \geq 6$	$(1,2,4,8,16,32,64)$, $(1,2,4,8,16,64,96)$, $(1,2,4,8,32,48,96)$, $(1,2,4,16,24,48,96)$, $(1,2,8,12,24,48,96)$, $(1,4,6,12,24,48,96)$
U_2 $k \geq 5$	$(2,3,6,12,24,48,96)$, $(2,3,6,12,24,48)$, $(2,3,6,12,24,96)$, $(2,3,6,12,48,72)$, $(2,3,6,12,72,96)$, $(2,3,6,24,36,72)$, $(2,3,6,36,48,96)$, $(2,3,12,18,36,72)$, $(2,3,18,24,48,96)$, $(2,6,9,18,36,72)$, $(2,9,12,24,48,96)$
U_3 $k \geq 5$	$(3,4,8,16,32,64)$, $(3,4,8,16,64,96)$, $(3,4,8,32,48,96)$, $(3,4,16,24,48,96)$, $(3,8,12,24,48,96)$
U_4 $k \geq 4$	$(4,5,10,20,40,80)$, $(4,5,10,20,40)$, $(4,5,10,20,80)$, $(4,5,10,40,60)$, $(4,5,10,60,80)$, $(4,5,10,80,100)$, $(4,5,20,30,60)$, $(4,5,20,60,90)$, $(4,5,30,40,80)$, $(4,5,40,50,100)$, $(4,10,15,30,60)$, $(4,10,15,60,90)$, $(4,10,30,45,90)$, $(4,15,20,40,80)$, $(4,20,25,50,100)$
U_5 $k \geq 4$	$(5,6,12,24,48,96)$, $(5,6,12,24,48)$, $(5,6,12,24,96)$, $(5,6,12,48,72)$, $(5,6,12,72,96)$, $(5,6,24,36,72)$, $(5,6,36,48,96)$, $(5,12,18,36,72)$, $(5,18,24,48,96)$
U_6 $k \geq 4$	$(6,7,14,28,56)$, $(6,7,14,56,84)$, $(6,7,28,42,84)$, $(6,14,21,42,84)$
U_7 $k \geq 4$	$(7,8,16,32,64)$, $(7,8,16,64,96)$, $(7,8,32,48,96)$, $(7,16,24,48,96)$
U_8 $k \geq 3$	$(8,9,18,36,72)$, $(8,9,18,36)$, $(8,9,18,72)$, $(8,9,36,54)$, $(8,9,54,72)$, $(8,9,72,90)$, $(8,18,27,54)$, $(8,18,54,81)$, $(8,27,36,72)$, $(8,36,45,90)$
U_9 $k \geq 3$	$(9,10,20,40,80)$, $(9,10,20,40)$, $(9,10,20,80)$, $(9,10,40,60)$, $(9,10,60,80)$, $(9,10,80,100)$, $(9,20,30,60)$, $(9,20,60,90)$, $(9,30,40,80)$, $(9,40,50,100)$
U_{10} $k \geq 3$	$(10,11,22,44,88)$, $(10,11,22,44)$, $(10,11,22,88)$, $(10,11,44,66)$, $(10,11,66,88)$, $(10,22,33,66)$, $(10,22,66,99)$, $(10,33,44,88)$

Table 4: Nested higher order Kronrod extensions $\mathcal{K}$ of the Chebyshev polynomials U_n. The table lists the most deeply nested extensions for $n \leq 10$ which were found. The maximal order $p_{\max}$ was set to 100 and the recursion limit $k_{\max}$ was never reached. The Chebyshev polynomials also possess a rich structure of deeply nested extensions.

L_n	$\mathcal{K} = (p_0, p_1, \ldots, p_k)$
L_1 $k \geq 3$	$(1,3,5,12,24)$, $(1,3,5,12,25)$, $(1,3,5,12,26)$, $(1,3,5,9)$, $(1,3,5,10)$, $(1,3,5,11)$, $(1,3,5,12)$, $(1,3,5,23)$, $(1,3,5,24)$, $(1,3,5,25)$, $(1,3,5,28)$, $(1,3,5,29)$, $(1,3,5,45)$, $(1,3,5,46)$, $(1,3,5,47)$, $(1,3,5,69)$, $(1,3,5,70)$, $(1,3,5,80)$, $(1,3,6,43)$, $(1,3,6,91)$, $(1,3,6,92)$, $(1,3,6,93)$, $(1,3,7,90)$, $(1,3,7,91)$, $(1,3,8,89)$, $(1,3,8,90)$, $(1,5,11,68)$
L_2 $k \geq 2$	$(2,4,7,29)$, $(2,4,8,86)$, $(2,4,9,86)$, $(2,4,7)$, $(2,4,8)$, $(2,4,9)$, $(2,4,10)$, $(2,4,13)$, $(2,4,21)$, $(2,4,22)$, $(2,4,23)$, $(2,4,30)$, $(2,4,41)$, $(2,4,42)$, $(2,4,43)$, $(2,4,44)$, $(2,4,45)$, $(2,4,47)$, $(2,4,53)$, $(2,4,68)$, $(2,4,69)$, $(2,4,70)$, $(2,4,71)$, $(2,4,72)$, $(2,4,73)$, $(2,4,74)$, $(2,4,96)$, $(2,4,97)$, $(2,5,29)$, $(2,5,30)$, $(2,5,38)$, $(2,5,39)$, $(2,5,48)$, $(2,6,50)$, $(2,6,51)$, $(2,6,54)$, $(2,6,79)$, $(2,6,80)$, $(2,7,49)$, $(2,7,77)$, $(2,9,48)$, $(2,10,58)$
L_3 $k \geq 2$	$(3,6,41)$, $(3,6,42)$, $(3,6,43)$, $(3,6,44)$, $(3,6,50)$, $(3,7,57)$, $(3,7,58)$, $(3,7,94)$
L_4 $k \geq 2$	$\emptyset$
L_5 $k \geq 2$	$(5,9,39)$, $(5,9,40)$
L_6 $k \geq 2$	$\emptyset$
L_7 $k \geq 2$	$\emptyset$
L_8 $k \geq 2$	$(8,15,26)$
L_9 $k \geq 2$	$\emptyset$
L_{10} $k \geq 2$	$\emptyset$

Table 5: Nested higher order Kronrod extensions $\mathcal{K}$ of the Laguerre polynomials L_n. The table lists the most deeply nested extensions for $n \leq 20$ which were found. The maximal order $p_{\max}$ was set to 100 and the recursion limit $k_{\max}$ was never reached. For this type of polynomial, deeply nested rules are extremely rare.

H_n	$\mathcal{K} = (p_0, p_1, \ldots, p_k)$
H_1 $k \geq 4$	$(1,2,6,10,16,68)$, $(1,2,6,10,18,66)$, $(1,2,6,10,18,68)$, $(1,2,6,10,16)$, $(1,2,6,10,18)$, $(1,2,6,10,22)$, $(1,2,6,10,24)$, $(1,2,6,10,96)$, $(1,2,6,12,28)$, $(1,2,6,12,34)$, $(1,2,6,12,36)$, $(1,2,6,12,48)$, $(1,2,6,14,22)$, $(1,2,6,14,24)$, $(1,2,6,14,28)$, $(1,2,6,14,32)$, $(1,2,6,14,34)$, $(1,2,6,14,78)$, $(1,2,6,14,80)$, $(1,2,6,14,82)$, $(1,2,6,24,36)$, $(1,2,6,24,40)$, $(1,2,6,24,44)$, $(1,4,8,14,96)$, $(1,8,14,22,90)$
H_2 $k \geq 4$	$(2,3,4,8,24)$, $(2,3,4,8,50)$, $(2,3,4,8,52)$, $(2,3,4,8,54)$, $(2,3,4,8,56)$, $(2,3,4,8,78)$, $(2,3,4,8,80)$, $(2,3,4,8,82)$, $(2,3,4,8,84)$, $(2,3,4,16,98)$, $(2,3,4,18,98)$, $(2,3,4,20,30)$, $(2,3,4,20,32)$, $(2,3,4,20,34)$, $(2,3,4,20,36)$, $(2,3,4,20,38)$, $(2,3,4,20,40)$, $(2,3,6,16,24)$, $(2,3,6,16,26)$, $(2,3,6,16,90)$, $(2,3,6,16,92)$, $(2,3,6,16,98)$
H_3 $k \geq 3$	$(3,6,10,16,68)$, $(3,6,10,18,66)$, $(3,6,10,18,68)$, $(3,6,10,16)$, $(3,6,10,18)$, $(3,6,10,22)$, $(3,6,10,24)$, $(3,6,10,96)$, $(3,6,12,28)$, $(3,6,12,34)$, $(3,6,12,36)$, $(3,6,12,48)$, $(3,6,14,22)$, $(3,6,14,24)$, $(3,6,14,28)$, $(3,6,14,32)$, $(3,6,14,34)$, $(3,6,14,78)$, $(3,6,14,80)$, $(3,6,14,82)$, $(3,6,24,36)$, $(3,6,24,40)$, $(3,6,24,44)$
H_4 $k \geq 3$	$(4,5,10,36,56)$, $(4,5,10,36)$, $(4,5,10,38)$, $(4,5,10,46)$, $(4,5,10,48)$, $(4,5,10,52)$, $(4,5,10,54)$, $(4,5,22,42)$, $(4,5,30,48)$
H_5 $k \geq 3$	$(5,8,14,96)$
H_6 $k \geq 3$	$(6,9,14,68)$, $(6,9,16,66)$, $(6,9,16,68)$
H_7 $k \geq 3$	$\emptyset$
H_8 $k \geq 3$	$(8,11,18,66)$
H_9 $k \geq 3$	$(9,14,22,90)$
H_{10} $k \geq 3$	$\emptyset$

Table 6: Nested higher order Kronrod extensions $\mathcal{K}$ of the Hermite polynomials H_n. The table lists the most deeply nested extensions for $n \leq 20$ which were found. The maximal order $p_{\max}$ was set to 100 and the recursion limit $k_{\max}$ was never reached.

B Computed Generators

The tables in this appendix contain the generator sets Λ for all default rules examined in section 6. The generators are ordered in the above-mentioned alternating order.

	Generator	Error
λ_0	0	± 0
λ_1	0.77459666924148337704	$\pm 8.9398 \cdot 10^{-128}$
λ_2	0.96049126870802028342	$\pm 2.9519 \cdot 10^{-127}$
λ_3	0.434243749346802558	$\pm 1.9264 \cdot 10^{-127}$
λ_4	0.99383196321275502221	$\pm 1.2033 \cdot 10^{-125}$
λ_5	0.22338668642896688163	$\pm 2.9048 \cdot 10^{-127}$
λ_6	0.88845923287225699889	$\pm 1.6417 \cdot 10^{-125}$
λ_7	0.62110294673722640294	$\pm 3.1186 \cdot 10^{-126}$
λ_8	0.99909812496766759766	$\pm 4.2615 \cdot 10^{-122}$
λ_9	0.11248894313318662575	$\pm 2.0256 \cdot 10^{-127}$
λ_{10}	0.98153114955374010687	$\pm 6.0247 \cdot 10^{-122}$
λ_{11}	0.33113539325797683309	$\pm 5.1636 \cdot 10^{-126}$
λ_{12}	0.92965485742974005667	$\pm 2.6398 \cdot 10^{-122}$
λ_{13}	0.53131974364437562397	$\pm 1.0295 \cdot 10^{-124}$
λ_{14}	0.8367259381688687355	$\pm 7.0227 \cdot 10^{-123}$
λ_{15}	0.70249620649152707861	$\pm 9.7952 \cdot 10^{-124}$
λ_{16}	0.99987288812035761194	$\pm 9.0618 \cdot 10^{-115}$
λ_{17}	0.056344313046592789972	$\pm 2.4195 \cdot 10^{-127}$
λ_{18}	0.99720625937222195908	$\pm 1.446 \cdot 10^{-114}$
λ_{19}	0.16823525155220746498	$\pm 5.9532 \cdot 10^{-126}$
λ_{20}	0.98868475754742947994	$\pm 8.3369 \cdot 10^{-115}$
λ_{21}	0.27774982202182431507	$\pm 1.5333 \cdot 10^{-124}$
λ_{22}	0.97218287474858179658	$\pm 3.0935 \cdot 10^{-115}$
λ_{23}	0.38335932419873034692	$\pm 2.7813 \cdot 10^{-123}$
λ_{24}	0.94634285837340290515	$\pm 9.2169 \cdot 10^{-116}$
λ_{25}	0.48361802694584102756	$\pm 4.9013 \cdot 10^{-122}$
λ_{26}	0.9103711569570042925	$\pm 2.6298 \cdot 10^{-116}$
λ_{27}	0.57719571005204581484	$\pm 8.4648 \cdot 10^{-121}$
λ_{28}	0.86390793819369047715	$\pm 4.8765 \cdot 10^{-117}$
λ_{29}	0.66290966002478059546	$\pm 9.9356 \cdot 10^{-120}$
λ_{30}	0.80694053195021761186	$\pm 8.102 \cdot 10^{-118}$
λ_{31}	0.73975604435269475868	$\pm 1.0763 \cdot 10^{-118}$

Table 7: Generators in the Legendre case $\mathcal{K} = (1, 2, 4, 8, 16, 32)$ computed to 20 decimal digits. Rigorous error bounds are provided by ball arithmetic.

	Generator	Error
λ_0	0	± 0
λ_1	0.86602540378443864676	$\pm 1.8457 \cdot 10^{-255}$
λ_2	1	± 0
λ_3	0.5	$\pm 4.44 \cdot 10^{-255}$
λ_4	0.96592582628906828675	$\pm 1.6752 \cdot 10^{-254}$
λ_5	0.25881904510252076235	$\pm 2.5144 \cdot 10^{-255}$
λ_6	0.7071067811865475244	$\pm 2.1372 \cdot 10^{-254}$
λ_7	0.99144486137381041114	$\pm 1.9027 \cdot 10^{-252}$
λ_8	0.13052619222005159155	$\pm 3.1477 \cdot 10^{-255}$
λ_9	0.92387953251128675613	$\pm 3.8807 \cdot 10^{-252}$
λ_{10}	0.38268343236508977173	$\pm 5.1667 \cdot 10^{-254}$
λ_{11}	0.79335334029123516458	$\pm 1.531 \cdot 10^{-252}$
λ_{12}	0.60876142900872063942	$\pm 3.995 \cdot 10^{-253}$
λ_{13}	0.99785892323860350674	$\pm 4.8189 \cdot 10^{-248}$
λ_{14}	0.065403129230143066815	$\pm 2.1204 \cdot 10^{-255}$
λ_{15}	0.98078528040323044913	$\pm 1.0712 \cdot 10^{-247}$
λ_{16}	0.19509032201612826785	$\pm 5.0556 \cdot 10^{-254}$
λ_{17}	0.94693012949510566426	$\pm 1.0193 \cdot 10^{-247}$
λ_{18}	0.3214394653031615807	$\pm 9.8952 \cdot 10^{-253}$
λ_{19}	0.89687274153268830389	$\pm 5.1395 \cdot 10^{-248}$
λ_{20}	0.442288690219001282	$\pm 1.0802 \cdot 10^{-251}$
λ_{21}	0.83146961230254523708	$\pm 2.0304 \cdot 10^{-248}$
λ_{22}	0.55557023301960222474	$\pm 1.4191 \cdot 10^{-250}$
λ_{23}	0.75183980747897739641	$\pm 5.3441 \cdot 10^{-249}$
λ_{24}	0.65934581510006886843	$\pm 9.1351 \cdot 10^{-250}$

Table 8: Generators in the Chebyshev (first kind) case $\mathcal{K} = (1, 2, 4, 6, 12, 24)$ computed to 20 decimal digits. Rigorous error bounds are provided by ball arithmetic.

	Generator	Error
λ_0	0	± 0
λ_1	0.70710678118654752440	$\pm 1.1302 \cdot 10^{-255}$
λ_2	0.92387953251128675613	$\pm 3.4002 \cdot 10^{-255}$
λ_3	0.38268343236508977173	$\pm 2.4588 \cdot 10^{-255}$
λ_4	0.98078528040323044913	$\pm 1.0265 \cdot 10^{-253}$
λ_5	0.19509032201612826785	$\pm 3.5259 \cdot 10^{-255}$
λ_6	0.83146961230254523708	$\pm 1.0815 \cdot 10^{-253}$
λ_7	0.55557023301960222474	$\pm 2.496 \cdot 10^{-254}$
λ_8	0.99518472667219688624	$\pm 5.6869 \cdot 10^{-251}$
λ_9	0.098017140329560601994	$\pm 3.0746 \cdot 10^{-255}$
λ_{10}	0.95694033573220886494	$\pm 1.1254 \cdot 10^{-250}$
λ_{11}	0.29028467725446236764	$\pm 4.1566 \cdot 10^{-254}$
λ_{12}	0.88192126434835502971	$\pm 5.8436 \cdot 10^{-251}$
λ_{13}	0.47139673682599764856	$\pm 5.9365 \cdot 10^{-253}$
λ_{14}	0.77301045336273696081	$\pm 2.4054 \cdot 10^{-251}$
λ_{15}	0.63439328416364549822	$\pm 6.3821 \cdot 10^{-252}$
λ_{16}	0.99879545620517239271	$\pm 3.7653 \cdot 10^{-245}$
λ_{17}	0.049067674327418014255	$\pm 3.1008 \cdot 10^{-255}$
λ_{18}	0.98917650996478097345	$\pm 1.0269 \cdot 10^{-244}$
λ_{19}	0.14673047445536175166	$\pm 5.0159 \cdot 10^{-254}$
λ_{20}	0.9700312531945439926	$\pm 9.1895 \cdot 10^{-245}$
λ_{21}	0.24298017990326388995	$\pm 1.0345 \cdot 10^{-252}$
λ_{22}	0.94154406518302077841	$\pm 7.649 \cdot 10^{-245}$
λ_{23}	0.33688985339222005069	$\pm 1.6499 \cdot 10^{-251}$
λ_{24}	0.90398929312344333159	$\pm 3.3936 \cdot 10^{-245}$
λ_{25}	0.42755509343028209432	$\pm 2.5664 \cdot 10^{-250}$
λ_{26}	0.8577286100002720699	$\pm 1.4468 \cdot 10^{-245}$
λ_{27}	0.51410274419322172659	$\pm 3.7758 \cdot 10^{-249}$
λ_{28}	0.80320753148064490981	$\pm 4.3992 \cdot 10^{-246}$
λ_{29}	0.59569930449243334347	$\pm 3.0138 \cdot 10^{-248}$
λ_{30}	0.74095112535495909118	$\pm 1.1218 \cdot 10^{-246}$
λ_{31}	0.67155895484701840063	$\pm 1.8774 \cdot 10^{-247}$

Table 9: Generators in the Chebyshev (second kind) case $\mathcal{K} = (1, 2, 4, 8, 16, 32)$ computed to 20 decimal digits. Rigorous error bounds are provided by ball arithmetic.

	Generator	Error
λ_0	0	± 0
λ_1	1.2247448713915890491	$\pm 2.6102 \cdot 10^{-255}$
λ_2	2.9592107790638377223	$\pm 3.2633 \cdot 10^{-254}$
λ_3	0.52403354748695764515	$\pm 8.0828 \cdot 10^{-255}$
λ_4	2.0232301911005156592	$\pm 4.6195 \cdot 10^{-254}$
λ_5	4.4995993983103888029	$\pm 7.1244 \cdot 10^{-253}$
λ_6	0.87004089535290290013	$\pm 3.6256 \cdot 10^{-254}$
λ_7	3.667774215946337 86	$\pm 1.1448 \cdot 10^{-252}$
λ_8	1.8357079751751868738	$\pm 4.852 \cdot 10^{-253}$
λ_9	2.2665132620567880275	$\pm 8.9175 \cdot 10^{-253}$
λ_{10}	6.3759392709822359517	$\pm 3.8855 \cdot 10^{-251}$
λ_{11}	0.17606414208200893503	$\pm 6.8732 \cdot 10^{-255}$
λ_{12}	5.6432578578857450628	$\pm 1.1977 \cdot 10^{-250}$
λ_{13}	1.5794121348467670857	$\pm 3.6322 \cdot 10^{-253}$
λ_{14}	5.0360899444730939687	$\pm 1.2618 \cdot 10^{-250}$
λ_{15}	2.5705583765842967091	$\pm 5.1481 \cdot 10^{-252}$
λ_{16}	4.0292201405043713648	$\pm 6.5727 \cdot 10^{-251}$
λ_{17}	3.3491639537131949774	$\pm 2.7947 \cdot 10^{-251}$

Table 10: Generators in the Hermite case $\mathcal{K} = (1, 2, 6, 10, 16)$ computed to 20 decimal digits. Rigorous error bounds are provided by ball arithmetic. We can confirm the claim made in [8] for their Table 4 (both columns) and assure that all digits shown are indeed correct.

	Generator	Error
λ_{18}	12.371183263294440156	$\pm 6.2996 \cdot 10^{-242}$
λ_{19}	0.36668252574926773363	$\pm 1.7765 \cdot 10^{-253}$
λ_{20}	11.773315693849850411	$\pm 2.3346 \cdot 10^{-240}$
λ_{21}	0.66761453794663251987	$\pm 1.6969 \cdot 10^{-252}$
λ_{22}	11.279571841264790728	$\pm 2.642 \cdot 10^{-239}$
λ_{23}	1.0853772883690724485	$\pm 3.7943 \cdot 10^{-251}$
λ_{24}	10.839884501585234819	$\pm 2.0142 \cdot 10^{-238}$
λ_{25}	1.3554874833640409297	$\pm 2.0233 \cdot 10^{-250}$
λ_{26}	10.435144794449726187	$\pm 9.2267 \cdot 10^{-238}$
λ_{27}	1.8804002593778771426	$\pm 3.9786 \cdot 10^{-249}$
λ_{28}	10.055514590896118546	$\pm 3.4517 \cdot 10^{-237}$
λ_{29}	2.4894835291142853745	$\pm 5.0127 \cdot 10^{-247}$
λ_{30}	9.6950986498409657256	$\pm 9.4588 \cdot 10^{-237}$
λ_{31}	2.7429887276487330543	$\pm 3.9256 \cdot 10^{-246}$
λ_{32}	9.3500178360366242267	$\pm 1.9321 \cdot 10^{-236}$
λ_{33}	3.1578423043107310587	$\pm 6.5944 \cdot 10^{-245}$
λ_{34}	9.0175517361800331664	$\pm 3.4879 \cdot 10^{-236}$
λ_{35}	3.5581744596318809581	$\pm 1.268 \cdot 10^{-243}$
λ_{36}	8.6957029638952971694	$\pm 5.2545 \cdot 10^{-236}$
λ_{37}	3.7936922531585261377	$\pm 5.3856 \cdot 10^{-243}$
λ_{38}	8.3829544155838454626	$\pm 5.7185 \cdot 10^{-236}$
λ_{39}	4.2688636547893383582	$\pm 7.0628 \cdot 10^{-242}$
λ_{40}	8.0781250284796943353	$\pm 5.6882 \cdot 10^{-236}$
λ_{41}	4.6477303329076984149	$\pm 1.4317 \cdot 10^{-240}$
λ_{42}	7.7802807323602445651	$\pm 4.7409 \cdot 10^{-236}$
λ_{43}	4.8019262436547872092	$\pm 3.184 \cdot 10^{-240}$
λ_{44}	7.4886797763487223782	$\pm 3.3395 \cdot 10^{-236}$
λ_{45}	5.2754516328221667421	$\pm 2.5212 \cdot 10^{-239}$
λ_{46}	7.2027436504485393396	$\pm 1.7826 \cdot 10^{-236}$
λ_{47}	5.4830796220220625119	$\pm 6.2053 \cdot 10^{-239}$
λ_{48}	6.9220548983808420548	$\pm 7.4588 \cdot 10^{-237}$
λ_{49}	5.8591159720395398957	$\pm 1.8806 \cdot 10^{-238}$
λ_{50}	6.6464009334963516572	$\pm 2.1116 \cdot 10^{-237}$
λ_{51}	6.1118124629258834825	$\pm 3.619 \cdot 10^{-238}$

Table 11: Higher generators in the Hermite case $\mathcal{K} = (1, 2, 6, 10, 16, 68)$ computed to 20 decimal digits. Rigorous error bounds are provided by ball arithmetic.

References

[1] Gustavo Avila and Tucker Carrington. Nonproduct quadrature grids for solving the vibrational schrödinger equation. *The Journal of Chemical Physics*, 131(17), 2009. 63

[2] Erwan Faou, Vasile Gradinaru, and Christian Lubich. Computing semiclassical quantum dynamics with hagedorn wavepackets, 2009. 2

[3] Laurent Fousse, Guillaume Hanrot, Vincent Lefèvre, Patrick Pélissier, and Paul Zimmermann. Mpfr: A multiple-precision binary floating-point library with correct rounding. *ACM Trans. Math. Softw.*, 33(2), June 2007. 9

[4] Walter Gautschi and Sotorios E. Notaris. An algebraic study of Gauss-Kronrod quadrature formulae for Jacobi weight functions. *Math. Comp.*, 51(183):231–248, 1988. 2, 10

[5] Walter Gautschi and Sotorios E. Notaris. Gauss–kronrod quadrature formulae for weight functions of bernstein–szegő type. *Journal of Computational and Applied Mathematics*, 25(2):199 – 224, 1989. 2, 10

[6] Walter Gautschi and Theodore J. Rivlin. A family of Gauss-Kronrod quadrature formulae. *Math. Comp.*, 51(184):749–754, 1988. 3

[7] Alan Genz. Fully symmetric interpolatory rules for multiple integrals. *SIAM Journal on Numerical Analysis*, 23(6):1273–1283, 1986. 2, 15, 16, 19, 20, 24

[8] Alan Genz and Bradley D. Keister. Fully symmetric interpolatory rules for multiple integrals over infinite regions with gaussian weight. *Journal of Computational and Applied Mathematics*, 71(2):299 – 309, 1996. 15, 19, 72

[9] George A. Hagedorn. Raising and lowering operators for semiclassical wave packets. *Annals of Physics*, 269(1):77–104, 1998. 2

[10] William Hart. Fast Library for Number Theory: An Introduction. In *Proceedings of the Third International Congress on Mathematical Software*, ICMS'10, pages 88–91, Berlin, Heidelberg, 2010. Springer-Verlag. 9, 17

[11] William Hart, Fredrik Johansson, and Sebastian Pancratz. FLINT: Fast Library for Number Theory, 2014. `http://flintlib.org`. 9, 17

[12] Markus Holtz. *Sparse Grid Quadrature in High Dimensions with Applications in Finance and Insurance*. Lecture Notes in Computational Science and Engineering. Springer, 2011. 24

[13] Fredrik Johansson. Arb: C library for arbitrary-precision floating-point ball arithmetic, 2014. `http://fredrikj.net/arb/`. 9

[14] David K. Kahaner and Giovanni Monegato. Nonexistence of extended gauss-laguerre and gauss-hermite quadrature rules with positive weights. *Zeitschrift für angewandte Mathematik und Physik ZAMP*, 29(6):983–986, 1978. 2, 11

[15] David K. Kahaner, Jörg Waldvogel, and L. W. Fullerton. Addition of points to gauss–laguerre quadrature formulas. *SIAM Journal on Scientific and Statistical Computing*, 5(1):42–55, 1984. 11

[16] Aleksandr Semenovich Kronrod. *Nodes and weights of quadrature formulas. Sixteen-place tables.* Authorized translation from the Russian. Consultants Bureau, New York, 1965. 1, 2

[17] Dirk P. Laurie. Calculation of gauss–kronrod quadrature rules. *Mathematics of Computation*, pages 1133–1145, 1997. 1

[18] Sanjay Mehrotra and Dávid Papp. Generating nested quadrature formulas for general weight functions with known moments. *ArXiv e-prints*, March 2012. `http://arxiv.org/abs/1203.1554`. 1, 2, 3

[19] Giovanni Monegato. A note on extended gaussian quadrature rule. *Mathematics of Computation*, 30(136):pp. 812–817, 1976. 11

[20] Giovanni Monegato. Positivity of the weights of extended Gauss-Legendre quadrature rules. *Math. Comp.*, 32(141):243–245, 1978. 2, 10

[21] Giovanni Monegato. Some remarks on the construction of extended gaussian quadrature rules. *Mathematics of Computation*, 32(141):pp. 247–252, 1978. 2, 10

[22] Giovanni Monegato. An overview of results and questions related to kronrod schemes. In G. Hämmerlin, editor, *Numerische Integration*, volume 45 of *International Series of Numerical Mathematics / Internationale Schriftenreihe zur Numerischen Mathematik / Série Internationale D'Analyse Numérique*, pages 231–240. Birkhäuser Basel, 1979. 3

[23] Giovanni Monegato. Stieltjes polynomials and related quadrature rules. *SIAM Review*, 24(2):137–158, 1982. 3

[24] Sotorios E. Notaris. Gauss-kronrod quadrature formulae for weight functions of bernstein-szegő type, ii. *Journal of Computational and Applied Mathematics*, 29(2):161 – 169, 1990. 10

[25] Erich Novak and Klaus Ritter. Simple cubature formulas with high polynomial exactness. *Constructive Approximation*, 15(4):499–522, 1999. 2, 20

[26] T. N. L. Patterson. The optimum addition of points to quadrature formulae. *Mathematics of Computation*, 22(104):pp. 847–856+s21–s31, 1968. 1

[27] Joan Serra-Sagristà. Enumeration of lattice points in l1 norm. *Inf. Process. Lett.*, 76(1-2):39–44, November 2000. 21

[28] Gábor Szegő. Über gewisse orthogonale polynome, die zu einer oszillierenden belegungsfunktion gehören. *Mathematische Annalen*, 110(1):501–513, 1935. 2, 10

[29] Joris van der Hoeven. Ball arithmetic. Technical report, HAL, 2009. `http://hal.archives-ouvertes.fr/hal-00432152/fr/`. 5

[30] Joris van der Hoeven. Ball arithmetic. In *Logical approaches to Barriers in Computing and Complexity*, number 6 in Preprint-Reihe Mathematik, pages 179–208, February 2010. 5

[31] Daniel Vladislav. Construction of gauss-kronrod-hermite quadrature and cubature formulas. 2004. 11

Recent Research Reports